MRS BULLETIN

Serving the International Materials Research Community

A Publication of the Materials Research Society

April 2007, Volume 32, No. 4

Polymer Nanocomposites

Also in This Issue:

Pb-Free Solder

Polymer Nanocomposites

Karen I. Winey and Richard A. Vaia,
Guest Editors

Abstract

Polymer nanocomposites (PNCs)—that is, nanoparticles (spheres, rods, plates) dispersed in a polymer matrix—have garnered substantial academic and industrial interest since their inception, circa 1990. This is due in large part to the incredible promise demonstrated by these early efforts: PNCs will not only expand the performance space of traditional filled polymers, but introduce completely new combinations of properties and thus enable new applications for plastics. Low volume additions (1–5%) of nanoparticles, such as layered silicates or carbon nanotubes, provide property enhancements with respect to the neat resin that are comparable to those achieved by conventional loadings (15–40%) of traditional fillers. The lower loadings facilitate processing and reduce component weight. Most important, though, is the unique value-added properties not normally possible with traditional fillers, such as reduced permeability, optical clarity, self-passivation, and increased resistance to oxidation and ablation. These characteristics have been transformed into numerous commercial successes, including automotive parts, coatings, and flame retardants. This issue of the *MRS Bulletin* provides a snapshot of these exemplary successes, future opportunities, and the critical scientific challenges still to be addressed for these nanoscale multiphase systems. In addition, these articles provide a perspective on the current status and future directions of polymer nanocomposite science and technology and their potential to move beyond additive concepts to designed materials and devices with prescribed nanoscale composition and morphology.

Introduction

Polymers have been a part of life since the beginning of humankind. From tar and shellac, tortoise shell and horns, to today's synthetic offerings such as polyolefins, epoxies, and engineering resins, polymers provide crucial materials for construction, commerce, transportation, and entertainment across the globe. Estimates of global polymer production range from 250 billion pounds to more than 400 billion pounds (approximately 114–181 billion kg) annually.

In the majority of their diverse applications, polymeric materials are not chemically or molecularly homogenous but are multicomponent systems. By adding fillers, such as minerals, ceramics, metals, or even air, materials scientists can generate an infinite variety of materials with unique physical properties and competitive production costs. For example, adding filler to a commodity thermoplastic such as polypropylene can achieve performance levels that would otherwise require a much more expensive engineering plastic. Similarly, combining different polymers to form a polymer blend or resin can increase the value of existing polymers.

Polymer nanocomposites incorporate a new spectrum of fillers that extend the function and utility of polymers while maintaining the manufacturing and processing flexibility inherent to plastics, thermosets, and resins. In particular, polymer nanocomposites have been successful with regard to overcoming traditionally antagonistic combinations of properties.

Since the first reports in the late 1980s,[1–6] the term "polymer nanocomposite" has evolved to refer to a multicomponent system in which the major constituent is a polymer or blend thereof and the minor constituent has at least one dimension below 100 nm. Polymer nanocomposite is an appropriate synonym for inorganic–organic hybrids and molecular composites and also encompasses mature commercial products such as polymers containing carbon black or fumed silica. This issue of *MRS Bulletin* focuses primarily on polymer nanocomposites containing nanoscale clays and various carbon nanotubes to illustrate the status of this rapidly evolving research and development enterprise.

The numerous reports of large property changes with very small additions of nanoparticles (<1–5 wt%) have fueled the view that nanoparticles are a magic pixie dust that delivers huge dividends. In fact, recent market surveys have estimated global consumption of polymer nanocomposites at tens of millions of pounds (~$250 million), with a potential annual average growth rate of 24%, to almost 100 million pounds in 2011 at a value exceeding $500–800 million.[7–9] Major revenues are forecast from large commercial opportunities such as automobile parts, coatings, flame retardants, and packaging, where lower-cost, higher-performance materials would improve durability and design flexibility while lowering unit price and life cycle cost.

Whatever the case for the long-term economic growth of polymer nanocomposites, the opportunities to deliver targeted material performance reside with the implications associated with nanoscale multiphase systems. There are important differences when the fillers shrink from microscale to nanoscale. This issue of the *MRS Bulletin* provides a snapshot of exemplary successes, future opportunities, and the critical scientific challenges still to be addressed for these nanoscale multiphase systems. In addition, these articles provide a perspective on the current status of polymer nanocomposite science and technology as well as future directions to move it beyond additive concepts to designed materials and devices with prescribed nanoscale composition and morphology.

The Nano Advantage

When fillers are nanoscopic, there are advantages afforded to filled polymers and composites that lead to performance enhancements. These advantages result primarily from filler size reduction and the concomitant increase in surface area. The size of the additive might drop by up to three orders of magnitude relative to conventional alternatives. In contrast, many nanotechnologies associated with electrical or optical properties benefit from new physical phenomena arising from quantum confinement effects induced by the nanoscale dimensions of the material. The literature about polymer nanocomposites contains many discussions about the implications and physical manifestations of the reduction in filler length scale.[10–14]

For example, compare a microcomposite and a nanocomposite with the same volume fraction of a secondary constituent (filler), where the spherical particles have volumes of 1 μm^3 or 1 nm^3 per particle, respectively. The mean particle–particle separation is smaller by three orders of magnitude, the total internal interfacial area increases by six orders of magnitude, and the number density of constituents increases by nine orders of magnitude in the nanocomposite. Although these numbers alone are impressive, the filler size must be viewed relative to the size of polymer molecules to capture the full potential impact of nanoscale fillers on composite properties.

Many properties are related to the size of the polymer chain, which can be expressed as the radius of gyration R_g (the second moment of the three-dimensional distribution of the monomers of the polymer chain—approximately the expanse of the molecule). R_g is on the order of 3–30 nm. Depending on the strength of interaction between the filler surface and the matrix, the polymer chains in close proximity to the filler will be perturbed with respect to those in the bulk (i.e., away from the interface). The thickness t of this interfacial region that surrounds the particle is, to first order, independent of the size of the particle. Thus, as the particle size decreases, the relative volume of this interfacial material, $V_{interface}$, with respect to the volume of the particle, $V_{particle}$, will increase.

Figure 1 shows this ratio, $V_{interface}/V_{particle}$, as a function of particle aspect ratio from plates (aspect ratio <1) to spheres to rods (aspect ratio >1). The filler size is expressed as δ, the ratio of the thickness of the interface to the smallest dimension of the particle. Micrometer-sized fillers have $\delta \sim 0.01$, so that at any aspect ratio, the volume of the particles exceeds that of the interfacial region. However, when the fillers are reduced to the nanoscale and $\delta \sim 1$–10, the volume of the interfacial region exceeds the volume of the particle. In addition, at a fixed value of δ, the aspect ratio has an effect on $V_{interface}/V_{particle}$, showing an expected increase from plates to rods to spheres as the fillers change from two-dimensional (plate) to one-dimensional (rod) to zero-dimensional (sphere) objects. The magnitude of this change increases dramatically as the filler size drops; for example, at δ 10, $V_{interface}/V_{particle}$ increases by two orders of magnitude between plates and spheres.

Furthermore, these calculations demonstrate the impact that even a small volume fraction of filler has on the surrounding polymers. For example, by dispersing a mere 1 vol% of a nanosphere (radius ~2 nm) in a polymer (interfacial thickness ~6 nm), the volume fraction occupied by the interfacial region is ~63 vol%, suggesting that more than half of the composite is affected by the presence of the second-phase particles. If the particle is increased to 20 nm in radius without changing the interfacial thickness or particle loading, the volume occupied by the interfacial region would be only ~1.2 vol%.

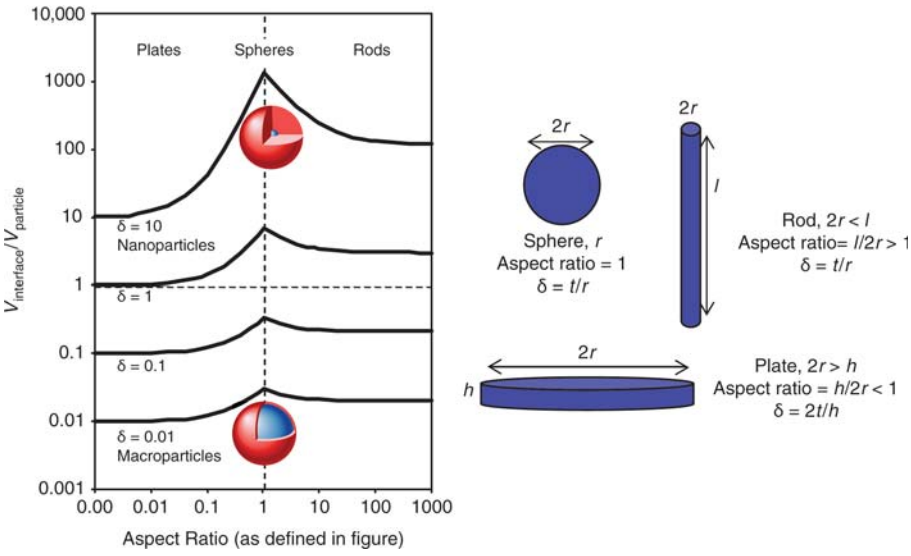

Figure 1. The ratio of interfacial volume to the particle volume ($V_{interface}/V_{particle}$) as a function of the particle aspect ratio and the ratio of the interfacial thickness to the particle size (δ). The aspect ratio and δ are defined in the schematic at right (r is radius, l is length, h is height). The interfacial thickness (red shell, t) is assumed to be independent of the particle size. As particles decrease in size to less than 100 nm, the interfacial volume around a particle can dominate the physical properties, and this is particularly evident for spheres and rods.

The importance of polymer–particle interactions is amplified in polymer nanocomposites such that the interface and the cooperativity between particles dominate the macroscopic properties. For example, weak forces between particles, such as van der Waals, are more pronounced for nano-sized particles because of lower surface roughness, smaller average particle separations, and thus higher dispersive forces. Also, because of the nanoscopic dimensions of the particles, the accessible aspect ratio of discrete secondary constituents can approach 100 or more. These high-aspect-ratio, nanoscale fillers can reach percolation thresholds at <1–5 vol% and thereby exhibit large increases in bulk mechanical and transport properties at these low loadings. The percolation threshold is the filler concentration at which the electrical conductivity increases sharply by orders of magnitude, indicating that conductive pathways span the macroscopic sample. Thus, the casual observation that nanofillers act as pixie dust is firmly rooted in the implications of reducing the size of the fillers by up to three orders of magnitude.

Scope and Impact

As with traditional filled plastics, an infinite variety of possible polymer–nanoparticle combinations conceptually affords tunability. Thus, given the diversity of possible properties and tolerable costs, there is no universal "best" nanoparticle filler for polymer nanocomposites. The best nanoparticle filler (or traditional filler, for that matter) is determined by meeting both a specific set of physical properties and a price point associated with a particular part or product. Table I compares the size, shape, properties, and uses of traditional fillers and newer nanoscale fillers. As noted earlier, a few traditional fillers have sizes below 100 nm, and nanoscale fillers can access high aspect ratios. Although there is considerable overlap in the elastic moduli and thermal conductivities between the traditional and nanoscale fillers, the electrical properties of the carbon-based nanofillers are in a class by themselves, with conductivities more than 100 times higher. This summary of fillers encourages one to imagine many possibilities for remarkable properties within the broad materials class of polymer nanocomposites.

The first key demonstration of polymer nanocomposites was provided by the pioneering work of Okada and co-workers at Toyota Central Research in the late 1980s.[1–4] By combining inclusion and colloidal chemistry of mica-type layered silicates (nanoclay) with surface-initiated

Table I: Characteristics of Traditional and Nanoscale Fillers: Shape, Size, Properties, Dimensions, and Uses.

	Approximate Shape[a]	Smallest Dimension (nm)[a]	Aspect Ratio[b]	Elastic Modulus (GPa)	Electrical Conductivity (S/cm)	Thermal Conductivity (W/m K)	Commercial Uses
Traditional Fillers							
Carbon black[32]	agglomerate of spheres	10–100	1–5	…	10–100	0.1–0.4	tires, hoses, shoes, elastomers
Carbon fiber[33]	rods	5,000–20,000	10–50	300–800	0.1–10	100–1000	aerospace, automotive, marine, sporting, medical
Carbon graphite[34]	plate	250–500	15–50	500–600	1–10	100–500	gaskets, seals
E-glass[35]	rod	10,000–20,000	20–30	75	…	…	marine, automotive, construction, filtration
Mineral: $CaCO_3$[36]	sphere platelet	45–70 600–4,000	~1 1–30	35	…	3–5	paper, paint, rubber, plastics
Mineral: silica[37,38]	agglomerate of spheres	8,000–30,000	5–10	30–200	…	1–10	reinforced plastics, thermal insulator, paint, rubber reinforcing agent
Mineral: talc, china clay[37,39]	platelet	5,000–20,000	5–10	1–70	…	1–10	paper, consumer goods, construction
Nanoscale Fillers							
Carbon nanofiber[40]	rod	50–100	50–200	500	700–1000	10–20	hoses, aerospace, ESD/EMI shielding, adhesives
Carbon MWNT[41]	rod	5–50	100–10,000	1,000	500–10,000	100–1000	automotive, sporting, ESD/EMI shielding
Carbon SWNT[42]	rod	0.6–1.8	100–10,000	1,500	1000–10,000	1000	filters, ESD/EMI shielding
Aluminosilicate nanoclay[43]	plate	1–10	50–1000	200–250	…	1–10	automotive, packaging, sporting, tires, aerospace
Nano-TiO_2[37,44]	sphere	10–40	~1	230,000	10^{-11}–10^{-12}	12	photocatalysis, gas sensors, paint
Nano-Al_2O_3[37,45]	sphere	300	~1	50	10^{-14}	20–30	seal rings, furnace liner tubes, gas laser tubs, wear pads

[a] Dispersible unit.
[b] Aspect ratio is defined as the long axis to short axis irrespective of shape. Note that this differs from Figure 1.
ESD is electrostatic discharge; EMI is electromagnetic interference; MWNT is multiwall carbon nanotube; SWNT is single-wall carbon nanotube.

polymerization, they demonstrated that only ~2–4 vol% of layered silicate sufficiently improved the mechanical properties of nylon-6 polymer at elevated temperatures to enable its use inside an automotive engine compartment.

Since then, the patent and literature activity has been astonishing (Figure 2).[15] From 1992 to 2004, the number of citations for polymer nanocomposites has doubled every two years, indicating that these materials are still on the steep part of the technology S-curve (Figure 2a). Since 2001, polymer nanocomposites represent ~43% of the broader nanocomposite field, which includes metals, ceramics, and thin films (Figure 2b). Of the publicly available literature on polymer nanocomposites, the majority (80%) is in peer-reviewed journals, whereas patents have maintained a constant fraction (8–10%). Together, layered silicates (nanoclays) and carbon nanotubes represent almost 50% of the ongoing investigations. Polymer–clay nanocomposites, however, might be reaching saturation, as evidenced by a diminishing growth rate in publications and patents per year. In contrast, polymer–carbon nanotube composites have rapidly accelerated since the availability of carbon nanotubes became widespread in the late 1990s and are still exhibiting a steady growth rate (Figure 2b).

After almost 20 years, the diversity in scientific investigations, technology advancements, processing innovations, and product development is staggering. A significant number of excellent review papers (e.g., clays[16–23] and carbon nanotubes[22–26]) and books[27–30] are available that chronicle and summarize the status of various nanoparticle–polymer combinations and the broad scientific and technological challenges that still need to be overcome.

This issue of *MRS Bulletin* provides six articles to illustrate the breadth of activity in polymer nanocomposites. Hunter et al. highlight the issues in polymer–nanoclay composites, where the most commercial activity currently exists. Baur and Silverman consider the opportunities in adding nanofillers to traditional engineering polymer composites that use continuous fiber reinforcements. Schadler and co-workers focus on the implications and engineering possibilities of larger interfacial areas per unit volume. Krishnamoorti addresses the issues of weak forces becoming significant for nano-sized components and strategies for overcoming their tendency to agglomerate. Winey et al. explore opportunities for nanofillers to modify electrical and thermal properties of polymers. Finally, Hule and Pochan consider the opportunities of polymer nanocomposites in the medical arena.

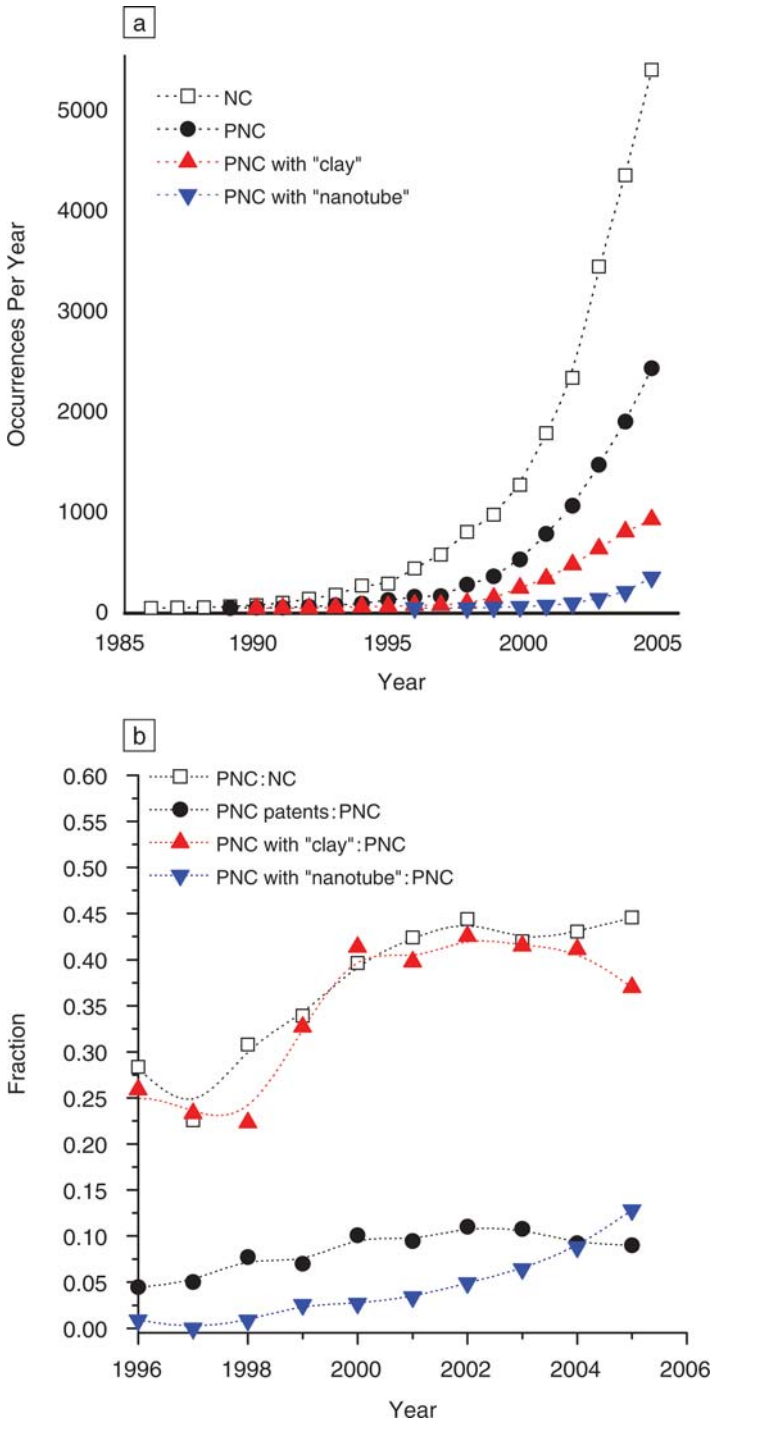

Figure 2. Growth trends of the polymer nanocomposite enterprise based on yearly publications catalogued in the CAPLUS and MEDLINE databases of the American Chemical Society.[15] (a) Number of occurrences per year of the term "nanocomposite" (NC, open squares) and "nanocomposite" appearing with "polymer" (PNC, solid circles). "Polymer nanocomposites" (PNC) is further refined to those discussing "clay" PNC (red symbols) and "nanotube" PNC (blue symbols). (b) Analysis of the number of citations per year, showing the total fraction of "nanocomposite" occurrences that discuss polymer nanocomposites (PNC:NC, open squares), as well as the total fraction of "polymer nanocomposite" occurrences that are patents (PNC patents, solid circles) that discuss clay-based PNCs (PNC with "clay," red symbols) and that discuss nanotube-containing PNCs (PNC with "nanotube," blue symbols).

Future Outlook

What's next? Where are the groundbreaking opportunities? What are the challenges that pervade polymer nanocomposites? Of extreme importance in all the potential markets is the establishment of a better, quantitative understanding of the occupational health risks.[31] For polymer nanocomposites, this is particularly important during the production of nanosized fillers and composite fabrication, as well as during recycling, incineration, or combustion.

Whereas the recent increased availability of the new nanoscale fillers has been a major contributor to the rapid development of polymer nanocomposites, robust structure–property–processing relationships are critical to further market infiltration. Relationships that provide *a priori* predictions of macroscopic properties for a given polymer, a specific nanoscale filler (or fillers), and a particular spatial arrangement of the filler are still in their infancy. For example, to what extent can existing continuum composite theories be modified to account for the implications that arise when the filler is comparable to the polymer in size? Are the properties currently being achieved in polymer nanocomposites as high as we can expect to obtain?

However, approaches to these challenges are not without precedent. The underlying science and constitutive relationships for these nanoscopic materials should share commonality with collections of nanoscopic polymer chains, whose framework has been developed through nearly a century of chemistry and physics and is the foundation of the global polymer industry. Future developments toward the full potential of nanoscale multicomponent polymer blends rely on these previous insights to tackle the ambiguities associated with smaller filler sizes, where the distinction between filler and polymer fade into filler-molecules and polymer-molecules.

Economically, given the current diversity in nanoparticle cost (carbon black and montmorillonite versus single-wall carbon nanotubes), two approaches are developing based on potential markets. The lower-cost nanoparticles provide competition to traditional filler technologies and have important advantages in commodity applications, whereas the higher-cost nanoparticles target higher-value industrial sectors such as medical and electronics. Rather than replacing existing materials and traditional filled plastics, a common business strategy is to develop new applications based on the uniqueness of polymer nanocomposites, such as shape-memory materials for morphing aircraft, self-passivating films for satellites, and piezoresistive materials for MEMs-based sensors. In addition, new processing tools and on-line controls are being developed to either (1) uniformly distribute nanofiller to produce homogeneous bulk properties or (2) spatially vary the nanofiller concentration to meet specific design criteria. One might refer to these two classes of polymer nanocomposites as nano-"filled" systems and nano-"composite" systems, respectively. By drawing inspiration from biology and engineered fiber-reinforced composites, polymer nanocomposites with spatially controlled morphology are beginning to provide viable options to critical components of active devices, such as fuel cell membranes, batteries, photovoltaics, sensors, and actuators.

Polymer nanocomposites have recently become part of established modern technologies, but the most significant accomplishments of these materials are still ahead of us. As an increasing number of scientists and engineers contribute to the understanding of polymer nanocomposites, what remains to be seen is which products will be critically enhanced and enabled by this broad and evolving class of materials.

Acknowledgments

The authors thank Minfang Mu (University of Pennsylvania) for compiling the data for Table I. K.I. Winey thanks Dupont for hosting her sabbatical visit and acknowledges funding from NSF-DMR-MRSEC-05–20020. R.A. Vaia thanks the Materials Research Laboratory at the University of California, Santa Barbara, for hosting his sabbatical visit.

References

1. Y. Fukushima, S. Inagaki, *J. Inclusion Phenom.* **5,** 473 (1987).
2. Y. Fukushima, A. Okada, M. Kawasumi, T. Kurauchi, O. Kamigaito, *Clays Clay Miner.* **23**, 27 (1988).
3. A. Usuki et al., *J. Mater. Res.* **8,** 1174 (1993).
4. Y. Kojima et al., *J. Mater. Res.* **8**, 1185 (1993).
5. R.A. Vaia, H. Ishii, E.P. Giannelis, *Chem. Mater.* **5**, 1694 (1993).
6. T.P. Lan, T.J. Pinnavaia, *Chem. Mater.* **6**, 2216 (1994).
7. A. McWilliams, "Nanocomposites, Nanoparticles, Nanoclays, Nanotubes" (NANO21C, BCC Research, Norwalk, CT, 2006).
8. "Polymer Nanocomposites Create Exciting Opportunities in the Plastics Industry" (Principia Partners, Jersey City, NJ, 2005).
9. A.M. Thayer, *Chem. Eng. News* **78,** 36 (October 16, 2000).
10. R.A. Vaia, E.P. Giannelis, *MRS Bull.* **26**, 394 (2001).
11. R.A. Vaia, H.D. Wagner, *Mater. Today* **7**, 32 (November 2004).
12. A. Bansal, H. Yang, C. Li, K. Cho, B.C. Benicewicz, S.K. Kumar, L.S. Schadler, *Nature Materials* **4,** 693 (2005).
13. R. Krishnamoorti, R.A. Vaia, E.P. Giannelis, *Chem. Mater.* **9**, 1728 (1996).
14. F.W. Starr, T.B. Schroeder, S.C. Glotzer, *Macromolecules* **35,** 4481 (2002).
15. SciFinder, Chemical Abstract Service (CAS) of the American Chemical Society, CAPLUS and MEDLINE databases, October 8, 2006. Data resulted from a keyword search on "nanocomposite" and selecting citations that included this concept (25,435 total citations). Results were refined using "polymer" (10,350 total citations), "nanotube or nanorod" (864 total citations), or "clay or (layered silicate) or montmorillonite" (3,938 total citations). Other keyword combinations did not drastically modify the refined number of citations (<2–3%).
16. E.P. Giannelis, *Adv. Mater.* **8**, 29 (1996).
17. M. Alexandre, P. Dubois, *Mater. Sci. Eng., R* **28**, 1 (2000).
18. S.S. Ray, M. Okamoto, *Prog. Polym. Sci.* **2**, 1539 (2003).
19. M. Okamoto, "Polymer/Clay Nanocomposites," in *Encyclopedia of Nanoscience and Nanotechnology*, H.S. Nalwa, Ed. (American Scientific, Stevenson Ranch, CA, 2004), vol. 8, p. 1.
20. E.T. Thostenson, C. Li, T.-W. Chou, *Compos. Sci. Technol.* **65**, 491 (2005).
21. L.F. Drummy, H. Koerner, B.L. Farmer, R.A. Vaia, *Advanced Morphology Characterization of Clay-Based Polymer Nanocomposites: CMS Workshop Lecture Series* (Clay Minerals Society, Chantilly, VA, 2006) vol. 14.
22. S.C. Tjong, *Mater. Sci. Eng., R* **53**, 73 (2006).
23. F. Hussain, M. Hojjati, M. Okamoto, R.E. Gorga, *J. Compos. Mater.* **40,** 1511 (2006).
24. X.-L. Xie, Y.-W. Maia, X.-P. Zhou, *Mater. Sci. Eng., R* **49**, 89 (2005).
25. M. Moniruzzaman, K.I. Winey, *Macromolecules (Review)* **39**, 5194 (2006).
26. T.J. Pinnavaia, G.W. Beall, *Polymer-Clay Nanocomposites* (Wiley, New York, 2001).
27. R. Krishnamoorti, R.A. Vaia, Eds., *Polymer Nanocomposites: Synthesis, Characterization, Modeling* (ACS Symposium Series, American Chemical Society, Washington, DC, 2001).
28. S.S. Ray, M. Bousmina, *Polymer Nanocomposites and Their Applications* (American Scientific, Stevenson Ranch, CA, 2006).
29. Y.-W. Mai, Z.-Z. Yu, Eds., *Polymer Nanocomposites CRC* (Woodhead Publishing, Cambridge, UK, 2006).
30. A.B. Morgan and C.A. Wilkie, Eds., *Flame Retardant Polymer Nanocomposites* (Wiley, New York, 2007).
31. "Environmental, Health and Safety Needs for Engineered Nanoscale Materials" (Committee on Technology, National Science and Technology Council, Washington, DC, 2006; www.nano.gov).
32. J.-B. Donnet, R.C. Bansal, M.-J. Wang, *Carbon Black* (Marcel Dekker, New York, ed. 2, 1993); J.C. Grunlan, W.W. Gerberich, L.F. Francis, *Polym. Eng. Sci.* **41**, 1947 (2001).
33. J.-B. Donnet, T.K. Wang, S. Rebouillat, J.C.M. Peng, *Carbon Fibers* (Marcel Dekker, New York, ed. 3, 1998; www.apsci.com/home.html).
34. A. Yasmin, I.M. Daniel, *Polymer* **45**, 8211 (2004); D.D.L. Chung, *J. Mater. Sci.* **37**, 1475

(2002); J.M. Keith, C.D. Hingst, M.G. Miller, J.A. King, R.A. Hauser, *Polym. Compos.* **27**, 1 (2006).
35. D.P.N. Vlasveld, P.P. Parlevliet, H.E.N. Bersee, S.J. Picken, *Composites Part A* **36**, 1 (2005); A. Pegormti, L. Fambfu, C. Migliaresi, *Polym. Compos.* **21**, 466 (2000).
36. K. Yang et al., *Polym. Comp.* **27**, 443 (2006); M. Lei et al., *J. Cryst. Growth* **294**, 358 (2006); T. Ding, E.S. Daniels, M.S. El-Aasser, A. Klein, *J. Appl. Polym. Sci.* **100**, 4550 (2006); E. Ramachandran, P. Raji, K. Ramachandran, S. Natarajan, *Cryst. Res. Technol.* **41**, 64 (2006).
37. C. Clauser, E. Huenges, in *Rock Physics and Phase Relations: A Handbook of Physical Constants* (American Geophysical Union, Washington, DC, 1995) p. 105.
38. L. Brabec et al., *Microporous Mesoporous Mater.* **94**, 226 (2006); I. Hackman, L. Hollaway, *Composites Part A* **37**, 1161 (2006).
39. V. Svehlova, E. Poloucek, *Angew. Makromol. Chem.* **214**, 91 (1994); E. Bailey, J.R. Holloway, *Earth. Planet. Sci. Lett.* **183**, 487 (2000); A. Kirak, H. Yilmaz, S. Guler, C. Guler, *J. Phys. D: Appl. Phys.* **32**, 1919 (1999).
40. Applied Sciences Inc. Home Page, http://www.apsci.com/home.html; H.Y. Ng, X. Lu, S.K. Lau, *Polym. Compos.* **26**, 66 (2005); C. Yu et al., *Trans. ASME* **128**, 234 (2006); J. Zeng et al., *Composites Part B* **35**, 245 (2004); T. Morita, H. Inoue, Y. Suhara, U.S. Patent 6,565,971 (May 20, 2003).
41. J. Zeng et al., *Composites Part B* **35**, 245 (2004); NanoLab Home Page, www.nano-lab.com/nanotubes-research-grade.html; M.-K. Yeh, N.-H. Tai, J.-H. Liu, *Carbon* **44**, 1 (2006); M. Fujii et al., *Phys. Rev. Lett.* **95**, 065502 (2005); T.W. Ebbesen et al., *Nature* **382**, 54 (1996).
42. E. Bichoutskaia, M.I. Heggie, A.M. Popov, Y.E. Lozovik, *Phys. Rev. B* **73**, 045435 (2006); S. Berber, Y.-K. Kwon, D. Tománek, *Phys. Rev. Lett.* **84**, 4613 (2000); U. Dettlaff-Weglikowska et al., *J. Am. Chem. Soc.* **127**, 5125 (2005).
43. H.S. Jeona, J.K. Rameshwarama, G. Kimb, D.H. Weinkauf, *Polymer* **44**, 5749 (2003); Y.-P. Wu, Q.-X. Jia, D.-S. Yu, L.-Q. Zhang, *Polym. Test.* **23**, 903 (2004); V.V. Murashov, *J. Phys.: Condens. Matter.* **11**, 1261 (1999); T.J. Pinnavaia, G.W. Beall, *Polymer-Clay Nanocomposites*, Wiley Series in Polymer Science (Wiley, New York, 2001).
44. S. Amarchand, T.R. Rama Mohan, P. Ramakrishnan, *Adv. Powder Technol.* **11**, 415 (2000); R.J. Fleming et al., *IEEE Trans. Dielectrics and Electrical Insulation* **12**, 745 (2005); The A to Z of Materials Home Page, www.azom.com/details.asp?ArticleID1179.
45. High Precision Machining of Hard Materials, Insaco Inc. Home Page, www.insaco.com/home.asp. □

Karen I. Winey

Richard A. Vaia

Jeff Baur

Brian C. Benicewicz

Shane E. Harton

Karen I. Winey, Guest Editor for this issue of *MRS Bulletin*, is a professor of materials science and engineering at the University of Pennsylvania. She earned her BS degree in materials science and engineering from Cornell University and her MS and PhD degrees in polymer science and engineering from the University of Massachusetts under the direction of Edwin L. Thomas.

Winey probes structure–property relationships in nanotube–polymer composites, ion-containing polymers, and block copolymers, where the properties of interest include electrical conductivity, thermal conductivity, mechanical properties and permeability. She received an NSF Young Investigator Award in 1994 and was elected fellow of the American Physical Society in 2003. Winey is currently chair of the Polymer Physics Gordon Research Conference scheduled for 2010. She recently published an invited review article entitled "Polymer Nanocomposites Containing Carbon Nanotubes" in *Macromolecules* (**39**, 5194–5205, 2006).

Winey can be reached at 3231 Walnut St., University of Pennsylvania, Philadelphia, PA 19104-6272, USA; tel. 215-898-0593, fax 215-573-2128, and e-mail winey@seas.upenn.edu.

Richard A. Vaia, Guest Editor for this issue of *MRS Bulletin*, is the lead of the NanoMaterials Strategy Group and chair of the NanoScience and Technology (NST) Strategic Technology Team at the U.S. Air Force Research Laboratory (AFRL). He received his PhD degree in materials science and engineering at Cornell University in 1995 and was a distinguished graduate from Cornell's Air Force ROTC.

Vaia's research group focuses on polymer nanocomposites, photonic technologies, and their impact on developing adaptive soft matter. His honors and awards include Air Force Outstanding Scientist (2002); MRL Visiting Professor at the University of California, Santa Barbara (2006); Air Force Office of Scientific Research Star Team (2003–2005, 2005–2007), and the Outstanding Engineers and Scientists Award (2006) from the Affiliate Societies Council of Dayton, Ohio. Vaia serves on the editorial boards of *Chemistry of Materials*, *Macromolecules*, and *Materials Today*. He is on the MRS board of directors, and is a member-at-large for the Division of Polymeric Materials Science and Engineering of the American Chemical Society. He has authored more than 100 papers and patents.

Vaia can be reached at the Air Force Research Laboratory, 2941 Hobson Way, Bldg. 654, Wright-Patterson Air Force Base, OH 45433-7750 USA; tel. 937-255-9184, fax 937-255-9157, and e-mail richard.vaia@wpafb.af.mil.

Jeff Baur is a senior research engineer for the Advanced Composites Branch within the Air Force Research Laboratory's Materials and Manufacturing Directorate. His received his PhD degree from the Massachusetts Institute of Technology's program in polymer science and technology in 1997.

Baur has held research and management positions within the Air Force Research Lab, Borden Chemical UV Coating Division, and at MIT's Institute for Soldier Nanotechnologies, and has published numerous papers in advanced electrical, optical, and mechanical properties of polymer composites. His current interests are in nanocomposites for improvement of fiber-reinforced

Rohan A. Hule

Douglas L. Hunter

Karl W. Kamena

Takashi Kashiwagi

Ramanan Krishnamoorti

composite structures and materials for morphing structures.

Baur can be reached at AFRL/MLBCO, 2941 Hobson Way, Wright-Patterson Air Force Base, OH 45433-7750 USA; tel. 937-255-9143, fax 937-656-4706, and e-mail jeff.baur@wpafb.af.mil.

Brian C. Benicewicz is director of the New York State Center for Polymer Synthesis and a professor of chemistry at Rensselaer Polytechnic Institute in Troy, N.Y. He received his BS degree from the Florida Institute of Technology in 1976 and his PhD degree in polymer chemistry from the University of Connecticut in 1980.

Benicewicz held positions at Celanese Research Co. and at Johnson & Johnson and was the deputy group leader at Los Alamos National Laboratory before joining Rensselaer in 1997. His research focuses on polymer nanocomposites, controlled radical polymerizations, fuel cell membranes, liquid-crystalline and electrically conducting polymers, and polymer synthesis.

Benicewicz can be reached at the Department of Chemistry and Chemical Biology, Rensselaer Polytechnic Institute, 110 Eighth St., Troy, NY 12180 USA; tel. 518-276-2534, fax 518-276-6434, and e-mail benice@rpi.edu.

Shane E. Harton is a postdoctoral research scientist in the Department of Chemical Engineering at Columbia University, working with Sanat K. Kumar. Harton received his PhD degree in materials science and engineering from North Carolina State University in 2005 under the advisement of Harald Ade.

As a graduate student, Harton's work primarily focused on thermodynamics of highly incompatible polymer/polymer interfaces, particularly the influences of the deuterium isotope effect. Harton's current work at Columbia University focuses on thermodynamics of polymer/inorganic interfaces, including compatibilization of polymer/inorganic nanocomposites.

Harton can be reached at the Department of Chemical Engineering, Columbia University, 500 W. 120th St., New York, NY 10027 USA.

Rohan A. Hule is a graduate student in the Department of Materials Science and Engineering and the Delaware Biotechnology Institute at the University of Delaware. After earning his BTech degree in polymer science and engineering from the University Institute of Chemical Technology in Mumbai, India, Hule studied rheology in the Complex Fluids and Polymer Engineering Group at the National Chemical Laboratory in Pune.

Hule's current research focuses on organic–inorganic hybrid nanomaterials, self-assembled hydrogels, and understanding structure–property relationships in bionanomaterials using polymer physics tools.

Hule can be reached by e-mail at hule@udel.edu.

Douglas L. Hunter is a senior scientist at Southern Clay Products Inc. (SCP), where he has worked since 1997. He earned his PhD degree in chemistry at Texas A&M University. Prior to SCP, he worked at Dow Chemical Co., beginning in 1975. At Dow, Hunter held a variety of positions working in early-stage catalyst and process development and technical service. The focus of his research at SCP has been polymer clay nanocomposites.

Hunter can be reached at Southern Clay Products, 1212 Church St., Gonzales, TX 78629 USA; tel. 830-672-1994 and e-mail dhunter@scprod.com.

Karl W. Kamena is the commercial manager of Cloisite® Nanoclays at Southern Clay Products Inc. He graduated from the University of Massachusetts in 1965 with a degree in chemical engineering.

Kamena worked with Dow Chemical Co. from 1965 to 1994 in a variety of technical and commercial positions. His experience at Dow ranged from product development and project management to business, marketing, public policy issues management, and government affairs. During the past ten years, Kamena has been involved with clay/polymer nanocomposite technologies in consulting capacities and working with companies. He is a member of the Society of Plastics Engineers.

Kamena can be reached at Cloisite® Nanoclays, 5508 Hwy. 290 West, Ste. 206, Austin, TX 78735 USA; tel. 512-358-3108, fax 512-899-2332, and e-mail kkamena@scprod.com.

Takashi Kashiwagi is a research professor in the Fire Protection Engineering Department of the University of Maryland and a guest researcher at the Fire Research Division of the National Institute of Standards and Technology. Kashiwagi earned his BS and MS degrees from Keio University and his PhD degree from Princeton University in aerospace mechanical science. His research interests include combustion of polymeric materials and flammability properties of polymer nanocomposites.

Kashiwagi can be reached at NIST, MS 8665, 100 Bureau Dr., Gaithersburg, MD 20899-8665 USA; tel. 301-975-6699, fax 301-975-4052, and e-mail takashi.kashiwagi@nist.gov.

Ramanan Krishnamoorti is a professor of chemical and biomolecular engineering and a professor of chemistry at the University of Houston (UH). After earning his PhD degree in chemical engineering from Princeton University in 1994, he held postdoctoral positions at the California Institute of Technology and Cornell University.

Krishnamoorti joined UH as an assistant professor in 1996 and was promoted to professor and appointed associate


Sanat K. Kumar


Sarah L. Lewis


Minfang Mu


Donald R. Paul


Darrin J. Pochan

dean for research in 2005. His primary research area is in the understanding of structure–processing–property relations for multicomponent polymeric materials, with recent extensions into biomaterials for drug delivery and the development of high-performance ceramic materials.

Krishnamoorti can be reached at the Department of Chemical Engineering, University of Houston, 4800 Calhoun Rd., Houston, TX 77204-4004 USA; tel. 713-743-4312, fax 713-743-4323, and e-mail ramanan@uh.edu.

Sanat K. Kumar is a professor in the Chemical Engineering Department at Columbia University. He received his BS degree from the Indian Institute of Technology, Madras, in 1981 and his PhD degree from the Massachusetts Institute of Technology in 1987. Kumar has held faculty positions at the Pennsylvania State University and Rensselaer Polytechnic Institute.

His research focuses on synthetic and bio polymers, nanocomposites, and nanomaterials. His work impacts the fields of biochemical engineering, composite materials, interfacial phenomena, nanotechnology, and polymers.

Kumar can be reached at the Department of Chemical Engineering, Columbia University, 500 W. 120th St., New York, NY 10027 USA; tel. 212-854-2193, fax 212-854-3054, and e-mail sk2794@columbia.edu.

Sarah L. Lewis is pursuing her PhD degree in materials science and engineering at Rensselaer Polytechnic Institute in Troy, N.Y. She received her MS degree in materials science and engineering from Lehigh University in 2003 and her BSc degree in biomedical materials science from the University of Manchester Institute of Science and Technology in 2001. Her research interests are in controlling and predicting properties in polymer nanocomposites.

Lewis can be reached at the Department of Materials Science and Engineering, Rensselaer Polytechnic Institute, 110 Eighth St., Troy, NY 12180 USA; tel. 518-276-3011, fax 518-276-8554, and e-mail lewiss@rpi.edu.

Minfang Mu is a PhD degree candidate in the Department of Materials Science and Engineering at the University of Pennsylvania. She received her BSc degree in chemistry and her MSc degree in the Department of Macromolecular Science at Fudan University, China. At Fudan University, Mu worked with Ming Jiang on self-assembly of protein-*graft*-dextran and polymer complexes. Currently, she is working on the diffusion behavior of polymers into carbon nanotube/polymer nanocomposites, as well as the preparation and characterization of composites with cellular nanotube networks.

Mu can be reached at the University of Pennsylvania, 3231 Walnut St., Philadelphia, PA 19104-6272, USA; tel. 215-898-2700 and e-mail minfang@seas.upenn.edu.

Donald R. Paul holds the Ernest Cockrell Sr. Chair in Engineering at the University of Texas at Austin and also is the director of the Texas Materials Institute. He joined the Department of Chemical Engineering at UT in 1967. Paul's research interests include polymer blends, membranes, processing, and nanocomposites. He was elected to the National Academy of Engineering in 1988 and to the Mexican Academy of Sciences in 2000, and has served as editor of *Industrial and Engineering Chemistry Research*, published by the American Chemical Society, since 1986.

Paul can be reached at the Department of Chemical Engineering, University of Texas at Austin, Austin, TX 78712 USA; tel. 512-471-5392, fax 512-471-0542; and e-mail drp@che.utexas.edu.

Darrin J. Pochan is an associate professor in the Materials Science and Engineering Department and the Delaware Biotechnology Institute at the University of Delaware. He joined the department in 1999 after earning his PhD degree in polymer science and engineering at the University of Massachusetts Amherst and having an NRC postdoctoral fellowship at the National Institute of Standards and Technology.

At the University of Delaware, Pochan has developed a research program around the construction of new materials and nanostructures via molecular self-assembly mechanisms. His recent honors include an NSF Career Award, the DuPont Young Faculty Award, and the Dillon Medal from the American Physical Society. Pochan also serves as associate editor for North America of *Soft Matter*, a new interdisciplinary journal from the Royal Society of Chemistry.

Pochan can be reached by e-mail at pochan@udel.edu.

Linda S. Schadler is a professor in materials science and engineering at Rensselaer Polytechnic Institute. She graduated from Cornell University in 1985 with a BS degree in materials science and engineering and received a PhD degree in materials science and engineering in 1990 from the University of Pennsylvania. Schadler joined Rensselaer in 1996.

She is a current member of the National Materials Advisory Board, and in addition to her research focus on interfaces in nanocomposites, she is the education and outreach coordinator for the NSF-funded Center for Directed Assembly of Nanostructures, headquartered at Rensselaer.

Schadler can be reached at the Department of Materials Science and Engineering, Rensselaer Polytechnic Institute, 110 Eighth St., Troy, NY 12180 USA; tel. 518-276-2022, fax 518-276-8554, and e-mail schadl@rpi.edu.

Linda S. Schadler

Edward Silverman

Edward Silverman is the advanced technology manager for advanced materials development at Northrop Grumman Space Technology. He holds a BE degree in chemical engineering from City College of New York and a PhD degree in chemical engineering from Stanford University.

Silverman has led the development of new lightweight composite resin transfer-molded joints, isogrid reflectors, and the thermally conductive material APG (annealed pyrolytic graphite). As the program manager of two NASA contracts, he compiled two handbooks on design guidelines for composite spacecraft components and on space environment effects on spacecraft materials. Silverman's current interest includes the development of nanotechnology for aerospace applications. He has published more than 50 papers in scientific journals and conferences and has received several awards for innovative research and development.

Silverman can be reached at Northrop Grumman Space Technology, One Space Park, M/S 01/2040, Redondo Beach, CA 90278 USA; tel. 310-813-9374, fax 310-812-8768, and e-mail edward.silverman@ngc.com. □

Processing and Properties of Polymers Modified by Clays

Douglas L. Hunter, Karl W. Kamena, and Donald R. Paul

Abstract

Layered smectite nanoclays are being developed for incorporation into a variety of host polymer systems. Nanoscopic phase distribution can impart enhanced stiffness at low addition levels and improve barrier and flame-retardant properties. When combined with other inorganic and organic modifiers, nanoclays can provide synergies to generate the desired formulation properties and cost/performance characteristics. Developments with existing nanoclay products using conventional amine chemistries are described for thermoplastic, thermoset, and rubber formulations. Nanoclays are demonstrating unique, multidimensional performance and processing capabilities. Commercial applications are emerging in a variety of diverse markets ranging from automotive to packaging.

Nanoclays and Host Polymers

"Nanoclay" is a term often used when referring to a clay mineral with a phyllosilicate or sheet structure having dimensions on the order of 1 nm in thickness. The mineral base can be natural or synthetic and is hydrophilic. The clay surfaces can be modified with specific chemistries to render them organophilic and therefore compatible with organic polymers. When small quantities are added to a host polymer, the resulting product is often termed a clay–polymer nanocomposite.[1–5]

Host polymers can be thermoplastic or thermoset, commodity or engineering/specialty plastics, crystalline or amorphous. Nanocomposite preparation can be done at the monomer stage by using *in situ* polymerization (e.g., polyamides and thermosets), by solution-blending organoclays with polymers, by mixing polymer latices with aqueous suspensions of unmodified clays, and finally by melt-compounding organoclays with thermoplastics.

Nanoclay Sources, Structure, and Properties

Many nanoclays are based on a clay classified as montmorillonite[6–8] (Figure 1a), a natural clay mineral of the smectite family that traces its origins to volcanic ash deposited millions of years ago in ancient brine seas where it slowly underwent alteration processes. Although montmorillonite is found in vast deposits around the world, it is always found with impurities such as gravel, shale, limestone, quartz, and feldspar, among others. This mixture of materials is known as bentonite (Figure 1b), and the montmorillonite is separated from the raw ore primarily through aqueous separation processes. The unique characteristic of the smectite clay minerals, including montmorillonite, that sets them apart from other clay minerals is their ability to swell in water.

Montmorillonite is classified as magnesium aluminum silicate, and each individual platelet has a thin-foil morphology, as shown in Figure 1a. The platelets are irregular in overall shape, with aspect ratios generally in the 50–150 range. A side view of a platelet reveals a uniform thickness of 0.94 nm, resulting in an extremely large surface area of ~750 m^2/g.

Each montmorillonite platelet or sheet is a 2:1 layered structure consisting of silica tetrahedral layers bonded to an inner alumina octahedral layer, as illustrated in Figure 2 by a molecular model of a small portion of a platelet. Other metals such as magnesium or iron can replace some of the aluminum atoms in the octahedral layer, or aluminum can replace a silicon atom in the tetrahedral layer and establish a charge deficiency. The resulting negative charge on the surface will attract any positive ions (cations), such as calcium or sodium ions, to neutralize the charge.

The cations on the clay surface can be easily exchanged for other cations. A measure of this capacity is commonly referred to as the cation exchange capacity (CEC) and is usually expressed as milliequivalents of cations per 100 g of clay.

It should be understood that each montmorillonite deposit found in nature is unique. Particle size, shape, and charge are different, and the replacement elements and positioning in either the octahedral or tetrahedral layers can have a significant effect on the characteristics and performance of the specific montmorillonite. Also, the impurities composing the overall bentonite deposit can be very different; removing non-montmorillonite impurities is essential to the overall performance of

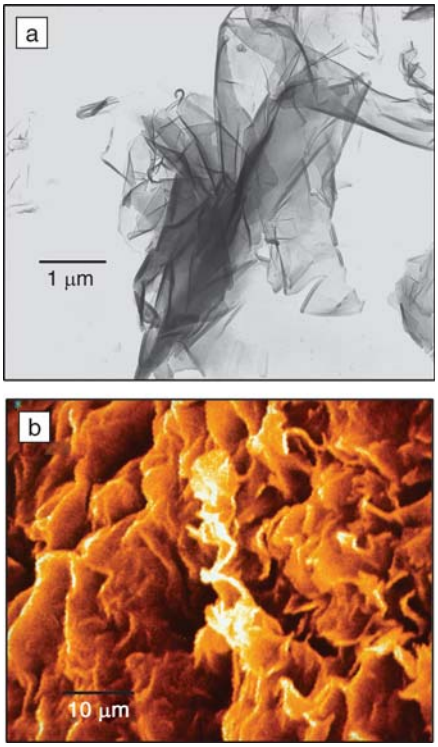

Figure 1. (a) Transmission electron microscopy image of refined montmorillonite. (b) Scanning electron microscopy image of bentonite rock.

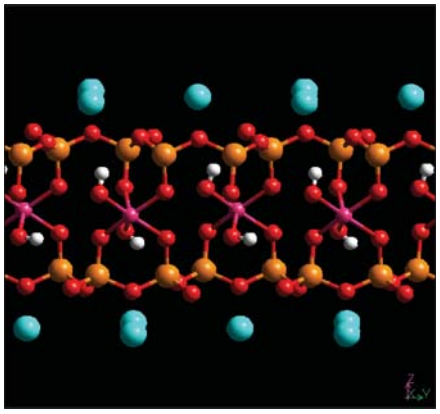

Figure 2. Molecular model of the edge of a montmorillonite platelet, showing the cations (e.g., Na^+ or Ca^{2+}) in blue, the silicon–oxygen tetrahedral layers in orange and red, and the aluminum–oxygen–hydroxyl octahedral layers in magenta, red, and white, respectively.

the montmorillonite in a nanocomposite, because impurities cannot be reduced to nanoscopic particle sizes.

The focus of this article is nanocomposites based on natural clay minerals, but synthetic nanoclays can also be used in nanocomposites. Synthetic clays may be prepared using a variety of chemical sources to provide the necessary elements such as silicon, oxygen, aluminum, magnesium, and others. Natural clays would appear to have an inherent raw material cost advantage, but the ability to control purity, charge density, and particle size is an appealing objective.

Nanoclay Chemistries and Functionalities

Unmodified, natural, and purified montmorillonite clays are extremely hydrophilic and fundamentally incompatible with hydrophobic organic polymers. The conventional way to prepare an organoclay is to replace the sodium ions on the surface of the sheets with an organic cation, often referred to as a surfactant, such as a quaternary ammonium salt (quat), as shown in Structure **1**. The pendant groups on the quat may be hydrogen atoms or methyl, benzyl, hydroxyethyl, or other groups with one or two relatively long alkyl tails (generally 16–22 carbons) derived from natural fatty acids like those from cocoa, tallow, rapeseed, and other oils. The ion exchange is typically done in a very dilute, purified aqueous solution. During the reaction, the clay loses its hydrophilicity and becomes oleophilic, at which point it precipitates from the aqueous phase and is filtered, dried, milled, and packaged.

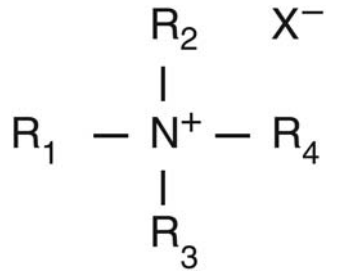

Structure **1**. General structure of a quaternary ammonium salt. R is an organic group and X is an anion.

The quat chemistry can be varied to produce dozens of organoclays. By modifying the surface polarity of the clay, the function of the ammonium ions is to thermodynamically alter the interaction with the polymer to assist in delamination of the clay platelets. Figure 3 shows molecular models of a typical organoclay according to early concepts[9] (Figure 3a) and more recent understanding (Figure 3b).[10]

In nonpolar polyolefin systems, a primary issue yet to be fully resolved is the identification of a chemistry (or combination of chemistries) that will provide a thermodynamic driving force for exfoliation. The most fruitful approaches have involved incorporating polarity into the polymer matrix by copolymerization, grafting, or blending; the most attractive option has been to use maleic anhydride–grafted polyolefins as compatibilizers in combination with a well-selected organoclay.

Another function of the quat chemistry is to weaken the inherent van der Waals forces attracting adjacent sheets of montmorillonite to facilitate delamination. Although it has been suggested that increasing the *d*-spacing between the sheets is desirable, empirical evidence would suggest a larger *d*-spacing is less important than improving compatibility between the polymer, the silicate surface, and the surfactant used to modify the clay.

Historically, nanoclays based on montmorillonite have been used in aqueous and organic solvent formulations to modify rheology in a thixotropic manner.[11] Typical application areas include paints and coatings, consumer care products, inks, ceramics and refractories, drilling fluids, greases, and polyester and epoxy composites. Because of montmorillonite's tremendous surface area of 750 m^2/g, just a few percent of completely dispersed platelets "solvate" in the liquid, creating a functional network and imparting the desired rheological properties to the system.

Preparation and Processing Considerations

Although nanocomposites can be prepared by a number of methods, much of the research and development activity leading to commercial interest is based on melt-compounding, for both manufacturing flexibility and economic considerations. Once the nanocomposite has been successfully prepared with good nanoclay dispersion and exfoliation, additional processing by normal extrusion and injection-molding methods are both applicable and may improve the efficiency of those downstream processing steps.

Preparing polyolefin-based nanocomposites is similar to preparing other types of nanocomposites but is more difficult because of the nonpolar nature of polyolefins and the lack of a thermodynamic driving force for exfoliation. Studies suggest that a combination of (1) chemistries used to

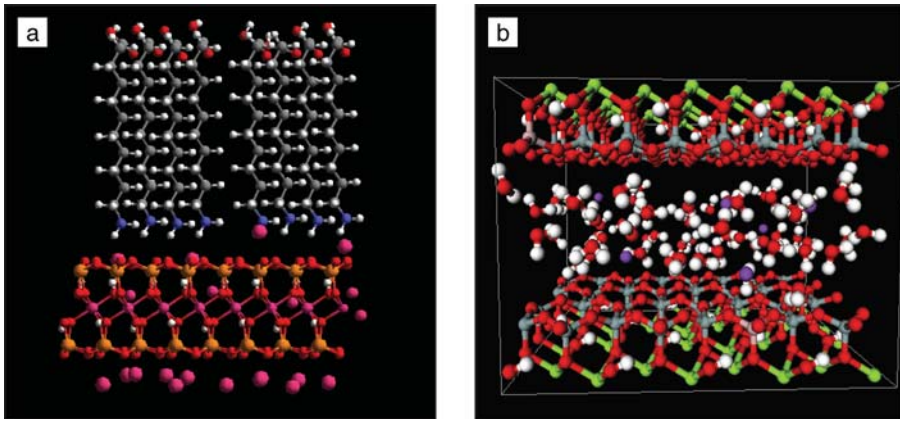

Figure 3. Two different models for organoclays. (a) Quaternary ammonium alkyl tails (gray) perpendicular to the platelet.[9] (b) More recent computer modeling shows the alkyl tails in a more random conformation between the platelets with some degree of entanglement.[10]

modify the clay surface, (2) compatibilizers such as maleated polypropylene, and (3) processing conditions will markedly increase the degree of dispersion and exfoliation of the nanoclay and thus enhance the properties and performance characteristics of the nanocomposites.

A nanoclay in its dry form consists of particles approximately 8–10 μm in diameter containing more than 1 million individual montmorillonite platelets. Conventional theory supposes that during the extrusion process, the polymer gradually enters the galleries between the platelets, and the distance between the platelets, the *d*-spacing, begins to expand until the van der Waals forces are overcome and the platelets are no longer linked together. We would propose,[12] however, that the exfoliation mechanism is more of a shearing process whereby hundreds or thousands of tactoids (particles that appear as spindle-shaped bodies under a polarizing microscope) composing the 8–10-μm particles are separated by a combination of mechanical and chemical forces, reducing them to smaller ribbons. Individual platelets peel from the ribbons to complete the exfoliation process. Figure 4a schematically illustrates this process, and Figures 4b and 4c show evidence for this mechanism from transmission electron microscopy (TEM) images taken in the early stages of exfoliation of an organoclay in a nylon-6 matrix.

For polypropylene-based nanocomposites, incorporation of maleated polypropylene into the formulation appears to aid in the dispersion and exfoliation process, apparently by acting as a compatibilizing agent with the clay edges, which are very different in character from the clay surfaces. The clay edges are also called broken-bond surfaces,[8] and, for example, the silica tetrahedral edge can have the functional groups $Si\text{-}O^-$, Si-OH, or Si^+, depending on pH.

As a general comment, during commercial scaleup of a thermoplastic polyolefin (TPO) nanocomposite product, we encountered a number of production issues, many of which were related to feeding a small amount of nanoclay (3–5% by weight of the bulk polymer) to attempt good distribution and dispersion. Clay agglomeration[13] can occur when clay particles are exposed to both increased temperature and pressure and can result during the feeding of nanoclay to make a nanocomposite. It can be a significant issue because agglomerates can account for a tremendous amount of individual clay platelets that cannot be exfoliated and benefit the overall polymer matrix. It must be stressed that when adding a small amount of nanoclay to a polymer, every step must be taken to maximize homogeneous distribution and microdispersion to facilitate the separation of tactoids and to ensure the proper temperature and pressure are attained to create shear conditions favoring exfoliation. We analyzed extruder screws for exfoliation by x-ray and TEM and showed that exfoliation occurs early in the extrusion process. When there is a strong enough affinity between the polymer and organoclay, this process may occur more or less spontaneously, given enough time; this is illustrated for Cloisite 93A[14] in PA6 held statically in a heated press under 69 MPa pressure for up to 120 min in Figure 5.

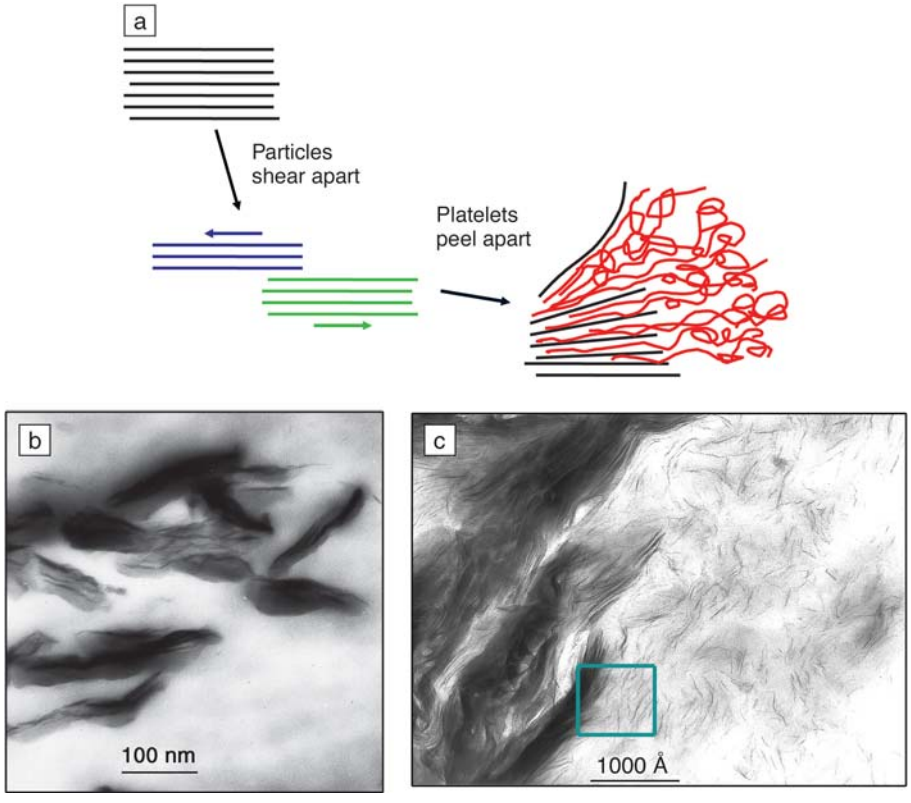

Figure 4. (a) Shearing-peeling mechanism for exfoliation of montmorillonite platelets in a polymer. Red ribbons are polymers penetrating between the platelets. (b), (c) Transmission electron micrographs showing evidence for the combination of (b) shearing tactoids to a consistent thickness and (c) peeling platelets off a tactoid. (Reprinted from Reference 12 with permission from Elsevier.)

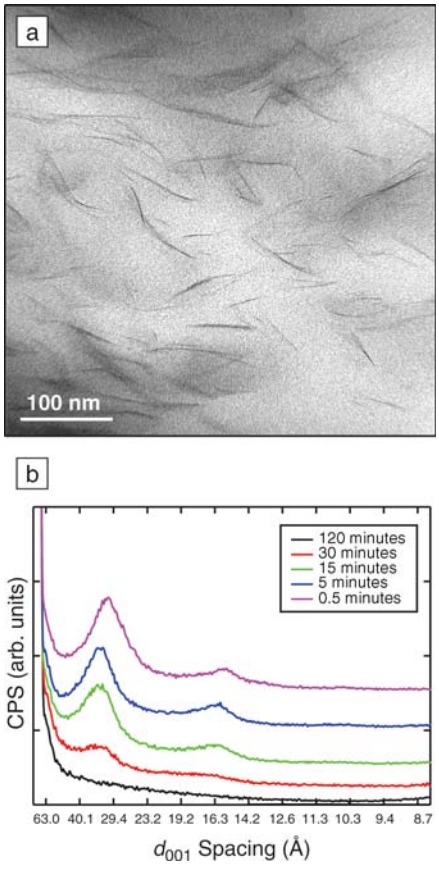

Figure 5. Evidence for static exfoliation of Cloisite 93A in PA6 as seen (a) by TEM and (b) by the evolution of x-ray scans with time in the melt. CPS is counts per second.

The process of moving from laboratory concept to production of commercial nanocomposites is beginning to become significant, especially as production engineers develop the necessary handling and processing parameters required to consistently prepare the same product.

Applications and Commercial Developments

In thermoset composites, nanoclays can be considered for a variety of functionalities, including improved syneresis control, improved dispersion of low-profile additives, decreased settling of fillers, improved surface appearance, improved processability, and better flow despite increased low shear rate viscosity. It would also appear that lower shrinkage can result, thereby enabling lower-density formulations. In transportation applications where the energy cost is particularly significant, lower mass can be an important benefit.

Interestingly, thermoset formulations have always been a combination of chemistries, fillers, additives, and curing agents, and nanoclays have been considered as one more synergistic ingredient to be used as a part of the whole. On the other hand, the development mindset in thermoplastics considers nanoclays as the single or primary inorganic additive. More recently, however, researchers are reporting developments based on synergy and combinations of additives. A producer of nylon products, for example, has commercialized a line of barrier resins that include nanoclay as the primary barrier and an active resin that serves as an oxygen scavenging agent; the two concepts work together to provide excellent barrier properties.

Similarly, early developments in the area of flame-retardant polymers focused on the use of nanoclays as the primary additive to impart flame-retardant performance to the host polymer. Products that have been commercialized or are in the late stages of the development process, however, employ a small amount of nanoclays (up to 5%) in combination with conventional additives such as magnesium hydroxide or aluminum trihydrate. Nanoclays promote extensive char formation, and the resulting synergies provide a flame-retardant polymer system with enhanced mechanical performance. Several companies are employing this approach in the wire and cable market.

A more conventional nanocomposite development has focused on TPO for automotive applications. Many organizations are in the process of developing clay/polyolefin nanocomposites with varying degrees of success. A number of commercial products have been introduced. While no one is yet claiming full exfoliation and complete technical success, competitive products are evolving, and newer and improved products are certain to emerge.

One example of an emerging product is from Basell Polyolefins, who, in conjunction with General Motors (GM) R&D and Southern Clay Products, has developed a line of nano-TPO resins. The first product was for a General Motors M-Van step assist in August 2001, and in February 2004, GM announced a second application, side trim moldings for their Impala line. This was quickly followed with additional trim and panel applications for the Hummer H2 sport utility vehicle. In each of these cases, the nanocomposite replaced a TPO formulation containing high loadings of talc. Figure 6 compares the relative efficiency of adding montmorillonite platelets versus talc particles for increasing modulus and reducing the coefficient of thermal expansion (CTE). It takes about four times more talc than montmorillonite to achieve the same level of property improvement.[15,16]

General Motors R&D has been a visible and active promoter of polyolefin as well as other types of nanocomposites. Their interest is based on a variety of factors:

- Mass savings
- Lower specific gravity
- Lighter weight, which requires less adhesive for attachment
- A large processing window
- Consistent physical and mechanical properties
- Elimination/reduction of "tiger striping" (a type of color defect in extruded or molded components)
- Improved appearance
- Improved knit line appearance
- Improved colorability and painting
- Sharper feature lines and grain patterns
- Improved scratch/mar resistance
- Low temperature ductility
- Improved recyclability

One of the more remarkable but perhaps unappreciated characteristics of nanoclays is their effect on improving the melt strength of thermoplastics. As is the case with thermosets, a higher melt strength of a given thermoplastic may enable the incorporation of other beneficial additives and, perhaps, unique processing techniques and parameters. One commercial product based on this property is nylon/glass fiber/nanoclay, which because of the higher melt strength of the formulation, can be blow-molded into large parts with high rigidity and strength.

An example of improved melt strength is shown in Figure 7, which shows the melt strength of linear low-density polyethylene (LLDPE) with Cloisite 20A. Again, it is seen that the addition of montmorillonite leads to an increase in melt tension, but a decrease in drawability. An optimal level of montmorillonite is about 1%. These results also show that as the ratio of linear low-density polyethylene grafted with maleic anhydride (LLDPE-*g*-MA) to Cloisite 20A is increased with the montmorillonite level held constant at ~4.7%, the melt strength increases because of the resulting improved exfoliation. A ratio of about 0.5 gives the best balance of drawability and melt tension.[17]

When nanoclay particles are added to a phase-separated polymer blend, the size of the dispersed phase can be dramatically reduced, as recently observed in blends of polypropylene,[15] polyamide,[18] and polystyrene[19] with elastomers. The rubber particle size in such blends is determined by a balance between the rates of droplet breakup and the coalescence of droplets; it has been proposed that the nanoclay particles interfere with the process of droplet coalescence such that smaller rubber particles are produced.[15,18] Rubber particle size is a key parameter in controlling toughness, and this effect of nanoclay

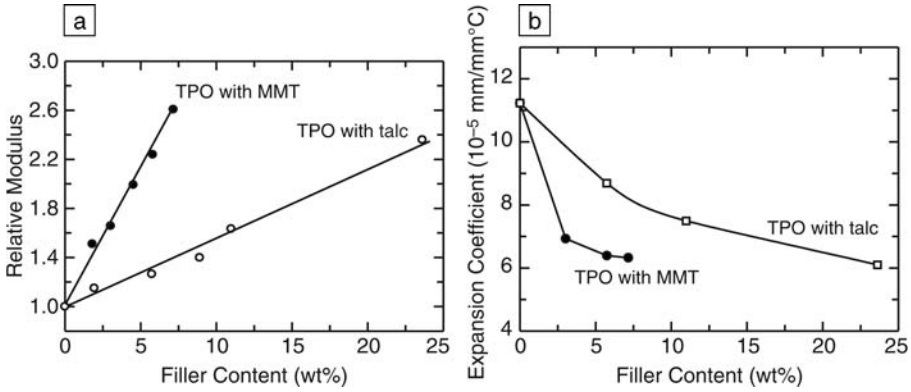

Figure 6. (a), (b) Comparison of the effect of adding montmorillonite (MMT) and talc to a thermoplastic olefin (TPO) on modulus and coefficient of thermal expansion. (Reprinted from References 15 and 16 with permission from Elsevier.)

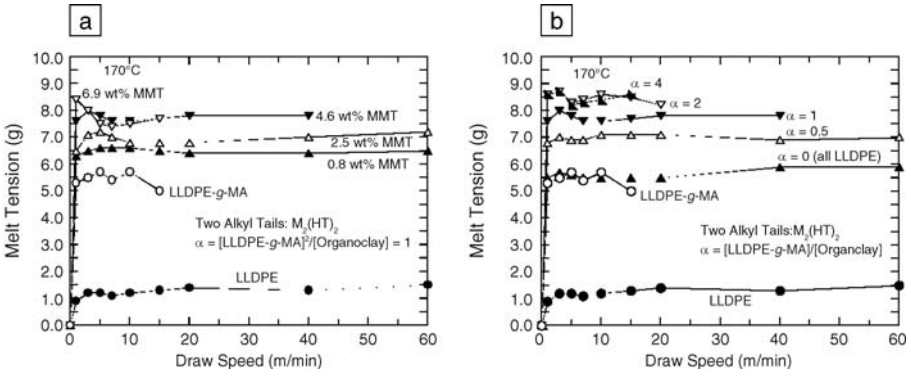

Figure 7. Melt strength for LLDPE nanocomposites containing Cloisite 20A. In (a), the amount of montmorillonite was varied at a fixed ratio of LLDPE-*g*-MA/Cloisite 20A, whereas in (b), the LLDPE-*g*-MA/Cloisite 20A ratio α was varied at a constant montmorillonite concentration of ~4.7%. (Reprinted from Reference 17 with permission from Elsevier.)

particles on polypropylene/rubber blends leads to a dramatic increase in toughness in such TPO materials.[15]

In addition to thermoset and thermoplastics, rubber formulations are being developed based on nanoclays in combination with other additives. As is the case with thermosets, rubber formulations are a complex recipe, and nanoclays are perceived more as synergistic additives than replacements.

ExxonMobil has announced improvements of about 35% in air impermeability of a tire inner liner by using less than 10 wt% organoclay in brominated isobutylene *p*-methylstyrene copolymers.[21] Some additional improvements are also possible if the improved air impermeability is taken advantage of by reducing the gauge of the inner liner; these advantages include reduced tire weight, lower tire operating temperature, and potential improvement in factory mixing and calendaring rates and potential cure time rates. These improvements to tire customers and the tire manufacturer are not possible by other compounding means.

Next-Generation Clay Nanocomposites

Although it is likely that additional nanocomposites will be developed and introduced as commercial products during the next several years, it is also apparent that conventional technologies using natural clays, quaternary amine chemistries, and existing polymer bases have some limitations.

Concurrent with the development of first-generation polyolefin nanocomposites, Southern Clay Products and other industry and research-based organizations are studying the fundamentals of nanocomposites. Whereas nature has provided an excellent starting point—natural montmorillonite clays—these natural materials can lack consistency in terms of particle shape, charge density, and charge positioning. Programs are underway to change the clay treatment chemistry using out-of-the-box approaches to make the organoclay more compatible with different types of resins, polymers, and rubbers. The quaternary amine chemistries required to modify the natural clay surfaces to make them more compatible with nonpolar polyolefin structures have inherent thermal stability limitations,[22] and once they have served the purpose of helping to exfoliate the individual clay platelets, the chemistry has no further function and can have deleterious effects on the final nanocomposite. Designing clays that would not require large quantities of added compatibilizing chemistries would have obvious benefits.

Summary

Clay/polymer nanocomposites are in the early stages of technology development but are beginning to have considerable commercial importance. Although there are some limitations to current technologies and products, R&D programs are accelerating and are expected to foster a number of new approaches.

Traditionally, the focus has been on the development and preparation of nanocomposites, with nanoclays being the principal non-polymer ingredient. Increasingly, however, we are seeing the development of polymer systems using a variety of modifier agents to generate the desired properties and cost/performance characteristics. Nanoclays are demonstrating unique, multidimensional capabilities to synergistically enhance overall polymer system performance.

References

1. E.P. Giannelis, *Appl. Organomet. Chem.* **12**, 675 (1998).
2. P.C. LeBaron, Z.W. Wang, T.J. Pinnavaia, *Appl. Clay Sci.* **15**, 11 (1999).
3. J.M. Garces et al., *Adv. Mater.* **12**, 1835 (2000).
4. M. Alexandre, P. Dubois, *Mater. Sci. Eng.* **28**, 1 (2000).
5. S.S. Ray, M. Okamoto, *Prog. Polym. Sci.* **28**, 1539 (2003).
6. H. van Olphen, *An Introduction to Clay Colloid Chemistry* (Wiley, New York, 1977).
7. R.E. Grim, *Clay Mineralogy* (McGraw-Hill, New York, 1968).
8. S. Yariv, H. Cross, *Organo-Clay Complexes and Interactions* (Marcel Dekker, New York, 2002).
9. G. Lagaly, *Naturwissenschaften* **68**, 82 (1981).
10. E. Hackett, E. Manias, E.P. Giannelis, *J. Chem. Phys.* **108**, 7410 (1998).
11. J.W. Jordon, F.J. Williams, *Kolloid-Zeitschrift* **137**, 40 (1954).
12. H.D. Dennis et al., *Polymer* **42**, 9513 (2001).
13. P.D. Fasulo, W.R. Rodgers, R.A. Ottaviani, D.L. Hunter, *Polym. Eng. Sci.* **44**, 1036 (2004).
14. Technical information about Cloisite nanoclays can be found at www.nanoclay.com.
15. H. Lee, P.D. Fasulo, W.R. Rodgers, D.R. Paul, *Polymer* **46**, 11673 (2005).
16. H. Lee, P.D. Fasulo, W.R. Rodgers, D.R. Paul, *Polymer* **47**, 3528 (2006).
17. S. Hotta, D.R. Paul, *Polymer* **45**, 7639 (2004).
18. B.B. Khautua, D.J. Lee, H.Y. Kim, J.K. Kim, *Macromolecules* **37**, 2454 (2004).
19. A. Karim, K. Yurekli, R. Krishnamoorti, *Proc. NATAS Annu. Conf. Thermal Analysis and Applications* **29**, 114 (2001).
20. M.Y. Gelfer, H.H. Song, L. Liu, B.S. Hsiao, B. Chu, M. Rafailovich, M. Si, V. Zaitsev, *J. Polym. Sci., Part B: Polym. Phys.* **41**, 44 (2003).
21. B. Rodgers, R.W. Webb, W. Weng, *ACS Rubber Div. Meet.*, paper 58 (November 2005).
22. W. Xie et al., *Chem. Mater.* **13,** 2979 (2001). □

Challenges and Opportunities in Multifunctional Nanocomposite Structures for Aerospace Applications

Jeff Baur and Edward Silverman

Abstract

One important application of nanocomposites is their use in engineered structural composites. Among the wide variety of structural applications, fiber-reinforced composites for aerospace structures have some of the most demanding physical, chemical, electrical, thermal, and mechanical property requirements. Nanocomposites offer tremendous potential to improve the properties of advanced engineered composites with modest additional weight and easy integration into current processing schemes. Significant progress has been made in fulfilling this vision. In particular, nanocomposites have been applied at numerous locations within hierarchical composites to improve specific properties and optimize the multifunctional properties of the overall structure. Within this article, we review the status of nanocomposite incorporation into aerospace composite structures and the need for continued development.

Introduction

Current advanced engineered materials systems, such as organic-matrix composites, have a myriad of applications including aerospace structures, sporting goods, high-performance automobiles, and boats. Composite aerospace structures often have extreme property demands that make the adoption of higher-performance materials systems, such as nanocomposites, inviting. However, there is also a strong need to balance the multiple demands of performance, weight, processability, risk, and/or life-cycle cost in selecting new structural materials. In this article, we discuss the current and potential impact of nanotechnology on composites, with a particular focus on their relevance to aerospace applications.

As air travel continues to grow, lightweight, multifunctional, and easily manufactured structural materials such as polymer matrix composites (PMCs) are being increasingly used. PMCs combat increased fuel and maintenance costs, which account for roughly 50% and 20%, respectively, of the operation costs, beyond ownership, of a commercial airplane.[1] Considering that the recent cost of launching a heavy lift system into low Earth orbit[2] is \$6000–\$20,000/kg and approximately \$36,000/kg for geosynchronous orbit,[3] PMCs are also being increasingly used for space structural applications.

PMCs are generally preferred over metals for moderate-temperature applications (<300°C), based on their weight savings, fatigue resistance, corrosion suppression, and significantly decreased part count (especially fasteners). Future aerospace systems and current developmental systems seek to further enhance both the mechanical and multifunctional properties of PMCs by incorporating nanoparticles.

Property Improvement of Composite Structures with Nanoparticles

A particular challenge for traditional composites is the integration, control, and exploitation of nanoparticle-enabled properties within a hierarchical structured composite made with commercially viable processing methods. Although industrial efforts continue to pursue low-cost processing methods for composite fabrication, the current large capital investment of composite processing equipment (automated fiber coating and positioning systems, equipment for infusing uncured resin into fiber preforms, high-temperature and high-pressure vessels for void-free composite curing, etc.) makes it initially preferable to use traditional composite processing schemes for integrating nanocomposites. Thus, nanoparticles can be incorporated in a number of different ways within the traditional composite material forms, including within a fiber, as a thin coating on a fiber, in place of a bundle of fibers (i.e., a fiber tow), as an inner layer, as a veil, as a coating, or as a part of the polymer resin system. Where the nanoparticles should be placed will depend on the property being sought and the ability to exploit the suite of properties imparted. An illustration of the potential multiscale incorporation is shown in Figure 1. A summary of approaches and possible applications of nanocomposites to aerospace structural composites is given in Table I.

In comparison, many of the current non-nanocomposite approaches to property improvement incorporate larger-scale conducting materials (foils, grids, coatings, etc.) that can often have increased weight, leading to manufacturing issues, or that complicate repairs because of phase discontinuities and their larger sizes. Nanocomposites provide an opportunity to lessen these traditional tradeoffs because properties are improved with small additions of nanoparticles, without significant changes in the manufacturing process and without the incorporation of an additional bulky phase that often requires formal connections. Overall, such a system

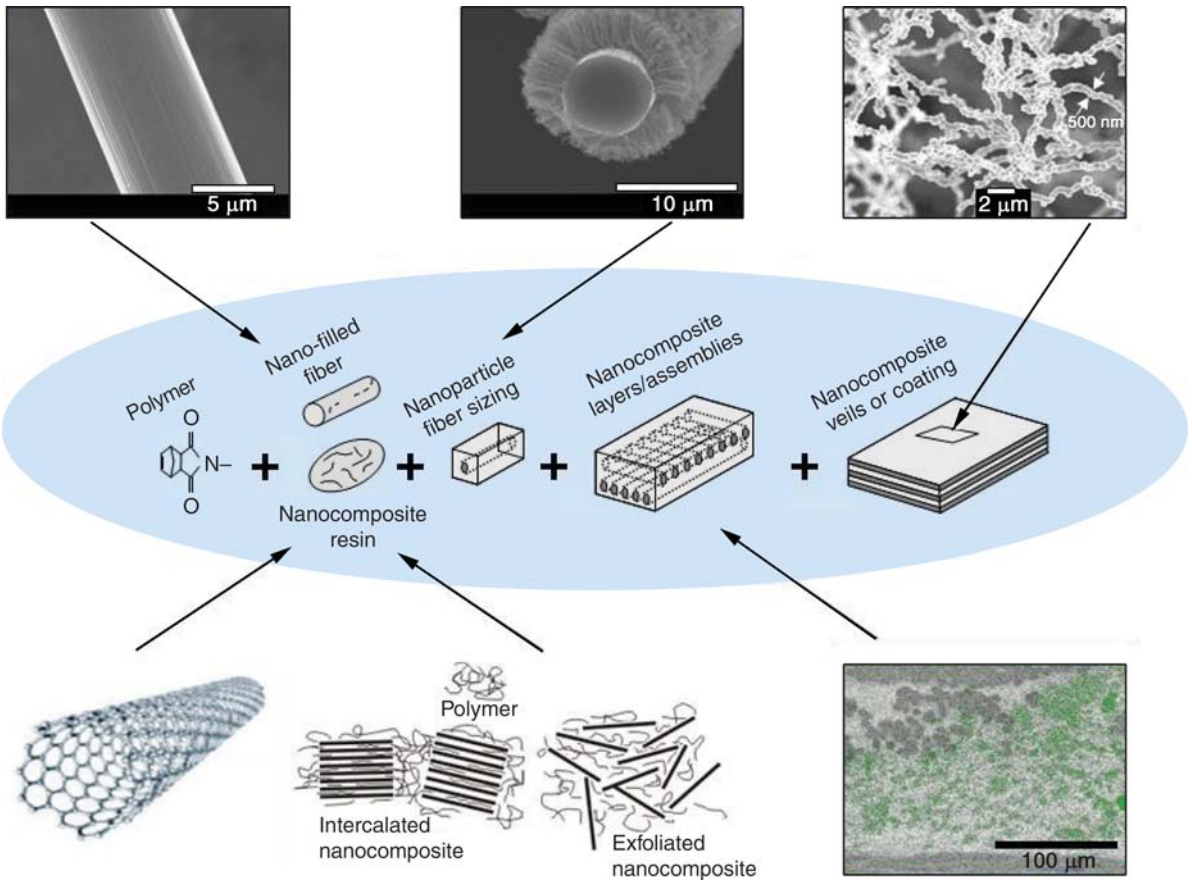

Figure 1. The potential hierarchical integration of nanoparticles within a multiscale composite.

is expected to eliminate redundancy, improve fabrication efficiency, reduce weight and volume, and decrease operating or repair costs. The following sections give some specific examples of improvements currently being made.

Physical/Chemical Properties

The ability of a solid material to maintain dimensional and chemical stability in adverse environments is important for both air and space structures. For example, some large, space-based optical structures require that the deviation in optical path length not exceed a few picometers as the satellite is cycling in and out of extreme thermal environments. Ideally, the structural material would be chemically inert to the radiation environment and resistant to dimensional or chemical changes as a function of temperature until the end of the service life of the material.

One of the most promising nanoscale fillers for enhancing the physical and chemical integrity of a polymer system without adding significant weight is layered silicates. Loadings of only a few percent exfoliated silicate nanoparticles in the appropriate polymer can result in significant enhancement of several physical properties, including resistance to atomic oxygen in low Earth orbit,[4] gas barrier properties for cryogenic tanks,[5] heat distortion temperatures, resistance to solvent swelling, and flammability resistance.[6] For example, previous work demonstrated the reduction of oxygen permeability from a value near 100 cc mil/m^2 day atm for the pristine polymer to values of 1 to 0.1 cc mil/m^2 day atm for film nanocomposites.[7] Figure 2 shows the decrease in helium permeability of a composite-overwrapped tank using layered silicates within the resin. There was also an additional 45%–55% decrease in structural weight with the elimination of the inner liner.[5]

Current reusable launch concepts that would use such tanks are envisioned to thermally cycle hundreds of times and require the tank to experience thermal extremes of about –240°C at the inner cryogenic fluid wall and up to ~343°C at the outer wall. Such thermal extremes will require management of the internal stresses that can lead to microcracking. A major contributor to the overall stresses is the stress induced by the coefficient of thermal expansion (CTE) mismatch between the carbon fiber and the thermosetting resin. Preferential swelling of the polymer by diffusing species (moisture, condensate, etc.) can also contribute to internal stresses. Fortunately, in addition to decreasing permeability, organically modified layered silicates decrease the CTE and the moisture expansion coefficient. For example, decreases in the CTE of 20%–50% for some epoxies[8,9] and about 20% for some polyimides[10] have been observed at modest layered silicate loadings. Decreases in moisture expansion values of 40%–80% for epoxy[11] and ~30%–40% for polyimides[10] have also been observed. Impeding the transport of oxidative species also appears promising, as indicated by the substantial increase in atomic oxygen resistance with a few percent of layered silicate dispersed in an epoxy matrix.[9] Other nanoparticles, such as functionalized carbon nanotubes (CNTs) and graphite flakes, have also been investigated[12–14] and

Table I: Summary of Approaches and Possible Applications of Nanocomposites in Aerospace Structural Composites.

Property	Common Nanocomposite Approach	Potential Application
Physical/Chemical		
Permeability	Inclusion of impermeable, high-aspect-ratio silicate or graphite flake in resin	Cryogenic tanks, durability to diffusion species
Outgassing	Inclusion of impermeable, high-aspect-ratio silicate or graphite flake in resin	Optical benches, interferometers, antenna truss structures
Oxidation resistance	Incorporate high-temperature, oxidation-resistant fillers (silicate, CNTs, POSS, etc.) that form passivating layers or slow oxidative erosion in resin or as coating	Thermal protection systems, atomic oxygen resistance, space structures
Electrical		
Electrostatic dissipation (ESD)	Incorporate high-aspect-ratio conductive particles such as CNTs, graphite flake, metals, as percolated networks in resin between conductive fibers	Charge-dissipating adhesives, coatings, and gap fillers
Electromagnetic interference (EMI)	Create films of highly percolated networks of conductive nanofillers (nickel nanostrand veil, SWNT buckypaper, etc.) that can both absorb and dissipate broadband frequencies	Bus compartment enclosures, electronic enclosures
Lightning strike	Incorporate conductive nanofillers (nickel nanostrands, CNTs, etc.) as highly percolated coatings, appliqués, resins, or veils that can carry large currents and have controlled failure modes	Composite aircraft exteriors
Thermal		
Thermal conductivity	Incorporate highly thermally conductive particles (CNTs, metals, etc.) into resin and optimize structure for heat transfer along continuous path to heat sink	Thermally conductive adhesives, gaskets, radiators, doublers, electronics boards, solid-state laser heat removal
Thermal protection systems	Use thermally conductive and insulating nanofillers within resin to assist larger structural components to direct heat away from protected systems or enhance mechanical properties at high temperature	Aircraft brakes, re-entry vehicles, missiles
Coefficient of thermal expansion	Incorporate nanofillers with low expansion coefficients and good matrix bonding such as functionalized CNTs, CNFs, silicate, into resin or as fiber sizing to reduce CTE mismatch with fiber by composite effect and restriction of polymer motion	Adhesives, space apertures with improved thermal cycling durability
Mechanical		
Toughness	Incorporate nanofillers, such as CNTs, layered silicate, and silica, into resin to increase energy dissipation on failure through deformation, pull-out, crack bridging, etc., at needed plies	Membrane structures, damage-tolerant structures
Modulus	Incorporate high-modulus nanoparticles like continuous CNT yarns/sheets as reinforcement or grow reinforcements between plies to increase out-of-plane modulus	Stable, precision structures
Compression strength	Incorporate high-strength nanoparticles such as functionalized CNTs into the resin	Propulsion tanks, fittings
Interfacial shear stress	Grow high-strength nanoparticles such as CNTs from fiber to tailor the interfacial properties as a smart sizing	High-temperature composites, vehicle health monitoring
Interlaminar shear strength	Incorporate nano-filled resins with increased toughness at mid-plies via coating or pre-pregging	Tubular structures

Notes: CNT is carbon nanotube; POSS is polyhedral oligomeric silsesquioxane, SWNT is single-wall carbon nanotube, CNF is carbon nanofiber, CTE is coefficient of thermal expansion.

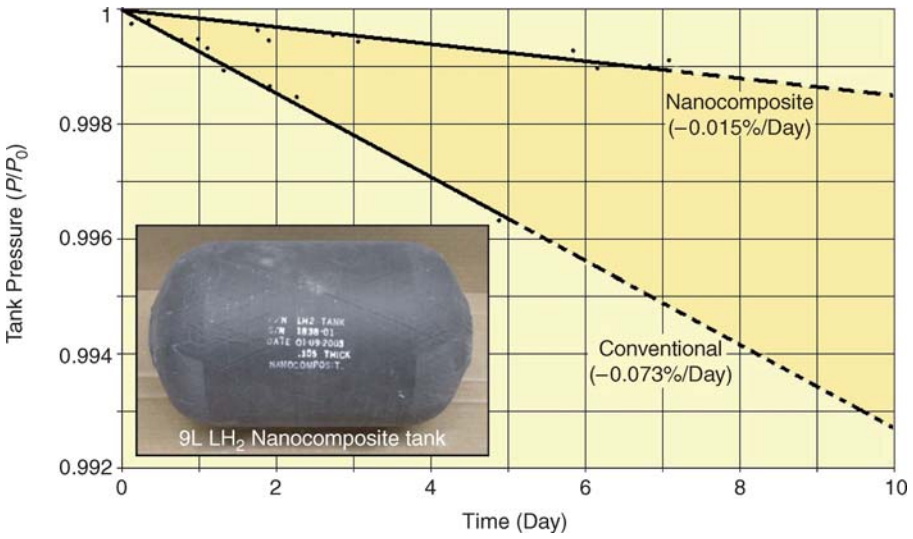

Figure 2. Comparison of leak rates for a nanocomposite-overwrapped tank using layered silicates within the resin. Nanoclays show reduced permeability to helium for tank applications (helium is used for leak detection). P_0 is the initial pressure of helium in the tank. Inset shows a photograph of a liquid-hydrogen tank.

may be able to impart multifunctional properties such as electrical and thermal conductivity.

Mechanical Properties

Mechanical improvements in traditional composite materials through the use of nanocomposites can be targeted toward improvement of resin-dominated properties or, eventually, toward fiber-dominated properties. Resin-dominated properties include interlaminar shear strength (ILSS), compression strength, and fatigue properties. Fiber-dominated properties include modulus and ultimate tensile strengths. The theoretically predicted high modulus and strength of nanoparticles such as single-wall carbon nanotubes (SWNTs) are of interest. For resin-dominated properties such as ILSS and toughness, a detailed understanding of the fracture mechanics within the nanocomposite morphology is needed to fully exploit the ultimate properties of nanocomposites. Characterization of the deformation and failure mechanisms in a manner similar to that used for traditional composites (pull-out, bridging, interfacial cracking, matrix cracking, etc.) are needed to more fully understand and exploit improvements made with nanocomposites. Although more work is needed, a 20% increase in ILSS for only 0.3 wt% functionalized double-wall carbon nanotubes has been reported in the literature for glass-fiber epoxy composite,[15] and a 180% increase for a similar epoxy/glass fabric composite with carbon nanofibers has been reported by a commercial material provider.[16]

A key benefit of nanocomposites for fiber-reinforced composites is the ability to selectively tailor the deformation mechanism at different locations within the composite. Thus, one might only need to use the nano-enhancement within selected plies. A recently reported extension of this concept is to grow carbon nanotubes directly on the fiber ply to create a mechanically and multifunctionally enhanced composite.[17] With these fiber-like, out-of-ply nanoreinforcements, the final composite begins to more closely resemble a hierarchical three-dimensional (3D) reinforced fabric rather than a composite laminate with nano-enhanced resin. This highlights the great flexibility of using nanoparticles within a composite material. Table II, which compares some of the properties of carbon nanotubes against more traditional aerospace materials, illustrates the basis of this potential. Although nanocomposite properties are discussed in more detail elsewhere,[18] these properties raise the intriguing possibility of applying the nanotubes as super-strong reinforcing fibers with strength and stiffness orders of magnitude higher than any other known material.

Although major advances have been made on the fabrication of carbon nanotube sheets[19–27] and yarns,[28–33] no one has yet assembled carbon nanotubes into yarns and sheets that retain the spectacular properties of the individual SWNTs. Individual single-wall nanotube properties include a tenfold higher strength than existing sheets and yarns, a higher thermal conductivity than diamond, a thousandfold larger current-carrying capability than copper, and many other fascinating and useful properties for active devices. Even though some of the produced CNT yarns are nearly as tough as the Kevlar fibers used for antiballistic vests, efforts to increase the strength, yarn toughness, and production capability continue. Correspondingly, the actual performance of nanotube/polymer composites has also been below the theoretically predicted performance.

Thermal Properties

Thermal management of aerospace structures is important for many applications including space platforms, re-entry vehicles, propulsion systems, electronics, and high-energy (e.g., laser) systems. For example, heat generated by spacecraft components often presents difficult thermal design problems because of the high and localized heat flux, the need for large total power dissipation, and the wide temperature changes over time. The increasing need to fly larger, higher-performance payloads with higher-density microprocessors for longer periods of time has escalated power dissipation and heat flux at the silicon level. Future military communication satellites will have higher-power-density microelectronics packaging design concepts that will increase the data processing throughput by five to ten times, resulting in a possible tenfold increase in the thermal density.[34]

Next-generation aerospace structures could potentially use more thermally conductive materials to spread out and judiciously direct heat flow in satellites, thermal protection systems, near-propulsion structures, electronic boxes, chip packaging, directed energy systems, radiators, and their accompanying thermal interfaces. CNTs offer some of the strongest promise, since the measured thermal conductivity of individual multiwall nanotubes (MWNTs) (3000 W/m K) is higher than diamond[35] and have predicted values even higher.[36] The theoretical thermal conductivity of SWNTs is 6000 W/m K,[37] which, when combined with exceptional tensile strength, could form the basis for a multitude of future high-performance materials.

Experimentally, unoptimized MWNT sheets have been measured to give a room-temperature thermal conductivity of about 150 W/m K. This is close to the thermal conductivity reported for magnetically oriented single-wall nanotube sheets,[38] but substantially higher that the <3 W/m K

Table II: Properties of Carbon Nanotubes Compared with Traditional Aerospace Materials.

Material	Specific Gravity (g/cm^3)	Yield Strength (GPa)	Elastic Modulus (GPa)	Thermal Conductivity (W/m K)	Electrical Resistivity ($\mu\Omega$ cm)	Normalized Strength-to-Mass Ratio
Carbon nanotube (SWNT theory)	1.4	65	1000	–6000	30–100	225
Measured SWNT yarns and sheets	1.4	1.8	80	150	150	7
Conventional carbon fiber, M55J	2.2	4	550	70	800	9
IM7 carbon composites	1.6	2.1	152	30	2000	7
Titanium	4.5	0.9	103	12	127	1
Aluminum	2.7	0.5	69	180	4.3	1

Note: SWNT is single-wall carbon nanotube.

reported for highly loaded (up to 20 wt%) vapor-grown carbon nanofibers (VGNFs) in epoxy.[39] Inefficient phonon transport between nanotubes is considered the major limitation to approaching the thermal conductivity of the individual nanotubes.[40] Because the phonon dispersion occurs at discontinuities such as tube ends, a simple argument would suggest that increasing nanotube length from 0.3 to 3 mm will increase nanotube yarn thermal conductivity tenfold, or from 150 to 1500 W/m K. However, creating nanotube junctions in which tubes efficiently exchange thermal energy to other nanotubes or carbon fibers would also significantly increase the thermal conductivity of composite resins. One of the first aerospace applications using this type of nanofiller could be thermally conductive adhesives and reinforced interface gaskets.

Electrical Properties

Many aerospace applications require electrically conducting, polymer-based composites for static discharge, electrical bonding, interference shielding, primary and secondary power, and current return through the structure. However, present carbon-reinforced polymer composites alone cannot provide robust solutions to satisfy these requirements because of the presence of insulating resin regions including the surface. Traditionally, secondary conductive materials such as foils, wires/straps, and coatings would be incorporated into the structure with additional processing steps. However, integrated composite structures that use percolated networks of conductive particles with high aspect ratios appear to be a preferred method for obtaining low-resistivity composites at low volume fractions and with little additional weight. For example, materials such as carbon nanofibers,[39,41] single-wall nanotube buckypaper (a collapsed film of CNTs),[42] nickel nanostrands,[43] or graphite flakes[14] have potential application in near-term electrostatic dissipation (ESD) and electromagnetic shielding systems, as discussed in detail next.

Control of Electrostatic Discharge

Composite structures, including graphite/epoxy and Kevlar, are known to locally charge to 4000 or 6000 V, respectively, when exposed to electron fluxes, despite the presence of a conductive path through carbon fibers.[44] To avoid discharging to a proximate ground and harming electronics or personnel, electrical shielding is required over the entire exposed surface. Materials that have resistivity values above 1×10^{13} ohm/square can develop a static charge that will not dissipate even when bonded. The measurement of ohm/square refers to the resistance (in ohms) of a surface film multiplied by the surface width and divided by the length. If one considers a square of equal length and width, the resistivity can be expressed as ohms per unitless square. A resistivity of 1×10^7 ohm/square is sufficient to dissipate charge for an electrically bonded structure and is generally the range at which the carbon filaments are adequately connected to the proximate ground. By adding high-aspect-ratio conductive nanoparticles to the resin-rich regions of a composite, the electrical connection with the proximate ground and the conducting carbon fibers can be assured at modest additional weight. For example, coatings of VGNFs and hybrid VGNF/graphene platelet nanocomposites on conventional composite substrates can reduce the surface resistivity from $>10^{12}$ ohm/square to 10^3–10^4 ohm/square to successfully satisfy the electrostatic discharge requirements for spacecraft applications.[45]

Conducting Adhesives

Good electrical bonding of a joint is needed to assist in controlling and dissipating the buildup of electrostatic charges. Typically, the requirement is less than 1000 Ω for bonds between composite materials and the structure. For bonding across joints in composite materials, an electrically conductive adhesive is filled with high amounts (up to 60% by volume) of powdered silver, nickel, or carbon black. However, this makes the adhesive bond weaker, and hence, a structural adhesive is needed in addition to the electrically conductive adhesive. Recent industry and government research efforts aim to develop a multifunctional, carbon, nanofiber-filled adhesive with high electrical conductivity that meets the requirements for lap shear strength and viscosity.[46]

Lightning Strike Protection

Another related application involving much larger currents (up to 200 kA) is lightning strike protection. With 40 aircraft accidents and 290 fatalities attributed to lightning strike incidents between 1963 and 1989,[47] this unpredictable act of nature can lead to loss of pilot control as well as burning, erosion, and distortion of the structure. As more structures use composite materials, strategies that use bulky films and meshes are being employed for protection. The key challenge is to either fully dissipate the energy or direct it into an easily repairable failure mode without compromising the structure or the flight.[48,49] New approaches that attempt to exploit lighter-weight conductive nanofilled composites are actively being explored by several researchers.[43]

Enclosures for Electromagnetic Shielding

Traditional enclosures of electronics for air and space structures have usually been made of aluminum and other electrically

conductive metals that provide electrostatic discharge protection, electromagnetic shielding, fault current return, an antenna ground plane, and intrinsic lightning protection. In recent years, composite materials have been used because of their light weight, high strength, and ease of fabrication. But extra steps must again be taken to achieve the desired electromagnetic properties. In this particular application, the electrical properties of the structure must meet the >60 dB shielding effectiveness level to shield against electrical interference. One traditional solution is to use a ~75-μm-thick aluminum foil co-cured with the graphite fiber composite. However, this is not the best solution because of cost, questionable adhesion, and limitation in the ability to repair or rework areas despite the favorable shielding efficiency.

An alternative approach is to use a lightweight veil of nickel nanostrands to achieve the desired level of shielding with good adhesion and the ability to repair. A composite with alternating layers of fibers oriented 0° and 90° relative to each other and with two top layers of nickel nanostrand veils showed shielding levels of >60 dB over the useful frequency range, as shown in Figure 3.[43] Hence, only a few tens of micrometers of a nanostrand composite film created a highly effective electromagnetic interference shield across a wide bandwidth. Although 60 dB is a respectable shielding level, it is anticipated that thicker or more concentrated nanostrands may provide even better broadband shielding with minimal weight increase.

Conclusion

In this article, we have provided a general overview of the near-term promise for nanotechnology within aerospace polymer-matrix structural composites. Whereas these composites are often considered light weight and integrated alternatives to traditional metals, they also have tradeoffs in dimensional stability, temperature capability, electrical conductivity, and thermal transport.

Nanocomposites are addressing many of the near-term needs of composite structures by providing mechanical and multifunctional improvements with modest additional weight. In the far term, one can envision integrated structures in which more advanced functions are embedded into the structure to actively manage mechanical, thermal, electrical, or optical loads, as well as actively select, sense, convert, store, and transmit the various energies within an intelligent structure.

Acknowledgments

We are very grateful to members of the Advanced Composites Branch, Katie Thorp, and Rich Vaia for the insightful discussions; to Liming Dai, Qiuhong Zhang, Jennifer Fielding, and Sirina Putthanarat for micrographs; and to the Air Force Office of Scientific Research and the Air Force Research Laboratory, Materials and Manufacturing Directorate, for partial support.

References

1. L.B. Ilcewicz, D.J. Hoffman, A.J. Fawcett, *Compr. Compos. Mater.* **6**, 87 (2000).
2. R.L. Burton, K. Brown, A. Jocobi, *J. Spacecraft Rockets* **43** (3), 696 (2006).
3. D.E. Koelle, *Acta Astronautica* **53**, 797 (2003).
4. H. Fong et al., *Chem. Mater.* **13**, 4123 (2001).
5. S. Campbell et al., *Int. SAMPE Symp. Exhib. Proc.* **48**, 1124 (2003).
6. E.T. Thostenson, L. Chunyu, T.-W. Chou, *Compos. Sci. Tech.* **65**, 491 (2005).
7. T. Ogasawara, Y. Ishida, T. Ishikawa, in *Proc. 11th US–Japan Conf. Composite Materials*, Yonezawa, Yamagata, Japan (2004).
8. I.-N. Jan et al., *Ind. Eng. Chem. Res.* **44**, 2086 (2005).
9. H. Koerner et al., *Chem. Mater.* **17**, 1990 (2005).
10. H.-L. Tyan, C.-Y. Wu, K.H. Wei, *J. Appl. Polym. Sci.* **81** (7), 1742 (2001).
11. J.-K. Kim, C. Hu, R.S.C. Woo, M.-L. Sham, *Compos. Sci. Tech.* **65**, 805 (2005).
12. Z. Liang et al., *Int. SAMPE Symp. Exhib. Proc.* **50**, 2331 (2005).
13. M. Moniruzzaman, K.I. Winey, *Macromolecules* **39** (16), 5194 (2006).
14. H. Fukushima, L.T. Drzal, B.P. Rook, M.J. Rich, *J. Therm. Anal. Calorim.* **85**, 235 (2006).
15. F.H. Gojny et al., *Composites Part A* **36**, 1525 (2005).
16. NanoSperse LLC product literature, www.nanosperse.com.
17. V.P. Veedu et al., *Nature Mater.* **5**, 457 (2006).
18. J.N. Coleman, U. Khan, W.J. Blau, Y.K. Gun'ko, *Carbon* **44**, 1624 (2006).
19. A.G. Rinzler et al., *Appl. Phys. A* **67**, 29 (1998).
20. M. Endo et al., *Nature* **433**, 476 (2005).
21. Z. Wu et al., *Science* **305**, 1273 (2004).
22. L. Hu, D.S. Hecht, G. Gruener, *Nano Lett.* **4**, 2513 (2004).
23. J.E. Fischer et al., *J. Appl. Phys.*, **93**, 2157 (2003).
24. Y.-L. Li, I.A. Kinloch, A.H. Windle, *Science* **304**, 276 (2004).
25. Y. Kim et al., *Jap. J. Appl. Phys.* **42**, 7629 (2003).
26. T.V. Sreekumar et al., *Chem. Mater.* **15**, 175 (2003).
27. H. Ago et al., *Adv. Mater.* **11**, 1281 (1999).
28. B. Vigolo et al., *Science* **290,** 1331 (2000).
29. R.H. Baughman, *Science* **290**, 1310 (2000).
30. B. Vigolo et al., *Appl. Phys. Lett.* **81**, 1210 (2002).
31. A.B. Dalton et al., *Nature* **423**, 703 (2003).
32. L.M. Ericson et al., *Science* **305**, 1447 (2004).
33. S. Kumar et al., *Macromolecules* **35**, 9039 (2002).
34. P.K. Schelling, L. Shi, K.E. Goodson, *Mater. Today* **8** (6), 30 (2005).
35. P. Kim, L. Shi, A. Majumdar, P.L. McEuen, *Phys. Rev. Lett.* **87**, 215502 (2001).
36. M.A. Osman, D. Srivastava, *Nanotech.* **12**, 21 (2001).
37. S. Berber, Y.-K. Kwon, D. Tomanek, *Phys. Rev. Lett.* **84**, 4613 (2000).
38. J. Hone et al., *Appl. Phys. Lett.* **77**, 666 (2000).
39. V.A. Buryachenko et al., *Compos. Sci. Tech.* **65**, 2435 (2005); K. Lafdi, M. Matzek, *Proc. 35th Int. SAMPE Tech. Conf.* **35**, 1 (2003).
40. A. Bagchi, S. Nomura, *Compos. Sci. Tech.* **66**, 1703 (2006).
41. Y.-K. Choi et al., *Carbon* **43**, 2199 (2005).
42. Z. Wang et al., *Composites Part A* **35**, 1225 (2004).
43. G. Hansen, *J. Adv. Mater.* **38** (3), 68 (2006); G. Hansen, *SAMPE J.* **41** (2), 24 (2005).

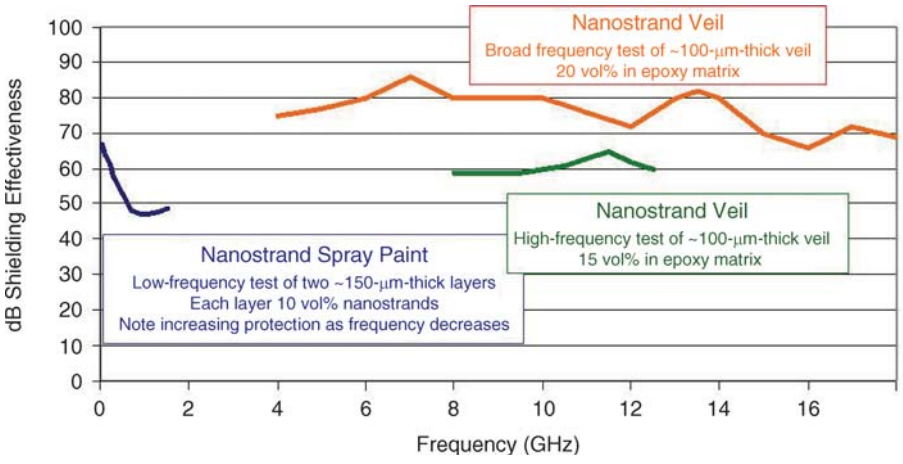

Figure 3. Summary of shielding effectiveness test results for composites with nickel nanostrand coating and epoxy-infused nickel nanostrand veil of two different thicknesses.

44. K.L. Bedingfield, R.D. Leach, M.B. Alexander, Eds., *Spacecraft System Failures and Anomalies Attributed to the Natural Space Environment* (NASA Reference Publication 1390, August 1996).
45. D.M. Barnett, S. Rawal, K. Rummel, *J. Spacecraft Rockets* **38** (2), 226 (2001).
46. T. Gibson, B. Rice, W. Ragland, E.M. Silverman, H.-H. Peng, K.L. Strong, D. Moon, *Int.. SAMPE Symp. Exhib. Proc.* **50**, 1713 (2005).
47. M. Cherington, K. Mathys, *Aviation Space Environ. Medicine* **66** (7), 687 (1995).
48. G. Gardiner, *High-Performance Compos.*, **14** (2), 44 (2006).
49. A. Fisher, R.A. Perala, J.A. Plumer, *Lightning Protection of Aircraft* (Lightning Technologies, Pittsfield, MA, 1985). □

Designed Interfaces in Polymer Nanocomposites: A Fundamental Viewpoint

Linda S. Schadler, Sanat K. Kumar, Brian C. Benicewicz, Sarah L. Lewis, and Shane E. Harton

Abstract

Using nanocomposites in design-critical applications requires an understanding of their structure–property–function relationships. Despite many reports of highly favorable properties, the behavior of polymer nanocomposites is not generally predictable. The ability to tailor the filler/matrix interaction and an understanding of the impact of the interface on macroscopic properties are key to designing their properties. Tailoring can be achieved by grafting short molecules or polymer chains from the surface with precise control over their chain length (1–1000 mers), graft density (0.01–1 chains/nm^2), and chemical architecture. The challenge is understanding the impact of the modified surfaces on the properties of the interfacial polymer, which can be more than 50% of the volume of the polymer matrix and, hence, can exert significant control over the macroscopic behavior of the nanocomposite. This article highlights the fundamental technical challenges that need to be overcome before spherical nanoparticle or nanotube composites can be designed. In particular, we discuss results from the recent literature that have significantly advanced our ability to predict and control nanocomposite properties through the use of designed interfaces.

Introduction

Nanoscale fillers blended with polymers ("nanocomposites") offer the real possibility of creating materials with properties that are not realizable with traditional, micron-scale fillers. These unusual properties arise because of three attributes of nanofillers. First, they can have properties distinct from micron-scale fillers. For example, carbon nanotubes are as stiff as graphite fibers, but are almost an order of magnitude stronger.[1] Second, nanoscale fillers play the role of small mechanical, optical, and electrical defects. These provide an opportunity for multifunctionality (e.g., scratch-resistant, transparent polymers[2]). Third, they create a large volume of interfacial polymer with properties different from the bulk, providing an opportunity for tailoring properties.

It is imperative to have a fundamental understanding of each of these aspects to understand structure–property–function relationships in these materials and to design composites with specific properties. In this review, focus is placed on the third aspect, and the role of the interface in modifying the thermomechanical properties of the composite is critically examined. Because this area of research is extremely broad, the discussion is further focused on the case of curved nanofillers (spherical and cylindrical); these systems are of particular interest because they provide a contrast to the case of composites with micron-scale spherical or cylindrical fillers, which have been studied for nearly half a century.

In traditional composites, the interface is critically important for controlling properties and has been the focus of significant research.[3] The interface is defined in the literature as the region in the vicinity of the particle surface where polymer properties are altered as compared with the bulk.[4] The size scale of the interface depends on the particular property measured: chain dimensions can be perturbed in the immediate vicinity of the surface (typically on the order of the size of the molecule, 10 nm),[5–7] but the chain center of mass diffusivity can be perturbed even 100 nm from the surface.[8,9] Whereas the interface is present in all composites, the difference between nanocomposites and traditional composites is the volume fraction of polymer that is affected in the two cases.

Figure 1 in the introduction by Winey and Vaia in this issue highlights this point. This figure implies conservatively that the interfacial volume occupies 5% of the composite for spherical fillers of 10-nm radius (thus, $\delta \approx 1$) at a loading of 1 vol %. In contrast, the interface volume at these loadings is negligible in a traditional composite.

Figure 1 in this article shows this effect pictorially.[10] Given the large fraction of polymer in the interface, the fundamental challenge to designing the properties of polymer nanocomposites is to understand the role of filler chemical modification as a vehicle for controlling interfacial polymer structure (and properties) with the goal of optimizing properties all the way from the nanoscale to the macroscopic level. At this point, this understanding is only qualitative and limits the ability to design composites with specific properties. For the purposes of this review, these fundamental challenges are distilled into two sets of questions:

1. Local Interfacial Properties: What is the effect of highly curved surfaces on the structure and dynamics of polymer chains? What is the size of the interface region? How do enthalpic interactions and entropic interactions control filler/matrix wettability and the resulting structure, dynamics, and properties of the polymer chains?
2. Consequences for Macroscopic Properties: How does the interface affect macroscopic properties such as the miscibility of polymers and particles (i.e., particle dispersion in the matrix)? Additionally, how does this dispersion quantitatively affect macroscopic properties, such as mechanical response and dielectric behavior? Can these macroscopic properties be predicted based on nanoscale information alone?

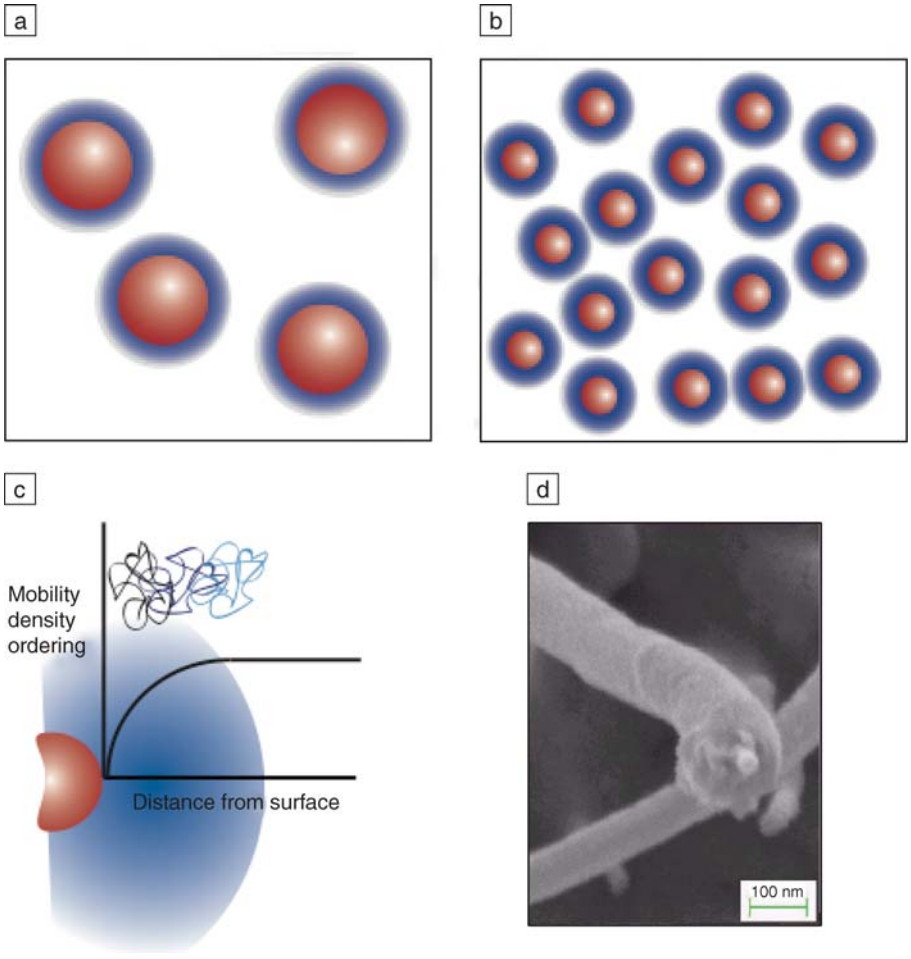

Figure 1. (a), (b) Schematic illustrations showing the difference in the volume of interfacial polymer (shown in blue) for nanocomposites compared with micron-scale composites. The area of red is about the same in the two images. (c) Schematic illustrations showing that the properties of the polymer change as a function of distance from the particle surface. (d) Scanning electron micrograph of a nanotube/polycarbonate fracture surface, showing the interface zone on the nanotube.[10]

With the questions defined, it is apparent that there is a need for systematic modeling and experimental studies that probe the effect of radius of curvature, and surface molecule chemistry, density, and length on the structure and dynamics of matrix polymer chains in the vicinity of a surface. For example, to predict particle dispersion requires "miscibility" maps similar to those derived for flat surfaces[11] (e.g., for melt intercalation into clays[12]). This dispersion will determine key quantities such as the structure and dynamics of the composite and thus enable us to relate nanoscale properties (e.g., wetting behavior, glass-transition temperature, or dielectric relaxation) to macroscale properties. When this knowledge is quantitatively integrated from the molecular scale to the macroscale, the design process to create nanocomposites with specific properties is enabled.

While recognizing that both sets of questions and their interplay are critical to the understanding of the role of the interface on the properties of the resulting nanocomposite, this article will address primarily question set 1, which has been the focus of considerable experimental and theoretical research in the last few years. The understanding of the relationship of interfacial properties with the macroscale properties of the nanocomposite (question set 2), which is critical to the applications of these materials in an engineering context, however, is at a nascent stage, and is hence only briefly discussed in this article. The article begins by identifying key components from the traditional composites and thin-film literature that apply to nanocomposite design. The article then selectively describes the toolbox of modification methods available for tailoring the interface. Finally, by considering separately the enthalpic and entropic effects at the interface, the challenges to the technical community are identified.

Building from Traditional Composites

Fortunately, there is a large body of literature in the field of traditional composites that provides an excellent starting point for understanding the behavior of polymer nanocomposites.[13,14] In addition, there are many models that provide accurate predictions of composite properties, for example, modulus and thermal conductivity.[15–17] At the micromechanical level, it is understood that aspect ratio, geometry, and interfacial shear stress are relevant parameters.[18] From this, it is expected (and observed) that nanoscale clays and high-aspect-ratio nanotubes should have the highest reinforcing capability.[19,20] These models also predict that percolation should not depend on filler size, but that higher-aspect-ratio fillers will be more efficient for altering transport properties across a composite. It is also well understood from traditional composites that controlled dispersion and alignment of fillers is critical for well-controlled properties.

Traditional composites exploit the unique role played by the interface. There are many methods for compatibilizing fillers with the matrix, and significant research has been done to understand the chemistry of filler surfaces and, hence, to tailor interactions with the matrix.[21] For example, work by McCullough's group[22] and Dibenedetto[23] bring rigor to understanding how the compatibility between the polymer matrix and fiber reinforcement is controlled by both enthalpic and entropic interactions between the two components. A review by Sottos and McCullough[24] makes a point that is still relevant today: "In order to develop and evaluate such models (that include the interphase) . . . the properties of the interphase must be accurately known." This is a significant issue in traditional composites, but it is even more crucial in polymer nanocomposites, where the interface represents a much larger volume fraction.

What Do Thin Films Teach Us?

Given the dominant role played by the interface, crucial guidance can also be drawn from the thin-film literature. One of the properties that is sensitive to polymer structure and mobility is the glass-transition temperature. Thus, it is often used as a metric to monitor thin-film behavior. Comprehensive work on polystyrene and poly(methyl methacrylate) thin films has shown that the glass-transition temperature T_g increases if the film interacts favorably with the substrate.[25–28] In limited cases, it has

been shown that increases in T_g reflect a reduction in the mobility of the interfacial polymer chains. On the other hand, in freestanding ultrathin films, T_g decreases (Figure 2, open circles).[29,30] Because of the small radius of curvature of the particles and the highly polydisperse particle spacing in typical situations, the application of the thin-film work is not straightforward. Recent work[31] by our group suggests that a quantitative correlation can be drawn between the thickness of thin films and the interparticle spacing in nanocomposites (Figure 2, solid circles) and that the interfacial width in the two cases is similar.[32,33] In addition, the glass-transition temperature of a polymer nanocomposite can be raised or lowered with the addition of nanoparticles with attractive or repulsive interaction with the matrix.[34,35] The mechanism causing these changes in T_g, however, is currently under discussion.[36] Thus, from thin films, it is known that the effect of a surface can impact the polymer structure and properties more than a radius of gyration away and that the chemical interaction at the surface is a critical parameter that affects whether the T_g increases or decreases.[37] This is important, because we shall assert that T_g can then be used in bulk nanocomposite systems as a measure of the particle/polymer interaction.[31]

Toolbox for Interfacial Modification

To design and tailor the interfaces for specific properties and applications, a "toolbox" of methods for interface modification is necessary. This toolbox should enable the control of molecule length, graft density, and chemical composition. The attachment of short molecules to the surface provides an opportunity for tailoring the energetics of the polymer–surface interaction. Silane coupling agents (i.e., silicon-containing molecules covalently attached to the particle surface) are frequently used to functionalize the surfaces of silicon, aluminum, zirconium, tin, titanium, and nickel oxides. Less stable bonds can be formed with other oxides.[38] They may also contain reactive groups that can copolymerize with the matrix monomers: these are commonly used in thermoset polymers to covalently incorporate fillers into the matrix.

An alternative approach that has gained considerable popularity recently is the covalent attachment of polymers to the filler surface.[39] There are generally two approaches to prepare polymer-grafted nanoparticles: grafting-to and grafting-from methods. Grafting-to methods, in which polymers bearing functional end groups are attached to the appropriate surface, are restricted to low grafting densities because of the steric hindrance imposed by the already grafted chains. In the grafting-from approach, the initiating sites are attached to the substrate surface.[40,41] Polymerization is then conducted from the particle surface to prepare polymer-grafted nanoparticles. Higher graft densities and molecular weights can be achieved. Recently, advances in controlled radical polymerization techniques (e.g., nitroxide-mediated polymerization, atom-transfer radical polymerization, and reversible addition-fragmentation chain-transfer polymerization) have greatly facilitated the controlled synthesis of these polymers and, thus, our ability to design these interfaces.[42–47]

Collectively, these methods (and others not mentioned) are exciting because a toolbox of methods is available that enables researchers to design interfaces with several levels of control over chemistry, chain length, chain density, and layer thickness. In some cases, short molecule modification will be ideal, in others a heterogeneous surface, whereas for a third, high graft densities with a homogeneous layer thickness may be desired. The challenge remains, however, to understand which interface structures are optimal for achieving specific composite properties.

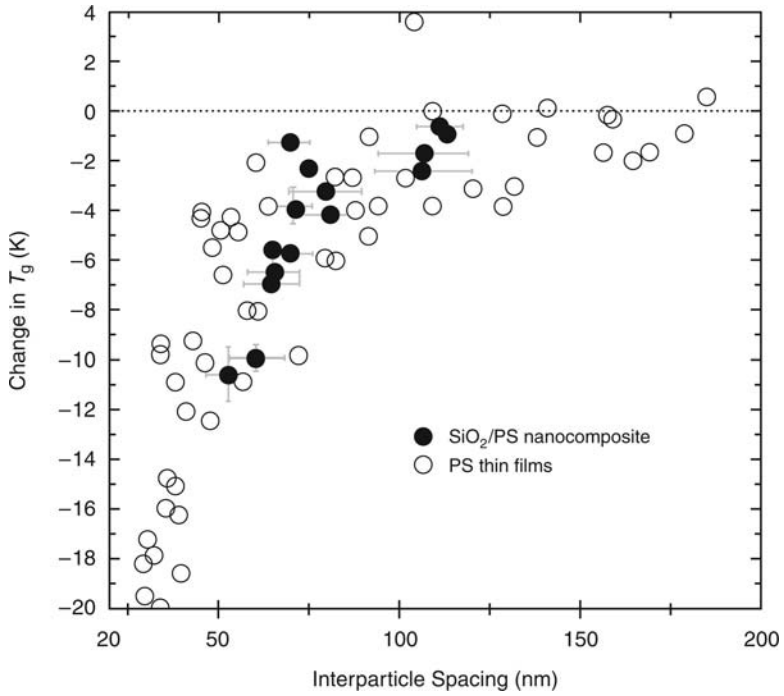

Figure 2. Comparison between the glass-transition response of polystyrene nanocomposites and polystyrene thin films as a function of interparticle spacing, which represents the film thickness for thin films and an average interparticle spacing in the nanocomposites. The x-error bars represent a 95% confidence level. Data from literature on freestanding ultrathin films[29] and supported films[30] are shown as open circles. (Taken from Reference 31.)

Characterization of Nanocomposites Formed from Functionalized Nanoparticles

The premise of this article is that to understand the structure–property–function relationships in nanocomposites, a fundamental understanding of the effect of the large surface area of nanofillers on the interfacial polymer structure and properties must be developed. It appears well accepted in the literature that the dispersion of the particles in a polymer matrix can be greatly facilitated by creating particle surfaces that are wet by the polymer. In addition, one fundamental property that is sensitive to the wetting properties of the interface and can be measured with relatively minor mechanical and electrical perturbations is the glass-transition temperature. This section, therefore, focuses on this property, where it is used as a measure of the filler/matrix interaction with the implicit understanding that the filler/matrix interaction is also known to affect the mechanical, optical, electrical, and thermal properties of bulk nanocomposites as well as dispersion.[2,46,47] It is the degree to which

each of these properties is affected by the interface that is not known quantitatively.

Enthalpic Control of Interfacial Properties

Consider first the role of short molecules on the filler/polymer interaction. In this case, entropic effects play a small role, and energetic interactions control the interfacial behavior. It is well known that the nanoparticle surface can be modified with silane coupling agents so as to affect many properties, including the glass-transition temperature. The hypothesis from the literature is that if the surface is attractive to the polymer, then T_g will increase. If it is neutral, T_g will not change, and if it is repulsive, or nonwetting, T_g will decrease.[23,48]

The adsorption energy of a polymer segment is the difference between the energy of interaction of a polymer segment with the surface (ε_{ps}) and the interaction of the same segment when it is interacting with another polymer segment (ε_{pp}), that is, $\varepsilon_{ps} - \varepsilon_{pp}$. If the interactions are modeled as being purely dispersive in character, then the solubility parameter of the surface and the polymer can describe the energetic interactions in the system.[49] In this situation, the adsorption energy of a segment to the surface is $\propto -\delta_p \times [\delta_s - \delta_p]$, where δ denotes the solubility parameter of the surface and the polymer, respectively, for subscripts p and s, and the negative sign after the proportionality sign is because the energy of interactions are generally negative while the solubility parameters are positive.

Thus, polymers will wet the surface if $\delta_s \geq \delta_p$, and the miscibility of the polymer and the particle, and hence the T_g shift, should scale with the difference in the solubility parameters. Additionally, the surface area of the particles can be used to normalize across particles of different size and volume fractions. Although these ideas were presented for micron-scale composites, they were only tested in limited cases and for positive interactions.[23]

To test this simple set of ideas on nanocomposites with a range of interactions, Figure 3 shows data from the literature for the changes in T_g in nanocomposites.[50,51] Cohesive energy density values were obtained from the literature[52] and in some cases were estimated based on similar materials or using group theory.[53] Figure 3 shows that these ideas work rather well for the range of systems examined here. Significantly more systems must be tested to establish the general power of this approach, which is analogous to the highly successful regular solution theory for bulk miscibility. It is important to note that there are significant limitations to this approach, including the error caused by specific interactions and estimation of surface area based on particle size. Nevertheless, it is encouraging to see the correlative ability of these ideas in understanding the behavior of T_g.

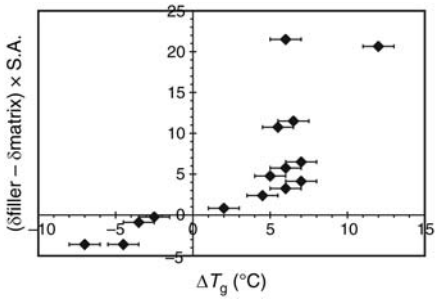

Figure 3. Plot showing the effect of the difference in the solubility parameters multiplied by the surface area as a function of glass-transition temperature. The glass-transition data include melt-processed ZnO/polystyrene[50] and calcium carbonate/poly(methyl methacrylate) composites[51] with several surface modifications as well as data generated by our group on solution-processed silica/polystyrene nancomposites using both as-received and fluorinated 15-nm silica.[64]

Entropic Control of Interfacial Properties

Wettability can also be controlled by entropy. Consider cases, therefore, where enthalpic interactions are minimized, such as when nanofillers with long-grafted polymer chains are placed in matrices of the same chemistry. This problem is essentially that of the wetting properties of curved brushes, especially when the particle sizes are in the nanoscale. Until a decade ago, most theoretical efforts in this area modeled flat surfaces and then accounted for the particle curvature at the level of the Derjaguin approximation. Although this approach should work for micron-scale particles, it is likely to be incorrect for spherical nanoparticles. More recent theories have recognized this fact and have explicitly accounted for the role of curvature in both theory[11,54] and simulations.[55] For chains grown from curved surfaces, the effective crowding decreases with increasing distance from the surface, because the volume available to the polymer segments increases with the square of the distance from the particle center. Thus, even though chains may be strongly extended at the particle surface, they may locally assume Gaussian conformations some distance away.[56]

Whereas this diminished crowding issue is well appreciated when curved brushes are placed in a small molecule solvent, the corresponding behavior in the presence of polymeric solvents is not clear. For flat surfaces and a given graft chain length, N_G, there exists a critical matrix length, N_{matrix}, beyond which free melt chains will not wet the brush. This autophobic dewetting effect is purely entropic in origin when the grafted and matrix chains are chemically identical and represents a balance of two competing tendencies. Wetting is favored because the system gains translational entropy by mixing brush chains with the matrix. This is balanced by the loss of entropy of the melt chains when they are placed in the geometrically crowded environment of the stretched brush. Theory and some experiments show[11] that this transition occurs when $N_{matrix} \approx N_G$ for the case of flat brushes.

Self-consistent mean-field calculations[57] for the wetting behavior of polymer melts on spherical surfaces with grafted polymer chains were used to explore the consequences of particle curvature.[58] The roles of brush molecular weight, brush density, and the particle radius of curvature were systematically explored while examining long-enough matrix chains to remain in the limit of infinite matrix molecular weight. Although the system has no net "excess" enthalpic interactions between the grafted polymer and the matrix homopolymer, there is an effective mean-field interaction (χ_{eff}) that arises because of the entropic penalty associated with the interface formed between the brush and the matrix chains. The effective mean-field interaction is estimated following the ideas of Helfand,[59] and the results show that for a fixed grafted chain length and grafting density, the interaction parameter becomes smaller with decreasing particle radius. Further, it scales with N_G as $\chi_{eff} \sim N_G^{-1.1}$ (Figure 4). Flory's theory for bulk miscibility[60] suggests that the grafted chains and matrix chains will mix if $N_{matrix} \leq N_G^{+1.1}$. This result is very similar in functional form to that derived for planar brushes,[5] except that the prefactors ignored in this scaling analysis are strongly dependent on particle radius.[61] This theoretical result suggests that longer grafted chains (i.e., higher N_G) indeed will be more wettable. Furthermore, miscibility is enhanced for smaller particles—a significant result, as it is hard to mix polymers with small bare nanoparticles.[62] Thus, these theoretical results confirm the hypothesis that the use of brushes should enable the facile tuning of the interfacial properties of these nanoparticles, presumably facilitating the creation of nanocomposites with any desired structure and properties.

Recent preliminary experiments lend credibility to the assertion that the wetting

behavior of the particles can be controlled by the use of grafted polymer chains.[62] Dense polystyrene chains were grown on silica particles with a nominal diameter of 14 nm using reversible addition-fragmentation, chain-transfer (RAFT) polymerization.[46,47] This method enables simultaneous control of both σ (0.05–0.8 chains/nm^2) and N_G (to molecular weights of more than 100,000 g/mol) of the grafted polymer without sacrificing the polydispersity index (PDI, <1.2) of the resulting chains. Figure 5 shows the effect of changing N_{matrix} with σ ≈ 0.27 chains/nm^2.[63] For N_{matrix}/N_G ratios of >1, the polystyrene matrix dewetted the particles and the glass-transition temperature of the matrix was reduced. For ratios <1, partial wetting and an increase in T_g were observed. This suggests that the controlling variable is N_{matrix}/N_G for the case of a fixed σ. Figure 5b shows a study[64] in which the N_{matrix}/N_G ratio was held constant and the σ was changed. The plot is the change in glass-transition temperature as a function of σN_G. It is encouraging to see that the data appear to follow an apparently universal law across this limited range. Although these are interesting results, it is not clear from theory what the scaling laws should be, and this is only a hint of the work that must be done to achieve understanding.

Relationship between Local Interface Behavior and Macroscopic Properties

So far, the focus has been on the first set of questions posed in the introduction. Reflecting on the second set of questions requires that two issues be understood: first, how do the nanoscale interactions at the particle/polymer interface affect the dispersion of the particles? This is particularly important, because it has been suggested that the mechanical (and presumably other macroscopic) properties of the resulting composites are sensitively determined by dispersion.[65] It has been recently appreciated across a wide range of systems (mainly micelles, star polymers, and more recently, particles with grafted brushes) that particle dispersion in polymer matrices is facilitated when the molecular weight of the polymer matrix is smaller than the brush chains.[66–68] However, it is unclear at this time if this result represents the equilibrium state of the system, or rather reflects the role of processing. This is highlighted in particular by the work of Bansal et al.,[63] who found that particles dispersed into matrices even when the matrix chains were much longer than the brush (i.e., even when the matrix did not wet the brush). Whereas this has become a topic of considerable interest in the community, with several unanswered issues, it is perhaps equally important that the relationship between the particle dispersion and macroscopic properties is not quantitatively understood at this time. Understanding this relationship, which is the second unanswered question, requires the development of multiscale models/experiments that can bridge across these scales. The use of micromechanical models can be helpful in predicting mechanical properties;[69] however, to design composites from the molecular scale to the macroscale, the role of the particle surface on interface region properties must be included not only for macroscopic property prediction[70,71] but to predict dispersion,[72] phase segregation,[73] and polymer crystalline structure.[74] Such multiscale tools are extremely challenging to develop[75,76] and require not only modeling/experiments at all scales, but bridging across these scales. These next few years will be exciting as this field continues to emerge and we begin quantitative design of nanocomposites.

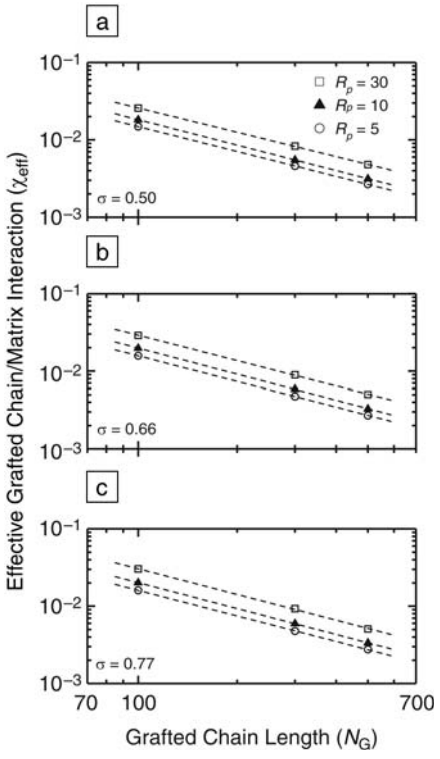

Figure 4. Plot of the effective interaction parameter, χ_{eff}, for a matrix of effectively infinite molecular weight as a function of graft chain length. The three plots correspond to three different grafting densities, (a) σ = 0.50, (b) σ = 0.66, and (c) σ = 0.77, where in each plot the three lines correspond to three different particle diameters. These diameters are in units of lattice units, where each site is ~1 nm. The dashed lines show that $\chi_{eff} \sim N_G^{-1.1}$.[57]

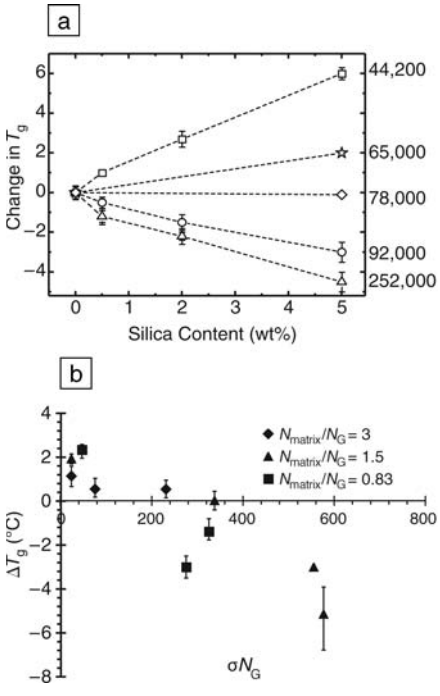

Figure 5. Plots of (a) the change in glass-transition temperature (ΔT_g) as a function of SiO_2 concentration for silica nanoparticles with 110,000 g/mol polystyrene on the surface, graft density of 0.27 chains per nm^2, and matrix of various molecular weights (in g/mol), shown at the right in the Figure. Dashed lines are a guide for the eye.[63] (b) The change in glass-transition temperature T_g for polystyrene-grafted silica/polystyrene nanocomposites as a function of the graft density σ, multiplied by the chain length of the grafted chain N_G.[64]

Summary and Conclusions

Our results unequivocally point to the critical role played by the polymer–particle interface in controlling the local polymer structure in polymer nanocomposites. This article demonstrates that both in the cases where energetic interactions dominate and for particles with long-chain brushes (where entropic factors are crucial), the thin-film literature and traditional-composites literature can provide significant insight. While this work has provided a brief overview of current developments in this field, it is important to stress that much more experimental information is required to gain a thorough fundamental understanding. More effort must be expended in understanding how these nanoscale interactions affect the macroscopic properties of

nanocomposites, a nascent area of research that is expected to be crucial in designing materials for use in any desired application.

Acknowledgments

The authors thank the Nanoscale Science and Engineering Initiative of the National Science Foundation under NSF award DMR-0117792. S. Kumar also thanks the NSF Division of Materials Research for funding the work reviewed in this article. Finally, the authors thank several people who provided insight and feedback on the thoughts presented in this article, including S. McKnight, R. Vaia, and E. Manias as well as C. Li.

References

1. M.M.J. Treacy, T.W. Ebbesen, J.M. Gibson, *Nature* **381**, 678 (1996).
2. P.M. Ajayan, P.V. Braun, L.S. Schadler, *Nanocomposite Science and Technology* (Wiley, Weinham, Germany, 2003) chap. 2.
3. A.T. Dibenedetto, *Mater. Sci. Eng. A* **302**, 74 (2001).
4. L.T. Drzal, M.J. Rich, and M.F. Koenig, *J. Adhesion* **16**, 33 (1983).
5. S. Granick et al, *J. Polym. Sci., Part B: Polym. Phys.* **41**, 2755 (2003).
6. R.L. Jones et al., *Nature* **400**, 146 (1999).
7. S.K. Kumar, M. Vacatello, and D.Y. Yoon, *J. Chem Phys.* **89**, 5206 (1988).
8. X. Zheng et al., *Phys. Rev. Lett.***79**, 241 (1979).
9. B. Frank et al., *Macromolecules* **29**, 6531 (1996).
10. W. Ding et al., *Nano Lett.* **3**, 1593 (2003).
11. I. Borukhov, L. Leibler, *Macromolecules* **35** (13), 5171 (2002).
12. R.A. Vaia, E.P. Giannelis, *Macromolecules* **30** (25), 8009 (1997).
13. T.W. Chou, *Microstructural Design of Fiber Composites* (Cambridge University Press, New York, 1992).
14. D. Gay, S.V. Hoa, S.W. Tsai, *Composite Materials: Design and Applications* (CRC Press, New York, 2003).
15. T. Reiter, G.J. Dvorak, V. Tyergaard, *J. Mech. Phys. Solids* **45**, 1281 (1997).
16. Z. Hashin, *J. Appl. Mech.* **50**, 481 (1983).
17. R.M. Christensen, *J. Mech. Phys. Solids* **38**, 379 (1990).
18. M.G. Bader, W.H. Bowyer, *J. Phys D: Appl. Phys.* **5**, 2215 (1972).
19. K.C. Yung, J. Wang, T.M. Yue, *J. Reinf. Plast. Compos.* **25**, 847 (2006).
20. A.B. Dalton et al., *Nature* **423**, 703 (2003).
21. J.D.H. Hughes, *Compos. Sci. Tech.* **41**, 13 (1991).
22. A.B. Pangelinan, R.L. McCullough, M.J. Kelley, *J. Polym. Sci., Part B: Polym. Phys.* **32**, 2383 (1994).
23. D.H. Droste, A.T. Dibenedetto, *J. Appl. Polym. Sci.* **13**, 2149 (1968).
24. N.R. Sottos, R.L. McCullough, *Flight-Vehicle Mater. Struct. Dyn.—Assess. Future Directions* **2** (2), 328 (1994).
25. J.A. Forrest, K. Dalnoki-Veress, *Adv. Colloid Interface Sci.* **94**, 167 (2001).
26. J.H. van Zanten, W.E. Wallace, W.-L. Wu, *Phys. Rev. E* **53** (3), R2053 (1996).
27. G.B. DeMaggio et al., *Phys. Rev. Lett.* **78**, 1524 (1997).
28. J.L. Keddie, R.A.L. Jones, R.A. Cory, *Faraday Discuss.*, **98**, 219 (1994).
29. J.A. Forrest, J. Mattsson, *Phys. Rev. E* **61**, R53 (2000).
30. L. Singh, P.J. Ludovice, C.L. Henderson, *Thin Solid Films* **449**, 231 (2004).
31. A. Bansal et al., *Nature Mater.* **4**, 693 (2005).
32. C.J. Ellison, R.L. Ruszkowski, N.J. Fredin, J.M. Torkelson, *Phys. Rev. Lett.* **92**, 119901 (2004).
33. C.J. Ellison, J.M. Torkelson, *Nature Mater.* **2**, 695 (2003).
34. B.J. Ash, L.S. Schadler, R.W. Siegel, *Mater. Lett.* **55** (1–2), 83 (2002).
35. C. Becker, H. Krug, H. Schmidt, in *Mater. Res. Soc. Symp. Proc.*, B.K. Coltrain, C. Sanchez, D.W. Schaefer, G.L. Wilkes, Eds. (Materials Research Society, Pittsburgh, PA, 1996), vol. 435, pp. 237–241.
36. M. Alcoutlabi, G.B. McKenna, *J. Phys.: Cond. Matter* **17**, R461 (2005).
37. W.-L. Wu, W.E. Wallace, J. Van Zanten, in *Mater. Res. Soc. Symp. Proc.*, T.-M. Lu, S.P. Murarka, T.-S. Kuan, C.H. Ting, Eds. (Materials Research Society, Pittsburgh, PA, 1995) vol. 381, pp. 147–151.
38. E.P. Pluddemann, *Silane Coupling Agents* (Plenum Press, New York, ed. 2, 1991).
39. E. Bourgeat-Lami, *J. Nanosci. Nanotech.* **2**, 1 (2002).
40. O. Prucker, J. Ruhe, *Macromolecules* **31**, 592 (1998).
41. J. Pyun, K. Matyjaszewski, *Chem. Mater.* **13**, 3436 (2001).
42. R.C. Advincula, *J. Dispersion Sci. Tech.* **24**, 343 (2003).
43. S.G. Boyes et al., *Surf. Sci.* **570**, 1 (2004).
44. S. Edmondson, V.L. Osborne, W.T.S. Huck, *Chem. Soc. Rev.* **33**, 14 (2004).
45. Y. Tsujii et al., *Adv. Polym. Sci.* **197**, 1 (2006).
46. C. Li, B.C. Benicewicz, *Macromolecules* **38**, 5929 (2005).
47. C. Li, B.C. Benicewicz, *Macromolecules* **39**, 3175 (2006).
48. M.E. Mackay et al., *Science* **311**, 1740 (2006).
49. J.L. Gardon, *J. Phys. Chem.* **67**, 1935 (1963).
50. M. Avella, M.E. Errico, G. Gentile, *Macromol. Symp.* **234**, 170 (2006).
51. C.-C.M. Ma, Y.-J. Chen, H.-C. Kuan, *J. Appl. Polym. Sci.* **98**, 2266 (2005).
52. A. Navrotsky, *Geochem. Trans.* **4**, 34 (2003).
53. D.W. Van Krevelen, *Properties of Polymers* (Elsevier, Amsterdam, 1980).
54. E.G. Zhulina, T.M. Birshtein, O.V. Borisov, *Eur. Phys. J. E* **20**, 243 (2006).
55. J. Klos, T. Pakula, *Macromolecules* **37**, 8145 (2004).
56. D.A. Savin et al., *J. Polym. Sci. B: Polym. Phys.* **40**, 2667 (2002).
57. S.E. Harton, S.K. Kumar, *Macromolecules* (2007) in review.
58. J.M.H.M. Scheutjens, G.J. Fleer, *J. Phys. Chem.* **83**, 1619 (1979).
59. E. Helfand, *Macromolecules* **25**, 1676 (1992).
60. P.J. Flory, *J. Chem. Phys.* **9**, 660 (1941).
61. E. Raphaël, P. Pincus, G.H. Fredrickson, *Macromolecules* **26**, 1996 (1993).
62. D. Ciprari, K. Jacob, R. Tannenbaum, *Macromolecules* **39** 6565 (2006).
63. A. Bansal, *J. Polym. Sci. B: Polym. Phys.* **44**, 2944 (2006).
64. S.L. Lewis, PhD thesis, Rensselaer Polytechnic Institute, Troy, NY (2006).
65. Z.Y. Zhu et al., *Macromolecules* **38**, 8816 (2005).
66. M.K. Corbierre, *Langmuir* **21**, 6063 (2005).
67. R. Hasegawa, Y. Aoki, M. Doi, *Macromolecules* **29**, 6656 (1996).
68. F.J. Esselink et al., *Phys. Rev. B* **48**, 13451 (1993).
69. C. Li, T.-W. Chou, *Compos. Sci. Tech.* **66**, 2409 (2006).
70. F.T. Fisher, L.C. Brinson, *Compos. Sci. Tech.* **61**, 731 (2001).
71. O. Borodin et al., *J. Polym. Sci. B: Polym. Phys.* **43**, 1005 (2005).
72. R. Hasegawa, Y. Aoki, M. Doi, *Macromolecules* **29**, 6656 (1996).
73. B. Jiang, C. Liu, C. Zhang, B. Wang, Z. Wang, *Compos. Part B: Eng.* **38**, 24 (2007).
74. Z. Xiao et al., *J. Polym. Sci. B: Polym. Phys.* **44**, 1084 (2006).
75. V.A. Buryachenko, *Compos. Sci. Tech.* **65**, 2435 (2005).
76. P.K. Valavala, G.M. Odegard, *Rev. Adv. Mater. Sci.* **9**, 34 (2005). □

Strategies for Dispersing Nanoparticles in Polymers

Ramanan Krishnamoorti

Abstract

Controlling the dispersion of nanoparticles in polymeric matrices is the most significant impediment in the development of high-performance polymer nanocomposite materials and results primarily from the strong interparticle interactions between the nanoparticles. This review examines the theoretical and experimental strategies employed in developing appropriate chemical and physical methods to achieve controlled dispersion of nanoparticles. Methods to characterize the state of dispersion, including force and electron microscopy, and scattering, electrical, and mechanical spectroscopy, are considered with special emphasis on achieving quantitative measures of the dispersion. Some of the outstanding issues, such as long-term aging and the implication for the dispersion of nanoparticles, development of high-throughput methods for rapid screening, and methods for in-line monitoring, are also discussed.

Introduction

The dispersion of nanoparticles in polymeric matrices is the fundamental challenge surrounding the development of polymer nanocomposites. In addition to the development of methods to characterize the dispersions of the nanoparticles (challenged by the multitude of hierarchical length scales), techniques for dispersing aggregated or ordered nanoparticles while not compromising the inherent advantages of the nanoparticles (such as their unique mechanical, thermal, and optical properties and extremely large internal surface area) remain a significant challenge.

The interparticle interactions are clearly a function of the chemical nature of the nanoparticles, with the shape of the nanoparticles, the distance between the nanoparticles, and the polydispersity of particle sizes being the most prominent secondary contributors. Israelachvili has summarized the interaction laws for different particles in vacuum (Table I), and these reveal the strong dependence of the interaction energies on the shape and aspect ratio of the nanoparticles.[1] Further, many nanoparticles form low-dimensional crystals or tight agglomerates that render their dispersion even more difficult. For instance, single-wall carbon nanotubes (SWNTs) have strong van der Waals interactions, resulting in parallel alignment and formation of a triangular lattice with an interaction energy of ~500 eV/μm of nanotube length,[2,3] which is partially responsible for the lack of dispersability of pristine SWNTs. The lack of dispersability of carbon nanotubes is illustrated by considering the concentrations of the nanotubes dispersible in a range of solvents, as shown in Table II.[4] A second example of the strong interactions between nanoparticles is observed in layered silicates, where it has recently been estimated that the cleavage energy for an unmodified montmorillonite is ~133 mJ/m^2, whereas for a similar octadecyl ammonium-modified montmorillonite (where the layers are an additional two nm apart), it is ~40 mJ/m^2, in excellent agreement with experiments.[5] Finally, for chemically identical materials, progressing from spherical nanoparticles (zero-dimensional) to cylindrical nanorods (one-dimensional) to nanoscale-thick sheets (two-dimensional) increases the energy of interaction per pair of nanoparticles and, therefore, increases the complexity of dispersion in a matrix polymer.

Thermodynamic Aspects of Dispersion

Mean-field, self-consistent field (SCF) with field theoretical and simulation methods have been used to understand the dispersion of nanoparticles in solvents and polymeric matrices. The most primitive model for dispersion of stiff rod-like moieties was considered by Onsager[6] and relied exclusively on entropic arguments to indicate that such stiff 1D materials even in the absence of attractive interparticle interactions would undergo an isotropic to nematic transition above a volume fraction that roughly scales as $1/x$, where x is the aspect ratio of the rod. This rather simplistic view captures many of the features associated with the attempted dispersion of carbon and boron nitride nanotubes, wherein extremely limited solubility of these materials is observed in many different small-molecule dispersants.

Vaia and Giannelis[7] have used a simple lattice-based thermodynamic model that examined the entropic and enthalpic contributions during the formation of a polymer layered-silicate nanocomposite to examine the driving forces for intercalation and exfoliation of organically modified layered silicates by long-chain polymers. In their estimation, despite the expected loss of conformational entropy of the confined polymers (even in an exfoliated system, as the free energy calculations are based per unit surface area of the silicate), the gain in conformational entropy of the surfactant tails compensates and leads to the primary conclusion that the enthalpy of the mixing process dominates the free energy considerations. Using the interfacial tension-based formalism of van Oss et al.,[8] Vaia and Giannelis[7] developed an expression for the enthalpy that contains contributions from both van der Waals interactions and polar (Lewis acid/base) interactions. Of these two sets of interaction terms, only the Lewis acid/base term could lead to a favorable enthalpy of mixing; this, combined with the fact that montmorillonite and other layered silicates have a considerable Lewis acid/base contribution, is the dominant thermodynamic driving force for the dispersion of layered silicates in a polymer matrix. This simple lattice-based model provides a straightforward understanding of the structural and chemical changes in the polymer or the surfactant used to functionalize the layered silicates that control dispersion and provides a first understanding of the complex role of thermodynamics in determining the dispersion of nanoparticles in polymers.

Table I: Interaction Laws for Different Particles.[1]

Type of Nanoparticle	van der Waals Interaction Energies
Two spheres (radii, R_1 and R_2) separated by distance D	$W = -\frac{A}{6D}\left(\frac{R_1R_2}{R_1+R_2}\right)$
Two parallel cylinders (radii, R_1 and R_2) separated by a distance D and of length L	$W = -\frac{AL}{12\sqrt{2}D^{3/2}}\left(\frac{R_1R_2}{R_1+R_2}\right)^{1/2}$
Two crossed cylinders (radii, R_1 and R_2) separated by a distance D	$W = -\frac{A}{6D}(R_1R_2)^{1/2}$
Two parallel plates separated by a distance D	$W = -\frac{A}{12\pi D^2}$

Notes: A (Hamaker constant) = $\pi^2C\rho_1\rho_2$, where C is the coefficient in the atom–atom pair potential, and ρ_1 and ρ_2 are the number of atoms per unit volume.

Table II: Room-Temperature Solubilities of Single-Wall Carbon Nanotubes.[4]

Solvent	Solubility in mg L^{-1}
1,2-dichlorobenzene	95
Chloroform	31
1-methylnapthalene	25
1-bromo-2-methylnapthalene	23
N-methylpyrrolidinone	10
Dimethylformamide	7.2
Tetrahydrofuran	4.9
1,2-dimethylbenzene	4.7
Pyridine	4.3
Carbon disulfide	2.6
1,3,5-trimethylbenzene	2.3
Acetone, ethanol, 1,3-dimethylbenzene, 1,4-dimethylbenzene, toluene	<1

A recent model by Mackay et al.[9] has suggested that the dispersion of nanoparticles in a polymer is a result of favorable enthalpy of mixing resulting from the increased molecular contacts between the polymer and the dispersed nanoparticle as compared with the case of aggregated nanoparticles, because of the increased accessible area on the nanoparticle caused by dispersion. Their results indicate that nanoparticles prepared from cross-linked polymers are capable of dispersing in polymers if the size of the nanoparticle is smaller than the radius of gyration of the polymer matrix. The effect, as elucidated by these authors, is only expected in nanoparticles and vanishes at the two limits of extremely small particles as well as for macroscopic particles. It is not readily obvious how these ideas can be extended to the case of nonporous spherical nanoparticles, functionalized spherical nanoparticles, and anisotropic porous and nonporous nanoparticles.

Schweizer and co-workers have used the polymeric reference interaction site model, a theory shown to work excellently to predict the phase behavior of polymer blends, to understand the thermodynamic behavior of nanocomposites comprising flexible polymers and spherical nanoparticles.[10] Miscibility is predicted as a result of a steric stabilization mechanism that results from a small polymer coating strongly adsorbed onto the nanoparticle. Interestingly, they note that the miscibility is relatively independent of polymer molecular weight for weak polymer–nanoparticle interactions, and in the case of strong bridging-induced attraction, an increase in miscibility is observed with increasing molecular weight.

Balazs and co-workers[11,12] have pioneered a method that uses SCF theory based on the theory of Scheutjens and Fleer to calculate the nanoscale interactions and act as input for a density functional theory (DFT), based on the Somoza–Tarazona formulation for anisotropic nanoparticles, that is then used to calculate the equilibrium behavior (phase diagram) of nanocomposites, especially those based on layered silicates. One efficient strategy that they discovered for the dispersion of the clay layers was using mixtures of majority non-functionalized (non-interacting) polymers and a small volume fraction of end-functionalized chains that, depending on the strength of the attractive interaction between the terminal group and the surface, could lead to immiscible, gel-like, and exfoliated structures with increasing attraction between the functionalized polymer and the nanoparticle.

Molecular dynamics (MD) and Monte Carlo simulations were used to understand the dispersion of nanoparticles—especially those of spherical nanoparticles and, to some extent, those of layered silicates and carbon nanotubes. Glotzer and co-workers have examined the mechanism of nanoparticle clustering in a dense non-entangled polymer melt using MD simulations of polyhedral nanoparticles.[13] Their results indicated that the dispersed-to-clustered-state transition was more akin to equilibrium polymerization than a first-order transition such as crystallization. On the other hand, coarse-grained MD simulations of stacks of platelets in a polymer melt indicate that the sliding of the platelets could lead to the breakdown of the platelet stacks; for kinetic reasons, these simulations required the use of non-functionalized (non-attractive) polymers blended with end-functionalized chains.[14] These simulation results are quite similar to the theoretical ones predicted by Ginzburg and Balazs using equilibrium phase diagram calculations based on SCF and DFT methods.[11] Nevertheless, as a result of the hierarchy of length scales and the importance of interparticle and matrix–nanoparticle interactions, it is clear that in order for such simulation methods to play a significant role in the development of dispersion methodologies in polymer nanocomposites, methods such as those employed in multiscale modeling[15] must be incorporated.

Experimental Strategies to Disperse Nanoparticles in Polymeric Matrices

Some of the most prominent methods to achieve dispersion of nanoparticles in polymer matrices have included functionalization of nanoparticles using weak (van der Waals, π-stacking) interactions, ionic interactions, and covalent functionalization. The use of surfactants and polymers interacting with weak forces with nanoparticles has received much attention in dispersing nanoparticles because of significant discoveries in the dispersion of carbon[2] and

boron nitride (BN)[16] nanotubes and, more recently, in the use of nanoemulsions to disperse single nanoparticles. This method clearly preserves many of the attractive properties of the nanoparticles, and in some cases, the stabilizing surfactant or polymers can be removed after dispersion. A good example of this method is the non-covalent supramolecular modification of carbon nanotubes (CNTs) by poly(*m*-phenylenevinylene)-*co*-(2,5-dioctoxy-*p*-phenylenevinylene) (PmPV)–based polymers and starch-based amylose polymers,[17] resulting in CNT dispersion in organic and aqueous solutions, respectively. In the case of the helical amylose, the CNTs are soluble in an aqueous solution of amylose–iodine complex by simultaneous favorable enthalpic interactions and entropy gain as the iodine is released from the complex.[17] Such an entropic–enthalpic combination to achieve dispersion is similar to that observed for many ionic polymers intercalating and exfoliating pristine clays in the presence of water. Recently, PmPV was used to disperse BN nanotubes in chloroform and other organic solvents,[16,18] and it is thought that the mechanism for dispersion is similar to that observed in non-covalent supramolecular modification of CNTs.

On the other hand, for the case of surfactant-assisted stabilization of CNTs, it has been observed that the solubilization occurs for anionic, cationic, and non-ionic surfactants at concentrations significantly lower than the critical micelle concentration. The mechanisms for such dispersion are speculated to be by the formation of rod-like micelles with the nanoparticle embedded at the core of the micelle, the formation of hemi-micelles on the outside of the nanoparticles, and the random adsorption of the surfactants onto the nanotubes. Although direct imaging using electron microscopy appears to be ambiguous regarding the dispersion mechanism, small-angle neutron scattering measurements suggest that random (disordered) adsorption of the surfactant is responsible for the dispersion,[19] and these measurements have been supported recently by computer simulation studies. Regardless of the dispersion mechanism, this use of surfactants and polymers interacting with weak forces with nanoparticles has been a powerful method to disperse nanotubes in solvent and polymeric matrices.

Ionic and covalent functionalization of nanoparticles has been perhaps one of the most extensively studied methods for the dispersion in polymer matrices. For instance, hydroxyl-terminated silica nanoparticles have been treated with organosilanes, and naturally occurring and synthetic layered silicates with hydrated metals populating the interlayer galleries have been ion-exchanged with cationic surfactants with long alkyl or aromatic groups to render them hydrophobic and organophilic. On the other hand, for the case of fullerenes and CNTs, covalent functionalization has proven to be a significant step toward increased solubilization and enhanced compatibility with a range of polymers. The covalent functionalization of CNTs has been reviewed extensively and is not detailed here.[20] The fullerene caps at the ends of the nanotubes are significantly more reactive than the side walls and were initially exploited to attach functional groups. More recently, the development of *in situ* generation and the reaction of organic diazonium compounds with nanotubes in the presence and absence of dispersing solvents and dispersing aids,[21,22] the functionalization by the use of free-radicals,[23] and direct fluorination[24] have enabled and enhanced the possible routes for developing well-dispersed polymer nanocomposites with CNTs.

Aside from the physical mixtures of such functionalized nanoparticles with polymer matrices, two interesting strategies of enhancing dispersion and interactions (physical and mechanical) between the nanoparticle and the matrix are "grafting-to" the nanoparticles with functional polymers and "grafting-from" the nanoparticles with radical, condensation, ring opening, or living or controlled polymerization processes. In fact, one of the pioneering polymer nanocomposites of nylon-6 with layered silicates was developed by the use of ring-opening polymerization with the initiator tethered to the layered silicate by ionic interactions.[25]

The development of controlled radical polymerization methods, such as atom transfer radical polymerization, nitroxide-mediated processes, and degenerative transfer methods, has diversified the range of monomers, functionality, composition, and dimensions of the macromolecules and the derived nanocomposites.[26] The tethering of well-defined polymers to nanoparticles (curved or flat) by grafting-to and grafting-from methods has been successfully demonstrated with thin films of hybrids in which the silica nanoparticles demonstrate a remarkable ordered 2D array, with the interparticle spacing dependent on the size of the tethered polymer chains.[26] Similarly, the grafting of tethered polymers from layered silicates by the use of ionic interactions and controlled polymerization methods has led to an efficient mechanism to ensure dispersion of these nanoparticles in matrices where only demixed or intercalated states were possible using solution and melt processing methods.[27]

Mechanical stresses generated by melt-state shear,[28] ultrasonication in solution,[29,30] and solid-state pulverization[31,32] are extremely effective in the dispersion of aggregated nanoparticles. In particular, ultrasonication has proven extremely popular in the dispersion of CNTs and is one of the few physical methods useful in the dispersion of nanotubes despite the known shortening of the CNTs when subjected to powerful ultrasonication.[30] On the other hand, melt-state processing in conventional polymer processing equipment such as twin-screw extruders results in large shear (and in some cases extension), leading to breakdown of the nanoparticle agglomerates and subsequent individualization and dispersion of the nanoparticles in the polymer matrix. Paul and co-workers[28] have provided an elegant summary of the mechanism for the shear-assisted dispersion of layered silicates in a polymer matrix as shown in Figure 1. This mechanism is similar to the shear-induced breakdown of the superstructure of carbon black and silica commonly observed during the processing of filled rubbers. However, for CNTs no such shear-induced dispersion has been demonstrated, which is perhaps reflective of the strong intertube interaction characteristic of CNTs. Solid-state pulverization at low temperatures provides a novel method to enable dispersion of nanoparticles and has been exploited by Vaia[31] and Torkelson[33] in dispersing layered silicates in polymer matrices. It has also been suggested that this method would be useful for the dispersion of nanotubes, although there is some evidence that suggests that ball milling of CNTs can lead to significant breakdown in the nanotube architecture.[34]

Recently, Schiraldi and co-workers have revived interest in the preparation of aerogels (and xerogels) of nanoparticles and followed it with infiltration by a polymer for the preparation of polymer nanocomposites, thereby avoiding the traditional thermodynamic and kinetic barriers.[35] Extensive work was performed on the development of ultralight, extraordinarily insulating silica aerogel-based polymer nanocomposites where sol-gel processing is combined with guest polymer, monomer, or nanoparticle inclusion followed by supercritical extraction of the solvent.[36] Extending this work, Schiraldi and co-workers[35] exploited freeze-drying of a clay dispersion in deionized water to create a clay aerogel with a density of 0.05 g/cm^3, followed by infiltration by *n*-isopropylacrylamide and subsequent *in situ* polymerization and cross-linking, resulting in a material that was a low-density, thermally responsive hydrogel composite.[35]

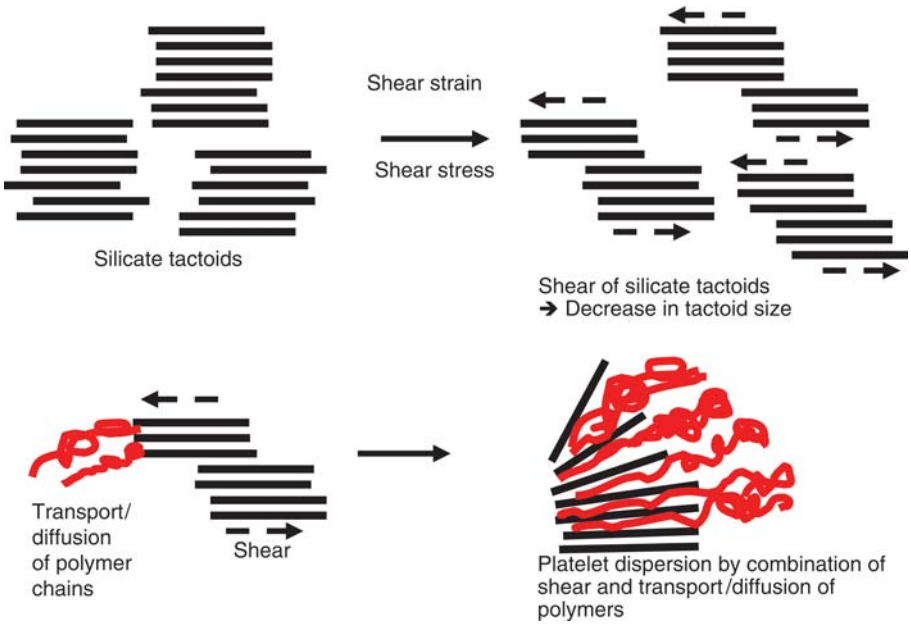

Figure 1. Proposed stepwise process of shear-assisted dispersion of layered silicates in a polymer matrix.[28] Shear is thought to break up the silicate tactoids (micron-sized clusters of silicate aggregates) by a sliding mechanism, consistent with computer simulations.[14] Then, acting in conjunction with the transport/diffusion of the polymer chains, shear enables the dispersion of individual nanometer-thick layers.

Characterization of Dispersion States

The most prominent ways to quantitatively characterize the dispersion state of nanocomposites include microscopy (electron and force), scattering (x-ray, neutron, and light), chemical spectroscopic methods, electrical and dielectric characterization, and mechanical spectroscopy. Although clearly dependent on the details of the nanoparticle, each of these methods can provide unique information on the state of dispersion, ranging from nanometer to micrometer in size scale, and, therefore, they are typically used in combination to provide detailed information on the hierarchical morphology usually present in such nanocomposites.

Electron microscopy has been most extensively used to determine the nanoscale dispersion in different nanocomposites and, in many cases, to qualitatively demonstrate the development of well-dispersed systems. The pioneering work of Gilman, Paul, and Vermogen et al.[37,38] demonstrated the quantitative interpretation of electron micrographs for the case of layered silicate-based nanocomposites by image analysis of several tens of micrographs (Figure 2). This work enabled a direct correlation of the nanoscale dispersion to macroscopic property measurements (mechanical, transport, and flame retardance). Many of these methods have been extended for the use of atomic force microscopy methods in characterizing dispersions of nanotubes and spherical nanodispersions in polymers and require many sets of images and detailed data analysis. Additionally, the development of three-dimensional reconstruction,[39] stereology, and high-resolution transmission electron microscopy and scanning electron microscopy methods[40] have all enabled significant improvements in the understanding of the 3D distribution and dispersion of the nanoparticles.

Radiation scattering and diffraction methods were applied to quantify the dispersion state of the nanoparticles in the matrix.[41] While providing a global (ensemble) average of the dispersion, these methods necessarily require the development of an analytical/numerical model to provide quantitative information regarding the dispersion. X-ray diffraction (XRD) is an invaluable method to provide a first-cut examination of dispersion of layered compounds such as clays and graphene sheets (Figure 3), because of the periodicity of the stacking and the disruption of the stack upon complete dispersion. XRD is also able to provide orientation information in these and multiwall carbon nanotube nanocomposites.[42] Nevertheless, XRD is seldom used as the definitive proof of exfoliation even in those cases, because issues such as surface sensitivity and orientation of the platelets can result in ambiguous results. On the other hand, small-angle x-ray and neutron scattering (SAXS and SANS) have been used to understand the dispersion of nanoparticles such as clays and nanotubes. The extensive SAXS and SANS studies on aqueous dispersions of laponite (a synthetic layered silicate) and montmorillonite, under both static and flow conditions, enabled the generalization of the scattering theory for anisotropic nanoparticles to extract information on the dispersion and alignment of such layered silicates dispersions.[43] These have been extended to the case of organically modified layered silicates in organic solvents by Ho and co-workers using analogies to the analysis of dispersed lamellar block copolymers.[44] Vaia and co-workers further generalized this approach to develop a model that enables the existence of a broad distribution of fully dispersed and stacked platelets (with a distribution of numbers of platelets per stack) and therefore determines quantitatively the extent of dispersion.[45]

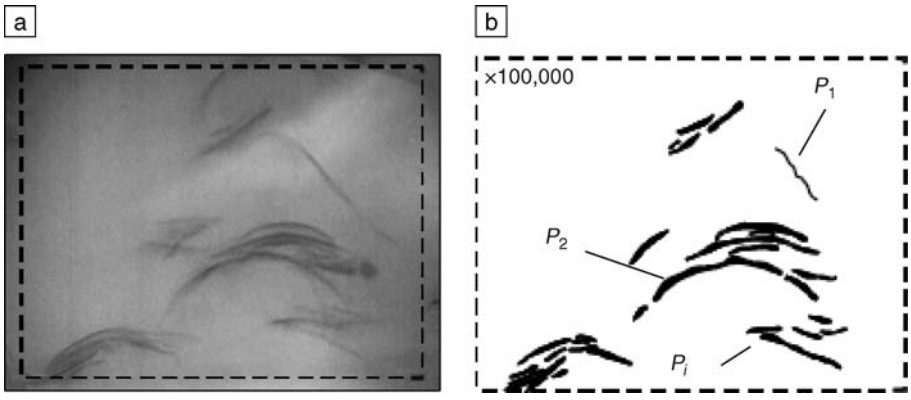

Figure 2. Quantitative analysis of (a) a layered silicate nanocomposite (imaged by transmission electron microscopy) using (b) image analysis methods described by Vermogen et al.[38] to describe the state of clay dispersion. P_i represents the particle number.

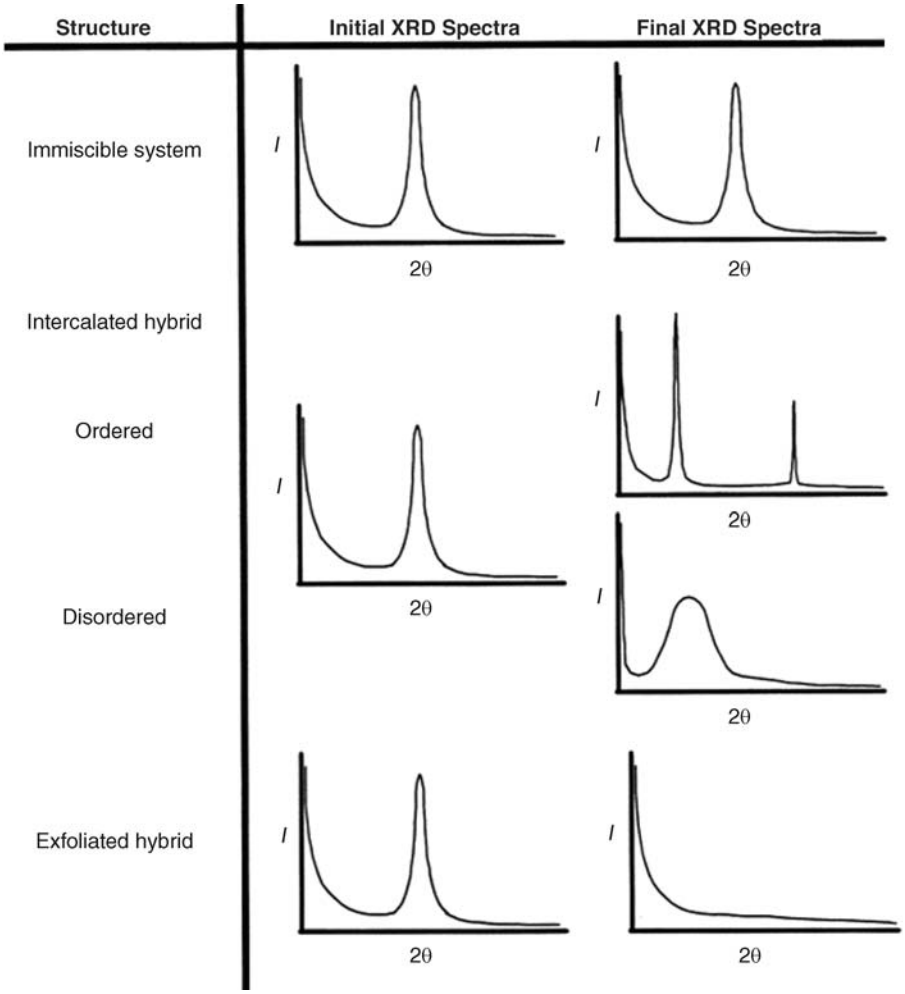

Figure 3. Schematic representation of the angular dependence of the x-ray diffraction (XRD) intensity for different states of dispersion of a layered silicate, from Vaia and Giannelis,[60] indicating the utility of XRD as an initial screening tool in determining the state of nanoparticle dispersion.

On the other hand, quantitatively understanding the dispersion of nanotubes in water, organic solvents, and polymers is still quite primitive.[46] Although it is expected that well-dispersed, non-interacting stiff rods (with length l and diameter d) would exhibit $I(\mathbf{q}) \sim \mathbf{q}^{-1}$ behavior [the scattering vector $\mathbf{q} = 4\pi/\lambda \sin(\theta)$, with λ and θ being the wavelength and half the scattering angle, respectively] for $\mathbf{q}$ values between $2\pi/l$ and $2\pi/d$,[47] there has been limited experimental proof for this scaling relationship.[48] The lack of proof is primarily a result of the low solubilities of CNTs and the uncertainties in guaranteeing well-dispersed and individualized states of the nanotubes in such dispersions.

Alternative measures of the dispersed state of nanoparticles have been sought by the use of chemical spectroscopic tools that are sensitive to local environments and confinement. For instance, Gilman and co-workers used the changes in absorption by organic dye molecules when subjected to changes in interactions and confinement to monitor the state of dispersion of clays in nanocomposites.[49] For the case of nanotubes, Strano and co-workers have demonstrated the use of fluorescence measurements to establish the state of dispersion of the nanotubes.[50]

On the other hand, two powerful macroscopic methods that have yielded significant quantitative measures of the dispersion of nanoparticles in nanocomposites have been mechanical spectroscopy and electrical (and dielectric) characterization. Whereas electrical characterization requires the use of inherently conductive nanoparticles, the rheological analogue to first approximation only requires differences in mechanical character between the matrix and the nanoparticle.[51] Focusing on the melt state (of the polymer or, equivalently, the liquid state of the matrix), a gradual transition from liquid-like to solid-like behavior with increasing nanoparticle concentration is observed in linear viscoelastic studies (Figure 4) and is thought to arise from the development of a geometrically percolated nanoparticle superstructure that exhibits many similarities to jammed and gel-like systems.[22,52–55] On the basis that the onset of solid-like behavior is a result of a geometrical percolation of the nanoparticles, the concentration for this percolation threshold can be used to determine the effective aspect ratio of the nanoparticles in the polymer matrix.[55,56] An important caveat in the use of rheology as a tool to gauge the mesoscale dispersion arises from the observation that such a solid-like response only develops in systems where the interactions between the matrix and the nanoparticles are strong and result in the development of a permanent network.[57]

Outlook

During the last ten years, the scientific and technological methods for dispersing and characterizing dispersions of nanoparticles in polymer matrices has significantly advanced, with the expectation that many of the current developments will lead to the ability to generalize these principles to arbitrary nanoparticles of differing chemical nature, size, shape, and aspect ratio that are becoming readily available as "designer" additives. In addition to the issues outlined here, there are three critical issues that need to be addressed for the successful commercial integration of such materials into materials manufacturing.

The first of these is related to slow "aging" processes during which the structure and properties of the nanocomposites change significantly. Considering the 3D hierarchical nature of the nanocomposites created, the size scale of the well-dispersed nanoparticles that leads them to exhibit both Brownian and non-Brownian dynamics in many cases and the strong and, in some cases, long-range interactions between the nanoparticles render this a crucial scientific issue to be understood. Clearly, accelerated testing methods, well developed for polymeric and polymer composite materials, are well suited to pursue for polymer nanocomposites. However, structural characterization that examines the dispersion and alignment state of nanoparticles must be an integral aspect of such considerations.[58]

The second critical aspect for the development of commercially successful nanocomposites is the integration of high-throughput testing methodologies, which

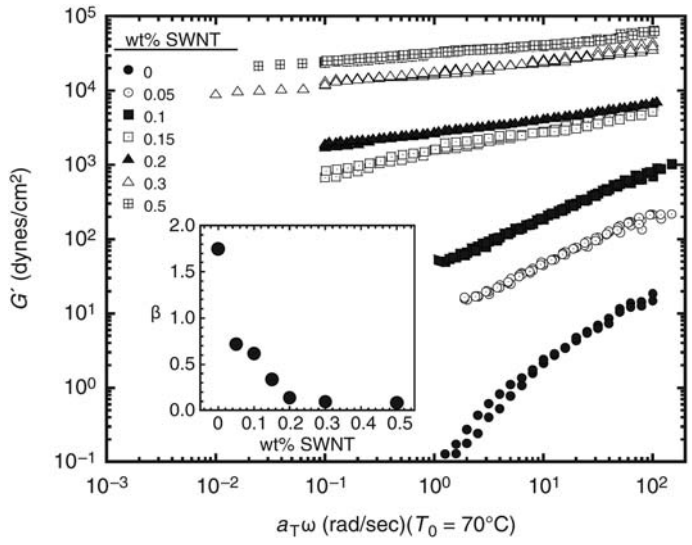

Figure 4. Use of melt-state rheology to demonstrate the development of a solid-like, geometrically percolated network structure. Linear dynamic storage modulus (G') as a function of reduced frequency $a_T\omega$ (where a_T is the temperature-dependent frequency shift factor and ω is the measurement frequency) is compared for different wt% loadings of single-wall carbon nanotubes in poly(ethylene oxide).[54] The low-frequency dependence of G' is described by a power-law dependence, $G' \propto (a_T\omega)^{\beta}$, with the composition dependence of β, the power law exponent, described in the inset of the figure.

dominate materials discovery processes, to probe the state of dispersion with changes in processing and nanoparticle chemistry and correlate with a multitude of mechanical, thermal, and physical properties so as to develop detailed structure–processing–property correlations in a rapid and system-specific manner.

Further, the development of in-line methodologies to provide rapid and sensitive probes to investigate the dispersion of the nanoparticles is crucial for their integration into traditional materials processing. A natural candidate is melt-rheological properties, but extracting dispersion issues from such measurements is complicated, as the rheological signature caused by dispersion is convoluted by changes in the alignment of the nanoparticles.[53] Additional candidates include optical probes such as diffusing wave spectroscopy, infrared, and fluorescence measurements.[49,59] Although there are some issues such as the penetration depth of these probes, they clearly provide a first attempt to address this important issue.

Acknowledgments

Many helpful discussions with Richard Vaia, Evangelos Manias, Sanat Kumar, and Jack Douglas are gratefully acknowledged. Financial support from the Texas Higher Education Coordinating Board through the Advanced Research Program and the Texas Institute for Intelligent Bio-Nano Materials and Structures for Aerospace Vehicles, funded by NASA Cooperative Agreement NCC-1–02038, is gratefully acknowledged.

References

1. J.N. Israelachvili, *Intermolecular Surface Forces* (Academic Press, San Diego, ed. 3, 2006).
2. D.A. Britz, A.N. Khlobystov, *Chem. Soc. Rev.* **35**, 637 (2006).
3. L.A. Girifalco, M. Hodak, R.S. Lee, *Phys. Rev. B* **62**, 13104 (2000).
4. J.L. Bahr, E.T. Mickelson, M.J. Bronikowski, R.E. Smalley, J.M. Tour, *Chem. Commun.,* 193 (2001).
5. H. Heinz, R.A. Vaia, B.L. Farmer, *J. Chem. Phys.* **124**, 224713 (2006).
6. L. Onsager, *Ann. N.Y. Acad. Sci.* **51**, 627 (1949).
7. R.A. Vaia, E.P. Giannelis, *Macromol.* **30**, 7990 (1997).
8. C.J. van Oss, M.K. Chaudhury, R.J. Good, *Chem. Rev.* **88**, 927 (1988)
9. M.E. Mackay et al., *Science* **311**, 1740 (2006).
10. J.B. Hooper, K.S. Schweizer, *Macromol.* **39**, 5133 (2006).
11. V.V. Ginzburg, A.C. Balazs, *Adv. Mater.* **12**, 1805 (2000).
12. A.C. Balazs, C. Singh, E. Zhulina, *Macromol.* **31**, 8370 (1998).
13. F.W. Starr, J.F. Douglas, S.C. Glotzer, *J. Chem. Phys.* **119**, 1777 (2003).
14. K.L. Anderson, A. Sinsawat, R.A. Vaia, B.L. Farmer, *J. Polym. Sci. Part B: Polym. Phys.* **43**, 1014 (2005); A. Sinsawat, K.L. Anderson, R.A. Vaia, B.L. Farmer, *J. Polym. Sci. Part B: Polym. Phys.* **41**, 3272 (2003).
15. N.P. Adhikari et al., *Phys. Rev. Lett.* **93** 188301 (2004).
16. C. Zhi et al., *J. Am. Chem. Soc.* **127**, 15996 (2005).
17. A. Star, D.W. Steuerman, J.R. Heath, J.F. Stoddart, *Angew. Chem. Int. Ed.* **41**, 2508 (2002).
18. C. Zhi et al., *J. Phys. Chem. B* **110**, 1525 (2006).
19. K. Yurekli, C.A. Mitchell, R. Krishnamoorti, *J. Am. Chem. Soc.* **126**, 9902 (2004).
20. A. Hirsch, O. Vostrowsky, *Funct. Mol. Struct.* **245**, 193 (2005).
21. J.L. Bahr, J.M. Tour, *Chem. Mater.* **13**, 3823 (2001); C.A. Dyke, J.M. Tour, *J. Phys. Chem. A* **108**, 11151 (2004).
22. C.A. Mitchell et al., *Macromol.* **35**, 8825 (2002).
23. Y.M. Ying et al., *Org. Lett.* **5**, 1471 (2003).
24. V.N. Khabashesku, W.E. Billups, J.L. Margrave, *Acc. Chem. Res.* **35**, 1087 (2002).
25. A. Usuki et al., *J. Mater. Res.* **8**, 1179 (1993).
26. J. Pyun, K. Matyjaszewski, *Chem. Mater.* **13**, 3436 (2001).
27. Z.M. Wang, H. Nakajima, E. Manias, T.C. Chung, *Macromol.* **36**, 8919 (2003); L. Xu et al., *Nanotechnology* **16**, S514 (2005).
28. T.D. Fornes, P.J. Yoon, H. Keskkula, D.R. Paul, *Polym.* **42**, 9929 (2001).
29. J. Zhao, A.B. Morgan, J.D. Harris, *Polym.* **46**, 8641 (2005).
30. C. Park et al., *Chem. Phys. Lett.* **364**, 303 (2002).
31. H. Koerner, D. Misra, A. Tan, L. Drummy, P. Mirau, R. Vaia, *Polymer* **47**, 3426 (2006).
32. K. Khait, J.M. Torkelson, *Polym. Plast. Technol. Eng.* **38**, 445 (1999).
33. J.M. Torkelson, A. Lebovitz, K. Kasimatis, K. Khait, "Method of producing exfoliated polymer-clay nanocomposite and polymer-clay nanocomposite produced therefrom," U.S. Patent Application No. 20060178465 (August 10, 2006).
34. N. Pierard et al., *Carbon* **42**, 1691 (2004).
35. S. Bandi, M. Bell, D.A. Schiraldi, *Macromol.* **38**, 9216 (2005).
36. L.A. Capadona, M.A.B. Meador, A. Alunni, E.F. Fabrizio, P. Vassilaras, N. Leventis, *Polymer* **47**, 5754 (2006); P. Innocenzi, G. Brusatin, *Chem. Mater.* **13**, 3126 (2001).
37. A.B. Morgan, J.W. Gilman, *J. Appl. Polym. Sci.* **87**, 1329 (2003); T.D. Fornes et al., *Polym.* **43**, 5915 (2002); H.R. Dennis et al., *Polym.* **42**, 9513 (2001).
38. A. Vermogen et al., *Macromol.* **38**, 9661 (2005).
39. A. Usuki, N. Hasegawa, H. Kadoura, T. Okamoto, *Nano Lett.* **1**, 271 (2001); E. Kumacheva, O.K.L. Lilge, *Adv. Mater.* **11**, 231 (1999).
40. L.F. Drummy et al., *J. Phys. Chem. B* **109**, 17868 (2005); J. Ryszkowska, in *Adv. Mater. Forum III, Pts. 1–2,* **514–516**, 1658 (2006); Z.L. Wang, *Adv. Mater.* **15**, 1497 (2003).
41. D.W. Schaefer, M.M. Agamalian, *Curr. Opin. Solid State Mater. Sci.* **8**, 39 (2004); B.J. Olivier et al., *Macromol.* **29**, 8615 (1996).
42. M. Gelfer et al., *Langmuir* **20**, 3746 (2004); A. Bafna, G. Beaucage, F. Mirabella, S. Mehta, *Polymer* **44**, 1103 (2003).
43. J.D.F. Ramsay, P. Lindner, *J. Chem. Soc. Faraday Trans.* **89**, 4207 (1993); J.D.F. Ramsay, S.W. Swanton, J. Bunce, *J. Chem. Soc. Faraday Trans.* **86**, 3919 (1990).
44. D.L. Ho, R.M. Briber, C.J. Glinka, *Chem. Mater.* **13**, 1923 (2001).
45. R.A. Vaia, W.D. Liu, H. Koerner, *J. Polym. Sci. Part B: Polym. Phys.* **41,** 3214 (2003).
46. D.W. Schaefer et al., *Chem. Phys. Lett.* **375**, 369 (2003).
47. M. Moniruzzaman, K.I. Winey, *Macromol.* **39**, 5194 (2006).

48. W. Zhou et al., *Chem. Phys. Lett.* **384**, 185 (2004).
49. P.H. Maupin, J.W. Gilman, R.H. Harris, S. Bellayer, A.J. Bur, S.C. Roth, M. Murariu, A.B. Morgan, J.D. Harris, *Macromol. Rapid Commun.* **25**, 788 (2004).
50. R.A. Graff et al., *Adv. Mater.* **17**, 980 (2005).
51. C. Park et al., *J. Polym. Sci. Part B: Polym. Phys.* **44**, 1751 (2006).
52. M. Surve, V. Pryamitsyn, V. Ganesan, *Langmuir* **22**, 969 (2006).
53. R. Krishnamoorti, K. Yurekli, *Curr. Opin. Colloid Interface Sci.* **6**, 464 (2001).
54. T. Chatterjee, K. Yurekli, V.G. Hadjiev, R. Krishnamoorti, *Adv. Funct. Mater.* **15**, 1832 (2005).
55. J. Ren, A.S. Silva, R. Krishnamoorti, *Macromolecules* **33**, 3739 (2000).
56. E.J. Garboczi, K.A. Snyder, J.F. Douglas, M.F. Thorpe, *Phys. Rev. E* **52**, 819 (1995).
57. S. Salaniwal, S.K. Kumar, J.F. Douglas, *Phys. Rev. Lett.* **89**, 258301 (2002); G. Schmidt et al., *Macromolecules* **33**, 7219 (2000); C.A. Mitchell, R. Krishnamoorti, *Macromolecules* **40**, 1538 (2007).
58. J.X. Ren, B.F. Casanueva, C.A. Mitchell, R. Krishnamoorti, *Macromolecules* **36**, 4188 (2003); V. Goel et al., *J. Polym. Sci. Part B: Polym. Phys.* **44**, 2014 (2006).
59. D.A. Tsyboulski, S.M. Bachilo, R.B. Weisman, *Nano Lett.* **5**, 975 (2005).
60. R.A. Vaia, E.P. Giannelis, *Macromolecules* **30**, 8000 (1997). □

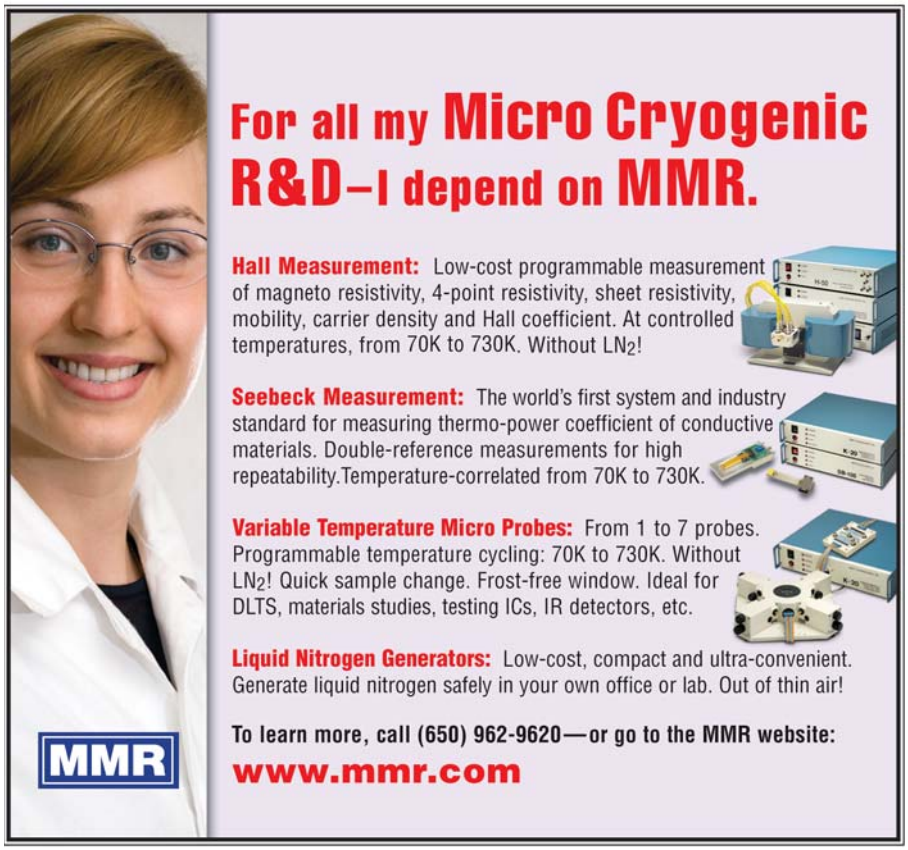

Improving Electrical Conductivity and Thermal Properties of Polymers by the Addition of Carbon Nanotubes as Fillers

Karen I. Winey, Takashi Kashiwagi, and Minfang Mu

Abstract

The remarkable electrical and thermal conductivities of isolated carbon nanotubes have spurred worldwide interest in using nanotubes to enhance polymer properties. Electrical conductivity in nanotube/polymer composites is well described by percolation, where the presence of an interconnected nanotube network corresponds to a dramatic increase in electrical conductivity ranging from 10^{-5} S/cm to 1 S/cm. Given the high aspect ratios and small diameters of carbon nanotubes, percolation thresholds are often reported below 1 wt%, although nanotube dispersion and alignment strongly influence this value. Increases in thermal conductivity are modest (~3 times) because the interfacial thermal resistance between nanotubes is considerable and the thermal conductivity of nanotubes is only 10^4 greater than the polymer, which forces the matrix to contribute more toward the composite thermal conductivity, as compared to the contrast in electrical conductivity, $>10^{14}$. The nanotube network is also valuable for improving flame-retardant efficiency by producing a protective nanotube residue. In this article, we highlight published research results that elucidate fundamental structure–property relationships pertaining to electrical, thermal, and/or flammability properties in numerous nanotube-containing polymer composites, so that specific applications can be targeted for future commercial success.

Introduction

Carbon nanotubes possess three important characteristics relative to the numerous available fillers: phenomenal electrical conductivity, nanoscopic size, and high aspect ratio. This combination of properties can lead to electrical percolation at low concentrations and has naturally spurred considerable activity in producing value-added polymer nanocomposites. Electrical percolation occurs when the filler has an electrical conductivity vastly higher than the polymer matrix. The higher electrical conductivities that are available in nanotube/polymer composites are being explored for a variety of potential applications, including housings for cell phones and computers, lightning-strike protection for airplanes, actuators, chemical sensors, photovoltaic devices (solar cells), electrical interconnects for plastic electronics, printable circuit wiring, transparent conductive coatings, and electromagnetic interference shielding. In fact, the first major commercial product from Hyperion Catalysis International that used multiwall carbon nanotubes (MWNTs) provides improved electrical conductivity that facilitates electrostatic coating for painting automobile bumpers.[1] A variety of potential applications are also being developed that require higher thermal conductivities, including heat exchangers and heat dissipation materials for electronics packaging.

This article provides a brief synopsis of fundamental research in polymer nanocomposites containing carbon nanotubes focusing on electrical, thermal, and flammability studies. Note that activity by small, medium, and large companies is considerable in this area, but is largely omitted here because of a lack of public information. Interested readers are directed to several recent review articles for more complete presentations.[2–8]

A word of caution before proceeding: one must appreciate that all known preparations of nanotubes give mixtures of nanotube chiralities, diameters, and lengths along with different types and amounts of impurities and structural defects. These variations impact the electrical and thermal properties of the nanotubes, as well as how the nanotubes are arranged in a composite. Furthermore, these nanotube characteristics can vary somewhat from one batch to the next from the same provider, not to mention the significant variations among the numerous synthesis methods used across the world to grow carbon nanotubes. Thus, it is challenging to quantitatively compare results among different groups without accounting for variations in nanotubes. Ultimately, companies will select nanotube suppliers based on cost, consistency, compatibility with their composite fabrication methods, and composite properties.

Electrical Conductivity of Polymers with Nanotubes

Electrical conductivity in filled polymers is typically discussed in terms of percolation phenomena when the filler has an electrical conductivity vastly higher than the polymer matrix. This is certainly the case with carbon nanotubes that have electrical conductivities ranging from semiconductive to metallic, whereas conventional polymers are insulating. The percolation threshold is the filler concentration at which the electrical conductivity increases sharply by orders of magnitude, indicating that conductive pathways span the macroscopic sample. Below the percolation threshold, electrons must travel through considerable amounts of insulating matrix between the conductive filler particles, whereas above the percolation concentration, electrons conduct predominantly along the

filler and move directly from one filler particle to the next.

Carbon nanotubes provide a new regime of fillers because of their high electrical conductivities, large aspect ratios, and nanometer-scale diameters and have revitalized the investigation of percolation phenomena. Significant increases in electrical conductivity have been reported at nanotube loadings considerably below the concentrations of traditional fillers in polymer matrices. For polymer composites with single-wall carbon nanotubes (SWNTs), the reported percolation thresholds range from 0.007 wt% to several wt%.[9] Percolation thresholds as low as 0.0025 wt% have been achieved in a polymer composite with long flexible bundles of aligned MWNTs.[10]

For composites with discrete fillers that are vastly more conductive than the matrix, the percolation threshold is determined by fitting experimental data to a power law,[11]

$$\sigma \propto (m - m_c)^{\beta_m}, \quad (1)$$

where σ is the electrical conductivity, m is the nanotube mass fraction, β_m is the critical exponent, and m_c is the concentration threshold. As an example, Figure 1a shows the electrical conductivity of polystyrene composites with functionalized SWNTs as a function of SWNT loading from 0 wt% to 10 wt%.[12] Nanotube concentrations of >0.3 wt% and >3 wt% SWNT loading are sufficient for applications in electrostatic painting and electromagnetic interference shielding, respectively. Fitting these data with the power law finds the concentration threshold to be 0.045 wt% (Figure 1b). When these authors used polycarbonate as the composite matrix, the concentration threshold increased to 0.110 wt%, demonstrating that electrical percolation might depend on the matrix as well as a variety of other factors, including processing, dispersion, and aspect ratio.

Whereas percolation concentration thresholds are frequently reported below ~1 wt%, there is considerable variability among the numerous nanotube/polymer composites. This observed range in percolation threshold stems primarily from the dispersion of the nanotubes, meaning the spatial distribution of the nanotubes. The van der Waals interactions between carbon nanotubes are notably larger than polymer–polymer van der Waals interactions because of the absence of hydrogen atoms, and have been calculated to be ~0.5 eV per nanometer.[13] This attraction coupled to their size leads to considerable aggregation of nanotubes, which typically reduces their aspect ratio, decreases the number of discrete filler bundles in a composite, and thereby increases the percolation threshold.[14] Numerous processing methods and chemical modification strategies have been developed to improve dispersion within polymer nanocomposites, where better dispersion generally has reduced the percolation threshold.

In addition to nanotube dispersion, the percolation threshold for the electrical conductivity in nanotube/polymer composites is also influenced by the nanotube aspect ratio. Note that higher-aspect-ratio nanotubes are typically more difficult to disperse, and it can be difficult to separate the two effects. Bryning et al. prepared SWNT/epoxy composites with nanotubes from two different sources (high-pressure carbon monoxide conversion and laser oven) having aspect ratios of ~150 and ~380, respectively, and found a smaller percolation threshold with the higher-aspect-ratio nanotubes.[9] Bai and Allaoui found more than an eightfold decrease in the threshold concentration in MWNT/epoxy composites when the MWNT length was increased from 1 to 50 μm.[15]

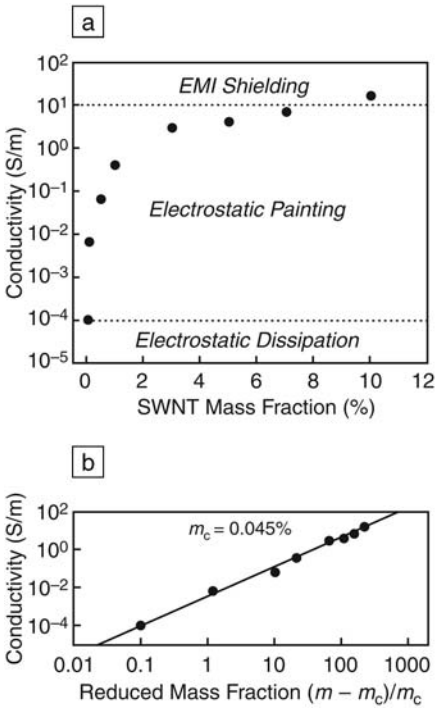

Figure 1. (a) Electrical conductivity of functionalized single-wall carbon nanotubes (SWNTs) in polystyrene composites as a function of SWNT loading. Dotted lines represent the conductivities required for various applications. (b) The power law dependence of the electrical conductivity according to Equation 1 gives a threshold concentration of 0.045 wt%; m is the nanotube mass fraction and m_c is the concentration threshold. (Reused with permission from Reference 12.)

It is widely accepted that chemical functionalization by covalent bonding disrupts the extended π conjugation of nanotubes and reduces the electrical conductivity of isolated nanotubes. However, we note that several researchers report that functionalization can improve the electrical properties of the composites. For example, Valentini et al. pointed out that amine-functionalized SWNTs in epoxy matrix enable migration of intrinsic charges, which contributes to the overall conductivity.[16] Tamburri et al. found that extensive functionalization of SWNTs with –OH and –COOH groups enhances the current in a conducting polymer (1,8-diaminophthalene) by factors of 90 and 140, respectively, whereas the untreated tubes showed an enhancement of only 20.[17] At present, it appears that the disadvantages of covalent chemical functionalization with respect to SWNT conductivity are outweighed by the improved dispersion enabled by functionalization. Similarly, noncovalent chemical functionalization, such as the addition of surfactant molecules, improves dispersion and generally improves electrical conductivity unless the dispersant remains between the nanotubes and increases the interfacial resistance.[18]

An underlying assumption in this discussion is that the composites are isotropic, that is, the nanotubes and/or nanotube bundles are randomly oriented in the sample. Alignment occurs at low concentrations when the polymer matrix flows, as in melt-fiber spinning[19] or shear deformation,[20] because the polymer chains are perturbed from random conformations to extended conformations along the flow direction by shear and extension forces and thereby align the nanotubes. When flow stops, entropic forces quickly drive polymers back to random conformations, whereas, in contrast, long nanotubes and nanotube bundles typically remain in their aligned arrangement. This nanotube alignment can remain indefinitely when the polymer matrix becomes glassy or semicrystalline upon cooling. Scanning electron microscopy readily detects nanotube orientation qualitatively, and quantitative measures of orientation have employed x-ray scattering from either the interlayer diffraction in MWNTs or the SWNT form-factor scattering.[21]

Nanotube alignment typically increases electrical conductivity in dry carbon nanotube mats, called "buckypaper," with high nanotube loadings (>30 vol%).[22] The situation is more complex with nanotube concentrations near the percolation concentration threshold. At low loadings, near-perfect alignment disconnects nanotubes,

thereby destroying the percolating pathways; the electrical conductivity approaches that of the polymer matrix. Du et al. studied the effect of nanotube orientation using a series of SWNT/poly(methyl methacrylate) (PMMA) composites in which the nanotubes were aligned using an extensional flow (Figure 2).[23] The extent of nanotube orientation was controlled by the melt-fiber processing conditions (extrusion rate, wind-up speed). The full width at half maximum (FWHM) refers to the azimuthal dependence of the form-factor scattering arising from the nanotube bundles, where 0° and 180° correspond to perfect alignment of SWNTs and isotropic distribution of SWNTs, respectively. At a fixed SWNT concentration (2 wt%), the electrical conductivity parallel to the alignment direction increases sharply with increasing FWHM (i.e., decreasing alignment). As with concentration, a power law was applied to determine the critical threshold for percolation with respect to alignment (inset in Figure 2). Figure 2 also indicates that there are intermediate levels of nanotube alignment (FWHM ~100°–140°), where the electrical conductivities are higher than the isotropic condition (FWHM 180°) because of fewer redundancies in the network; this effect is more pronounced at lower SWNT loading. Given that typical industrial polymer processing methods (injection molding) use considerable shear forces, nanotube alignment can vary across a piece, so strategies will be required to address the accompanying variations in electrical conductivity.

Alternative approaches to high electrical conductivity create heterogeneous distributions of nanotubes in which the nanotube-rich phase is continuous within a macroscopic sample. One example of this approach starts with nanotube buckypaper that is prepared by filtering a nanotube suspension to yield a porous, flexible nanotube material consisting of interconnected nanotube bundles. Buckypaper can be infiltrated with polymers or with polymer precursors that are subsequently polymerized to give composites with >20 vol% nanotubes.[24,25] Epoxy-based nanotube composites of this type are being developed for lightning-strike protection. A second example begins with a polymer latex that consists of an aqueous suspension of polymer particles prepared by emulsion polymerization. Nanotubes are added to the suspension, the solvent is removed, and as the latex particles consolidate into a dense film, the nanotubes are trapped between the particles and form a continuous minority phase that is electrically conductive.[26] This route is particularly well suited for preparing electrically conductive thick films with nanotube loadings of ~1 wt% without compromising the processability of the latex.

The electrical conductivities in nanotube/polymer composites are readily understood in terms of a percolating network of highly conductive, high-aspect-ratio fillers with minimal tube–tube resistance. Consequently, research to date finds strong dependencies of the composite electrical properties on the following nanotube characteristics: spatial distribution, orientation, length, and functionalization. Note that these characteristics are certainly not independent, that is, functionalization typically alters the spatial distribution. As these materials are developed, the correlations among processing, structure, and properties will be refined for specific fabrication methods, materials, and applications.

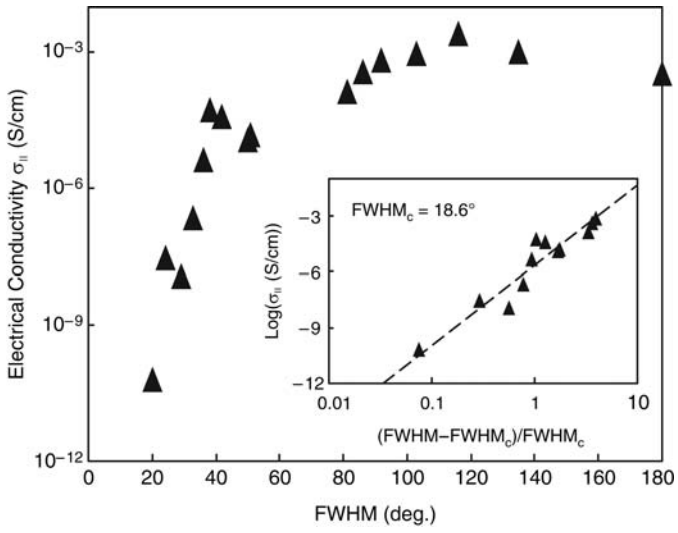

Figure 2. Electrical conductivity of poly(methyl methacrylate) composite fibers with 2 wt% single-wall carbon nanotubes (SWNTs) as a function of nanotube alignment as given by a full width at half maximum (FWHM) from scattering measurements. Electrical conductivity measured along the composite fibers at room temperature. Inset: log–log plot of conductivity versus reduced FWHM determines the critical alignment, FWHM$_c$. (Reused with permission from Reference 23.)

Thermal Conductivity of Polymers with Dispersed Nanotubes

The excellent thermal conductivity of individual nanotubes led to early expectations that nanotubes will vastly enhance the thermal conductivity of polymers, as nanotubes do with the electrical conductivity. However, the thermal conductivities of nanotube/polymer composites have increased to only a few W/m K and fail to show a dramatic percolation threshold. There are two important differences between thermal and electrical conductivity in nanotube/polymer composites that provide insight into the relatively poor performance of the nanocomposites as thermal conductors: property contrast between nanotubes and polymers and interfacial thermal resistance. Of course, the thermal conductivity of nanotube/polymer composites also depends on the nanotube characteristics described in the section "Electrical Conductivity of Polymers with Nanotubes," including dispersion, alignment, and aspect ratio, but these are less important here.

First, there is the issue of contrast in thermal versus electrical conductivity. The highest reported nanotube thermal conductivities are on the order of 10^3 W/m K, whereas typical thermoplastics and thermosets have ~10^{-1} W/m K. Note that the thermal conductivity of isolated nanotubes is an active area of research, with some reports giving values as low at 30 W/m K and others illustrating the influence of nanotube size and type.[27–28] Thus, a larger fraction of phonons entering a nanotube/polymer composite are likely to travel through the matrix than electrons, because the contrast in thermal conductivity, $\kappa_{nanotube}/\kappa_{polymer}$, is at most ~$10^4$, in comparison with the electrical conductivity contrast, $\sigma_{nanotube}/\sigma_{polymer}$, of ~$10^{14}$–$10^{19}$.

Second, atomic vibrations or phonons dominate the thermal conductivity of carbon materials, leading to high interfacial thermal resistance between nanotubes. This interfacial thermal resistance arises from the constraint that the energy contained in high-frequency phonon modes within the nanotubes must first be transferred to low-frequency modes through phonon–phonon coupling in order to be

exchanged with the surrounding medium. Huxtable et al. has estimated the thermal conductance to be ~12 MW/m^2 K at a nanotube–polymer interface.[29] Simulations of heat transfer between two nanotubes without an intervening matrix material also show high thermal resistance.[29] This result is consistent with the low thermal conductivity of SWNT buckypaper (~30 W/m K for the unaligned buckypaper[30]) as compared to that of the individual SWNTs (~6600 W/m K, theoretical prediction[7]). From a comparative study of different nanotubes (SWNTs; MWNTs; and double-wall nanotubes, DWNTs) in epoxy composites, Gojny et al. suggest that MWNTs have the highest potential to improve the thermal conductivity of polymer composites, because of the relatively low interfacial area (therefore, less phonon scattering at the interface) and the existence of shielded internal layers that promote the conduction of phonons and minimize the matrix coupling losses.[31] Efforts are now focused on clever methods to reduce this interfacial thermal resistance by covalently bonding functional groups onto nanotubes[32,33] and by introducing extensive nanotube overlap.[34]

Here, we summarize some promising experimental findings. Biercuk et al. prepared an epoxy composite with 1 wt% raw (not purified) laser-oven SWNTs that showed a 125% increase in thermal conductivity at room temperature.[35] Choi et al. reported a 300% increase in thermal conductivity at room temperature with 3 wt% SWNTs in epoxy, with an additional increase (10%) when aligned magnetically.[36] Du et al. developed an infiltration method that produced a bicontinuous morphology of epoxy and a nanotube-rich phase (Figure 3) and showed a ~220% increase in thermal conductivity at ~2.3 wt% SWNT loading.[37] As discussed previously for electrical conductivity, spatially heterogeneous or two-phase materials demonstrate methods that circumvent the need for good dispersion to produce favorable properties. Overall, improving the thermal conductivity of polymers using carbon nanotubes is proving more challenging than improving electrical properties, but progress is steady. Currently, the thermal conductivities of nanotube/epoxy composites fall far below commercial silver flake/epoxy composites (50–65 wt% silver content and several to 30 W/m K) that are widely used in packaging microprocessors.

Flammability in Polymers with Dispersed Nanotubes

The flammability of polymeric materials can be significantly reduced by the addition of a small quantity of carbon nanotubes. During flammability experiments, nanotube/polymer composites with well-dispersed nanotubes form a freestanding nanotube network that remains robust after burning, thus serving as a protective layer and providing good flame-retardant effectiveness.[38,39] The nanotube concentration and dispersion are critical for producing this protective nanotube network. The size of the carbon filler (SWNTs; MWNTs; and carbon nanofiber, CNF) also has an impact on the physical structure of the protective layer and the flame-retardant effectiveness, as detailed later.[40] CNF is graphite fiber with small diameters of 60–200 nm and lengths in the range of tens to hundreds of microns.

The mass loss rate curves of samples having a mass fraction of 0.5 wt% of SWNTs, MWNTs, or CNF under an external radiant flux of 50 kW/m^2 in nitrogen (no flaming but sample heating similar to fire conditions) are shown in Figure 4. The liquid-like PMMA bubbled violently, and no residue remained in the container at the end of the test. The 0.5% SWNT/PMMA nanocomposite was solid-like throughout the test and effectively suppressed bubbling. The residue is a continuous nanotube network (see Figure 4) and effectively reduced the mass loss rate of the PMMA by roughly 70%. The 0.5% MWNT/PMMA composite formed numerous discrete structures that agglomerated as the test progressed, leading to the formation of a discontinuous residue. The mass loss rate of the 0.5% MWNT/PMMA was significantly lower than that of the PMMA but not as low as that of the 0.5% SWNT/PMMA. The 0.5% CNF/PMMA composite is a slightly viscous liquid that bubbled vigorously during the test and left only a thin, fragile residue. The mass loss rate of the 0.5% CNF/PMMA was not significantly different from that of the PMMA. These results indicate that the order of flame-retardant effectiveness is SWNTs, MWNTs, and CNF at 0.5 wt% loading.

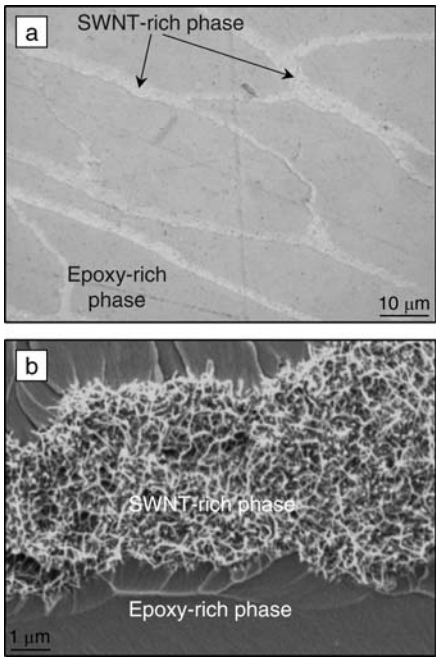

Figure 3. (a) Optical and (b) scanning electron microscopy images of a SWNT/epoxy composite fabricated by infiltrating a freestanding nanotube network. This composite exhibits a heterogeneous morphology in which the nanotube-rich phase is both the minority phase and continuous across the sample. (Modified from Reference 37.)

The development of a mechanically and thermally robust filler network provides critical protection during burning and improves the flammability properties of the polymer nanocomposites. Such a structure appears to form when a filler network exists in the initial sample. The presence of a network can be detected by viscoelastic measurements on the samples as a function of filler type and concentration. The frequency dependence of the shear-storage modulus (G') indicates whether a composite behaves like a liquid ($G' \sim \omega^2$) or like a solid ($G' \sim \omega^0$), where ω is the frequency of the dynamic experiment. As the filler concentration increases, a transition from a Newtonian liquid to an ideal Hookean solid accompanies the formation of a filler network structure in the composite (Figure 5). For larger fillers (e.g., CNF), a higher loading is necessary to exhibit solid-like behavior in the composite. Solid-like behavior in the composite at 200°C corresponds to an ability to form a protective layer during burning. This strong correlation between viscoelastic properties and flame-retardant effectiveness of polymer nanocomposites provides a convenient method for screening materials. For example, the 4% CNF/PMMA composite is solid-like at 200°C and has a mass loss rate of the PMMA similar to the 0.5% SWNT/PMMA (see Figure 4), because the higher concentration enabled the formation of a CNF network.

Remaining Challenges and Outlook

The high aspect ratios and small diameters of carbon nanotubes permit network structures to form within polymer matrices at remarkably low concentrations. The specific threshold concentration depends on the size of the individual nanotubes (length and diameter); the extent of nanotube dispersion into isolated nanotubes, bundles, ropes, or fiber; the spatial distribution of these objects; and their local

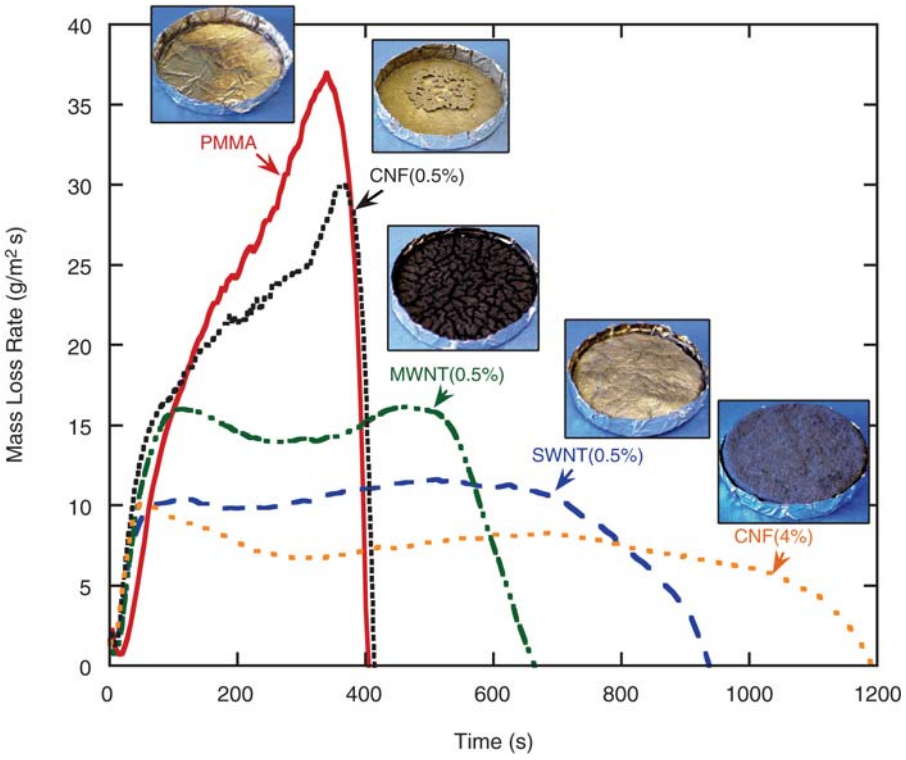

Figure 4. Effects of filler type on mass loss rate of poly(methyl methacrylate) and (insets) residue photographs collected at the end of the flammability tests. The tests were conducted at an external radiant flux of 50 kW/m^2 in nitrogen. Abbreviations: PMMA is poly(methyl methacrylate), CNF is carbon nanofiber, MWNT is multiwall carbon nanotube, and SWNT is single-wall carbon nanotube. (Modified from Reference 40.)

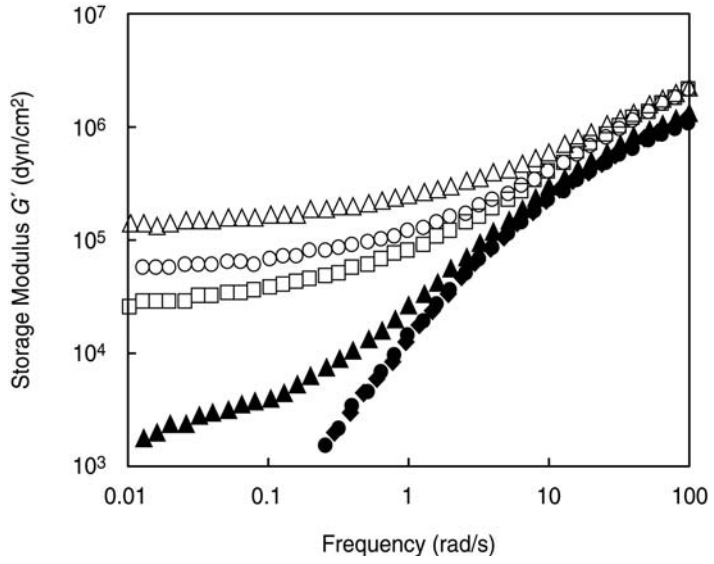

Figure 5. Rheological response transitions from liquid-like behavior ($G' \sim \omega^2$) to solid-like behavior ($G' \sim \omega^0$) as a function of increasing SWNT loading in poly(methyl methacrylate): 0 wt% (solid diamonds), 0.1 wt% (solid circles), 0.2 wt% (solid triangles), 0.5 wt% (open squares), 1.0 wt% (open circles), and 2.0 wt% (open triangles). (Modified from Reference 14.)

and global orientation. Above a critical concentration, a nanotube network can (1) sufficiently constrain the motion of thermoplastics to produce solid-like behavior; (2) form a protective layer that significantly improves flame-retardant efficiency; and (3) provide pathways for electrical conduction, leading to dramatic increases in electrical conductivity.

Carbon nanotubes have unequivocally demonstrated their ability to convert an insulating polymer matrix into a conductive nanocomposite. Electrical conductivity is likely to continue to increase as sizable quantities of metallic (or at least, predominantly metallic) nanotubes become available either by controlling the nanotube synthesis or by removing the semiconductive nanotubes. It remains to be seen whether well-dispersed nanotubes or spatially heterogeneous nanotube distributions will be favored for specific applications, given the complex interplay of cost, processability, and properties. For applications requiring the processability of thermoplastic or thermoset composites with improved electrical conductivity, the outlook is excellent both in terms of performance and the number of potential applications. The improvements in flammability properties also indicate a positive trajectory for nanotube/polymer composites. In contrast, thermal conductivity in nanotube/polymer composites requires a substantial scientific breakthrough before its future is assured.

Emerging areas of opportunity in nanotube/polymer composites include combining nanotubes with conventional fillers or other nanoscale fillers. The motivations for combining fillers include the goals of improving multiple properties simultaneously, incorporating nanotubes into existing commercial processing methods, and making the price point of the composite attractive to new applications. The principles involved will remain the same, but the level of complexity increases dramatically with two or more fillers. Another emerging area will be the incorporation of nanotube fibers into polymer matrixes. Nanotube fibers have been wet-spun from acid suspensions of SWNTs,[41] spun from chemical vapor deposition–grown nanotubes,[42] and twisted from densely grown arrays of MWNTs,[43] and will provide a new class of carbon-based fibers to the field of continuous fiber composites.

Looking beyond carbon nanotubes, electrical and thermal conductivities and flammability properties of polymer nanocomposites may benefit from other nanoscale fillers, particularly nanowires and nanorods. Nanowires and nanorods are high-aspect-ratio particles ($l/d > 100$)

prepared by using catalytic nanoparticles in a chemical vapor deposition or solution method and by electroplating material into porous templates. Metals, semiconductors, and ceramics have been made as nanowires and can be either single-crystal or polycrystalline. The dispersion, fabrication, characterization, and testing methods developed for nanotube/polymer composites will readily be adapted for nanowire- or nanorod-based polymer nanocomposites.

In summary, we have highlighted research results that elucidate fundamental structure–property relationships pertaining to electrical, thermal, and/or flammability properties in numerous nanotube-containing polymer composites. MWNTs are already established commercially as fillers that improve electrical conductivity in polymers. As research continues, specific potential applications will define materials properties and materials scientists will endeavor to design nanotube–polymer composites that meet both the targeted materials and cost criteria. In the coming decade, the number of commercial nanotube–polymer composites with improved electrical, thermal, or flammability properties will certainly increase.

Acknowledgments

K.I. Winey and M. Mu acknowledge funding from the National Science Foundation (DMR-MRSEC 05-20020) and valuable discussions with F. Du, R. Haggenmueller, and M. Moniruzzaman. T. Kashiwagi acknowledges funding from the National Institute of Standards and Technology (5D1022).

References

1. W.A. de Heer, *MRS Bull.* **29** (4), 281 (2004).
2. M. Moniruzzaman, K.I. Winey, *Macromolecules* **39,** 5194 (2006).
3. C.A. Cooper, R.J. Young, M. Halsall, *Compos. Part A* **32**, 401 (2001).
4. G. Gao, T. Cagin, W.A. Goddard, *Nanotechnology* **9**, 184 (1998).
5. T. Uchida, S.J. Kumar, *J. Appl. Polym. Sci.* **98**, 985 (2005).
6. P.L. McEuen et al., *Phys. Rev. Lett.* **83**, 5098 (1999).
7. S. Berber, Y.K. Kwon, D. Tomanek, *Phys. Rev. Lett.* **84**, 4613 (2000).
8. J.N. Coleman, U. Khan, Y.K. Gun'ko, *Adv. Mater.* **18**, 689 (2006).
9. M.B. Bryning, M.F. Islam, J.M. Kikkawa, A.G. Yodh, *Adv. Mater.* **17**, 1186 (2005).
10. J.K.W. Sandler et al., *Polymer* **44**, 5893 (2003).
11. J.-M. Benoit et al., *Synth. Met.* **121**, 1215 (2001).
12. R. Ramasubramaniam, J. Chen, H. Liu, *Appl. Phys. Lett.* **83**, 2928 (2003).
13. C.A. Dyke, J.M. Tour, *J. Phys. Chem. A* **108**, 11151 (2004).
14. F. Du et al., *Macromolecules* **37**, 9048 (2004).
15. J.B. Bai, A. Allaoui, *Compos. Part A* **34**, 689 (2003).
16. L. Valentini, I. Armentano, D. Puglia, J.M. Kenny, *Carbon* **42**, 323 (2004).
17. E. Tamburri et al., *Carbon* **43**, 1213 (2005).
18. E.K. Hobbie, J. Obrzut, S.B. Kharchenko, E.A. Grulke, *J. Chem. Phys.* **125**, 044712 (2006).
19. R. Haggenmueller et al., *Chem. Phys. Lett.* **330**, 219 (2000).
20. J. Xu et al., *J. Phys. Chem. B* **110**, 12289 (2006).
21. J.E. Fischer et al., *J. Appl. Phys.* **93**, 2157 (2003).
22. R.S. Lee et al., *Nature* **388**, 255 (1997).
23. F. Du, J.E. Fischer, K.I. Winey, *Phys. Rev. B* **72**, 121404 (2005).
24. J.N. Coleman et al., *Appl. Phys. Lett.* **82**, 1682 (2003).
25. Z. Wang et al., *Compos. Part A* **35**, 1225 (2004).
26. J.C. Grunlan, A.R. Mehrabi, M.V. Bannon, J.L. Bahr, *Adv. Mater.* **16**, 150 (2004).
27. H.L. Zhong, J.R. Lukes, *Phys. Rev. B* **74**, 125403 (2006).
28. X.H. Yan, Y. Xiao, Z.M. Li, *J. Appl. Phys.* **99**, 124305 (2006).
29. S.T. Huxtable et al., *Nature Mater.* **2**, 731 (2003).
30. J. Hone et al., *Appl. Phys. Lett.* **77**, 666 (2000).
31. F.H. Gojny et al., *Polymer* **47**, 2036 (2006).
32. S. Shenogin et al., *Appl. Phys. Lett.* **85**, 2229 (2004).
33. C.H. Liu, S.S. Fan, *Appl. Phys. Lett.* **86**, 123106 (2005).
34. H. Huang, C. Liu, Y. Wu, S. Fan, *Adv. Mater.* **17**, 1652 (2005).
35. M.J. Biercuk et al., *Appl. Phys. Lett.* **80**, 2767 (2002).
36. E.S. Choi et al., *Appl. Phys. Lett.* **94**, 6034 (2003).
37. F. Du et al., *J. Polym. Sci. B* **44**, 1513 (2006).
38. T. Kashiwagi et al., *Polymer* **45**, 4227 (2004).
39. T. Kashiwagi et al., *Polymer* **46**, 471 (2005).
40. T. Kashiwagi et al., *Nature Mater.* **4**, 928 (2005).
41. L.M. Ericson et al., *Science* **305**, 1447 (2004).
42. Y.L. Li, I.A. Kinloch, A.H. Windle, *Science* **304**, 276 (2004).
43. M. Zhang, K.R. Atkinson, R.H. Baughman, *Science* **306**, 1358 (2004). □

Polymer Nanocomposites for Biomedical Applications

Rohan A. Hule and Darrin J. Pochan

Abstract

Bionanocomposites have established themselves as a promising class of hybrid materials derived from natural and synthetic biodegradable polymers and organic/inorganic fillers. Different chemistries and compositions can lead to applications from tissue engineering to load-bearing composites for bone reconstruction. A critical factor underlying biomedical nanocomposite properties is interaction between the chosen matrix and the filler. This article discusses current efforts and key research challenges in the development of these materials for use in potential biomedical applications.

Introduction and Challenges

Bionanocomposites form a fascinating interdisciplinary area that brings together biology, materials science, and nanotechnology. New bionanocomposites are impacting diverse areas, in particular, biomedical science. Generally, polymer nanocomposites are the result of the combination of polymers and inorganic/organic fillers at the nanometer scale. The extraordinary versatility of these new materials springs from the large selection of biopolymers and fillers available to researchers. Existing biopolymers include, but are not limited to, polysaccharides, aliphatic polyesters, polypeptides and proteins, and polynucleic acids, whereas fillers include clays, hydroxyapatite, and metal nanoparticles.[1]

The interaction between filler components of nanocomposites at the nanometer scale enables them to act as molecular bridges in the polymer matrix. This is the basis for enhanced mechanical properties of the nanocomposite as compared to conventional microcomposites.[2] Bionanocomposites add a new dimension to these enhanced properties in that they are biocompatible and/or biodegradable materials.

For the sake of this review, biodegradable materials can be described as materials degraded and gradually absorbed and/or eliminated by the body, whether degradation is caused mainly by hydrolysis or mediated by metabolic processes.[3] Therefore, these nanocomposites are of immense interest to biomedical technologies such as tissue engineering, bone replacement/repair, dental applications, and controlled drug delivery. Table I lists some biopolymers commonly used in biomedical applications.

Current opportunities for polymer nanocomposites in the biomedical arena arise from the multitude of applications and the vastly different functional requirements for each of these applications. For example, the screws and rods that are used for internal bone fixation bring the bone surfaces in close proximity to promote healing. This stabilization must persist for weeks to months without loosening or breaking.[3] The modulus of the implant must be close to that of the bone for efficient load transfer.[4,5] The screws and rods must be noncorrosive, nontoxic, and easy to remove if necessary.[6] Thus, a polymer nanocomposite implant must meet certain design and functional criteria, including biocompatibility, biodegradability, mechanical properties, and, in some cases, aesthetic demands. The underlying solution to the use of polymer nanocomposites in vastly differing applications is the correct choice of matrix polymer chemistry, filler type, and matrix–filler interaction. This article discusses current efforts and focuses on key research challenges in the emerging usage of polymer nanocomposites for potential biomedical applications.

Hydroxyapatite–Polymer Nanocomposites

Producing bionanocomposites based on biomimetic approaches has been a recent focus of researchers. Among these materials, hydroxyapatite (HAP)–polymer nanocomposites have been used as a biocompatible and osteoconductive substitute for bone repair and implantation.[7,8] As the main inorganic component of hard tissue, HAP [$Ca_{10}(PO_4)_6(OH)_2$] has long been used in orthopedic surgery. However, HAP is difficult to shape because of its brittleness and lack of flexibility. HAP powders can migrate from implanted sites, thus making them inappropriate for use. Moreover, these powders do not disperse well and agglomerate easily.[9] Therefore, the incorporation of HAP in polymeric nanocomposites to overcome processing and dispersion challenges is of great interest to the biomedical community. Consequently, a desirable material for use in clinical orthopedics would be a biodegradable structure that induces and promotes new bone formation at the required site.

To date, primarily polysaccharide and polypeptidic matrices have been used with HAP nanoparticles for composite formation. Yamaguchi and co-workers have synthesized and studied flexible chitosan–HAP nanocomposites.[9] The matrix used for this study, chitosan (a cationic, biodegradable polysaccharide), is flexible and has a high resistance upon heating because of intramolecular hydrogen bonds formed between the hydroxyl and amino groups.[10,11] The resulting nanocomposite, prepared by the coprecipitation method, is mechanically flexible and can be formed into any desired shape.[9]

Nanocomposites formed from gelatin and HAP nanocrystals are conducive to the attachment, growth, and proliferation of human osteoblast cells.[12] Collagen-based, polypeptidic gelatin has a high number of functional groups and is currently being used in wound dressings and pharmaceutical adhesives in clinics.[13] The flexibility and cost-effectiveness of gelatin can be combined with the bioactivity and osteoconductivity of HAP to generate potential engineering biomaterials. The traditional problem of HAP aggregation was overcome by precipitation of the apatite crystals within a polymer solution.[14,15] The porous scaffold generated by this method exhibited well-developed structural features

Table I: Biopolymers Commonly Used in Biomedical Applications.

Biopolymer	Structure
Chitosan	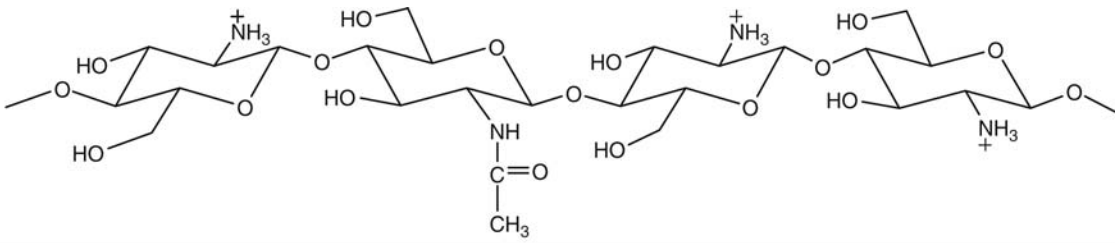
Collagen	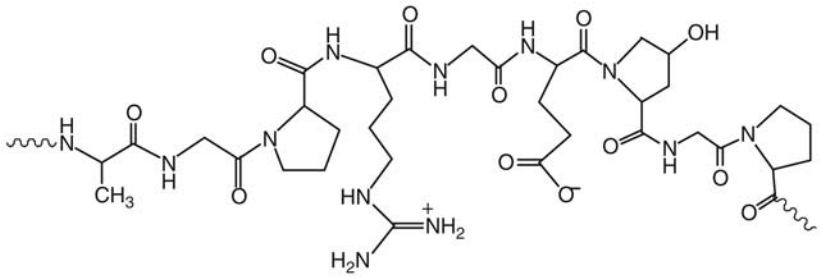
Poly(lactic acid) (PLA)	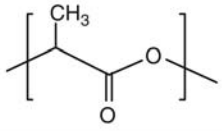
Poly(ε-caprolactone) (PCL)	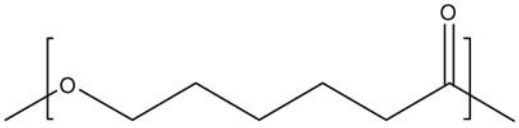
Poly(L-lysine) (PLL)	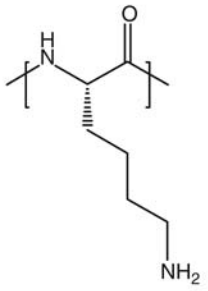

and pore configuration to induce blood circulation and cell ingrowth. Such nanocomposites have high potential for use as hard-tissue scaffolds.[12]

Three-dimensional porous scaffolds from biomimetic HAP/chitosan–gelatin network composites with microscale porosity have shown adhesion, proliferation, and expression of osteoblasts.[16] A low-magnification scanning electron micrograph of such a scaffold showing uniform pore sizes and walls is shown in Figure 1. Porosity is critical for tissue-engineering applications because it enables the diffusion of cellular nutrients and waste, and provides for cell movement.[17]

Polysaccharides, such as alginate, provide a natural polymeric sponge structure that has been used in tissue-engineering scaffold design. The weak, soft alginate scaffolds can be strengthened with HAP and have widespread applications.[18] Composite membranes from HAP nanoparticles and chitosan/collagen sols have also been synthesized to study connective-tissue reactions.[19,20]

Studies that target the nucleation of calcium phosphates and bone cell signaling within the matrix have used acidic macromolecules as the nanocomposite matrix.[21] Specifically, amino acids like aspartic acid and glutamic acid have been used as the matrix protein. Both of these amino acids are known to play an important role in intercellular communication and osteoblast differentiation that increases extracellular mineralization. Related studies have also highlighted the significance of aspartic acid in the treatment of osteoporosis and other bone dysfunctions.[22]

Aliphatic Polyester Nanocomposites

Aliphatic polyesters have been the predominant choice for materials in degradable drug delivery systems. Homopolymers and copolymers derived from glycolic acid or glycolide, lactic acid or lactide, and

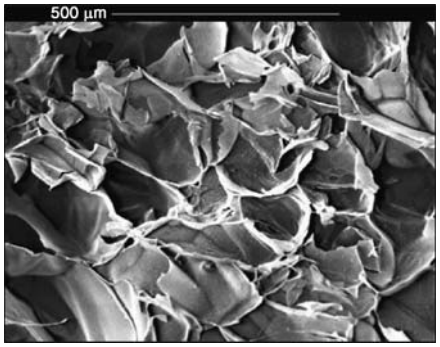

Figure 1. Low-magnification scanning electron micrograph of a hydroxyapatite (HAP)–polymer/chitosan–gelatin scaffold prepared from HAP/chitosan–gelatin/acetic acid mixture. The uniform porosity observed in the micrograph is advantageous for tissue-engineering applications. The chitosan–gelatin concentration used was 2.5 wt%; HAP/chitosan–gelatin, 30/70 parts by weight. (Reproduced from Reference 16.)

ε-caprolactone form the bulk of this research. Most of these polymers degrade by acid- or base-catalyzed hydrolytic cleavage of the backbone or by enzymatic activity.[23]

Of the polyesters that show promise in biomedical fields, poly(L-lactic acid) (PLLA) is the most prevalent. Although reports of the use of PLLA can be found in the 1960s, a phenomenal amount of work has been performed recently. PLLA has widespread applications in sutures, drug delivery devices, prosthetics, scaffolds, vascular grafts, bone screws, pins, and plates for temporary internal fixation.[24] Good mechanical properties and degradation into nontoxic products[25] are the main reasons for such an array of applications. Additionally, PLLA is U.S. Food and Drug Administation–approved and available commercially in a variety of grades. As a material, PLLA is relatively hard and crystalline with a melting point between 170°C–180°C and a glass-transition temperature T_g of ~60°C–67°C. Another factor contributing to the use of PLLA in biomedical applications is its ability to be copolymerized and blended to obtain a nanocomposite-like product with desirable properties. The racemic version of the polymer, poly(D,L-lactide) (PDLLA), sometimes simply called PLA, is amorphous with a T_g of around 50°C–60°C.

Studies also have been done to evaluate the potential of PLLA as a bone reinforcement material. The mechanical properties of neat PLLA might be inadequate for high load-bearing applications.[26] This necessitates the incorporation of reinforcements like oriented fibers, HAP, or clays to form nanocomposites. Such studies report an increase in the flexural modulus, strength, and moduli values commensurate with bone replacement implants.[27]

"Self-reinforced" composites have also been synthesized by incorporation of oriented PLA fibers in a matrix of the same material.[28] Past work in our group[29] involved the synthesis of PLLA–organoclay nanocomposites via the exfoliation adsorption film-casting technique, in which both the matrix and the filler are sonicated separately in a common solvent. The two solutions are then mixed and cast on a substrate under controlled evaporation conditions, resulting in a film.

Exfoliation in the case of Cloisite 30B clay was ascribed to favorable enthalpic interactions between the diols of the organic modifier and carbonyl bonds of the PLLA backbone with polymer crystallinity being suppressed at complete exfoliation.[29] This unusual phenomenon necessitated in-depth studies that revealed lower crystallinity and crystallization rates and higher radial spherulitic growth rates resulting from the addition of highly miscible organoclay in PLLA.[30] Subsequent time-lapsed Fourier transform infrared (FTIR) studies attributed this behavior to the precedence of intrachain interactions, specifically, PLA 10_3 helix formation and backbone reorientation, over interchain interactions, as opposed to neat PLLA.[31–33]

Poly(glycolic acid) (PGA) is another aliphatic polyester with applicability for biomedical use. However, unlike PLLA, PGA is readily soluble in water. Mechanical properties of self-reinforced PGA have been investigated and are found to worsen on exposure to distilled water.[23] Thus, water solubility and its high melting point limit the use of PGA in bionanocomposites.

Another biodegradable and nontoxic aliphatic polyester discussed in the biomedical nanocomposite literature is poly (ε-caprolactone) (PCL). Synthesized by the ring-opening polymerization of ε-caprolactone, it has a melting temperature of 61°C and a T_g of −60°C. The rubbery state permits the diffusion of low-molecular-weight species at body temperature, thus making PCL a promising candidate for controlled release and soft-tissue engineering. The range of properties can be furthered by copolymerization with other lactones such as glycolide, lactide, and poly(ethylene oxide) (PEO) or by nanofiller incorporation. Both techniques have been adopted and have shown great potential for biomedical applications.[23] Nanocomposite polymer–clay hydrogels have also been studied extensively by microscopy and scattering techniques.[34]

Recently, electrospinning has been used as an alternative scaffold fabrication technique in soft-tissue transplantation and hard-tissue regeneration. This method provides woven mats with individual fiber diameters ranging from 50 nm to a few microns. The interconnected, porous network so formed is desirable for drug delivery as well as biomedical substrates for tissue regeneration, wound dressing, artificial blood vessels, and other uses. Electrospinning helps tailor the mechanical, biological, and kinetic properties of the scaffolds by varying parameters such as polymer solution properties and processing conditions (e.g., electrical force, the distance between the electrospinning needle and the oppositely charged surface acting as ground, spinneret geometry, and solution flow rate).[35] However, some of the restrictions of this method, like controlling the pore size and softness of the electrospun mat, currently prevents it from being used for hard-tissue applications. Studies incorporating montmorillonite clay[36] (MMT) in a PLLA solution that was subsequently electrospun into a mat found improved mechanical and biodegradation characteristics and ideal pore sizes (microns) for cell growth, blood vessel invasion, and nano-sized pores for nutrient/waste transfer.[37]

Polypeptide-Based Nanocomposites

Polypeptides as matrices provide an additional array of opportunities in materials design and application in terms of a unique ability to adopt specific secondary, tertiary, and quaternary structures, a feature not available with synthetic polymers. Functionality can also be incorporated by the use of natural and non-natural amino acids with desired activity at specific sites along the polypeptide backbone. Our group has been investigating the incorporation of polypeptides, particularly, poly(L-lysine) (PLL), as the matrix polypeptide and MMT as the filler.[38] Initial work[39] produced nanocomposites from PLL and MMT that exhibited enhanced mechanical properties and thermal properties comparable to other widely explored biomaterials and engineering thermoplastics. A transmission electron micrograph showing the intercalated MMT layers in a PLL–MMT nanocomposite is shown in Figure 2.

The potential applicability of these materials was further investigated by studying the effect of the molecular weight of the polypeptide on the secondary conformation of the final nanocomposite matrix. PLL is a good choice for such a study because it can display a variety of secondary structures: the random coil, α-helix, or β-sheet in aqueous solution. Moreover, transitions

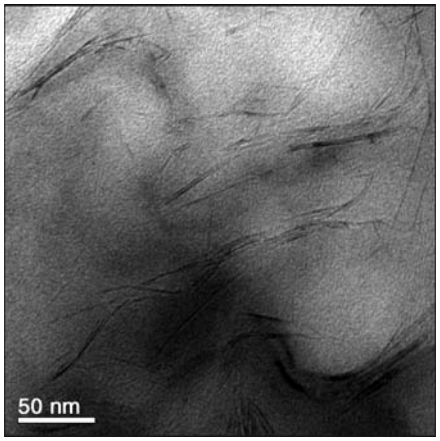

Figure 2. Bright-field transmission electron micrograph of a 5 wt% poly(L-lysine)-montmorillonite clay nanocomposite film, showing intercalated regions. The image was obtained on a microtomed film (<80 nm) at 200 kV. (Reproduced from Reference 38.)

between conformations can be easily achieved using pH, temperature, salt concentration, or alcohol content as an environmental stimulus. The secondary structure transitions in the liquid as well as the solid state and related thermodynamics have been accurately mapped using circular dichroism (CD), FTIR, and Raman spectroscopy. PLL folds preferentially in the β-sheet structure at the high concentrations relevant to nanocomposite film formation regardless of solution conformation from which films were cast. The transition from α-helix to β-sheet is directly dependent on molecular weight, with high-molecular-weight films showing a consistent β-sheet conformation and exhibiting a kinetic dependence on temperature. We hope this insight into the mechanism of secondary structural control in polypeptides will foster the design of new peptidic nanomaterials for specific desired applications in the biomedical arena.[38]

Efforts in our group[40] have also been directed at responsive hydrogels constructed via self-assembly of short 20-residue peptides. These synthetic peptides are designed to intramolecularly fold under desired aqueous conditions and subsequently intermolecularly self-assemble into supramolecular networks.[40] The network scaffold is comprised of stiff, fibrillar structures that exhibit varied morphology, including twisted or untwisted single fibrils and fibril laminates.

Materials like these, in addition to proteins, introduce the possibility of fibril incorporation into nanocomposites as reinforcement with biodegradable matrices. Such unique nanocomposites combine the degradability and strength of the gel matrix with control over functionality and morphology of the fibrillar fillers. Potential applications of such nanomaterials include drug delivery matrices, tissue-engineering scaffolds, and bioengineering materials, to name a few.

Nanocomposites from Other Polymers and Fillers

Nanocomposites from bioactive molecules and clays have also been reported. One such example is smectite nanocomposites that use the ability of smectites to induce specific cointercalation of purines and pyrimidines. Thus, thymine and uracil are absorbed on MMT appreciably if solutions also contain coabsorbed adenine.[41]

Layered double hydroxides (LDHs) present a layered structure comprised of di-and trivalent metal cations [M(II) and M(III)] coordinated by six oxygen anions. The substitution of M(III) cations induces an overall positive charge that is counterbalanced by exchangeable interlayer anions. Thus, LDHs can serve as hosts for polymeric intercalation. An attractive, potential application of LDHs is controlled drug release carriers. Several bioactive compounds like DNA and pharmaceuticals have been incorporated within LDH hosts.[42]

Poly(urethane urea) (PUU) segmented block copolymers are common in ventricular assist devices and total artificial hearts as blood sacs. One of the main disadvantages of PUUs in these devices is their relatively high permeability to air and water vapor, a result of the diffusion through the poly(tetramethylene oxide) soft segments that are present as the majority component of the copolymer. The use of organically modified layered silicates seems particularly attractive among the variety of approaches taken to reduce permeability while maintaining desired biocompatibility and mechanical properties. This can be ascribed to the dramatic increase of barrier properties because of intercalated or exfoliated high-aspect-ratio (~1000) clay layers in the polymer matrix. Studies on the PUU–clay system have shown increases in the modulus and strength of the nanocomposite. However, in contrast to conventional composite systems, this enhancement does not come at the expense of ductility. In fact, it is reported that the ductility increases with clay loading.[43] A convincing explanation for this remarkable behavior has not yet emerged. Nonetheless, a significant reduction in gas permeability with an increase in mechanical properties has been shown.

Just as nanocomposites used for various biomedical applications have different requirements, nanocomposites used for dental applications have unique necessities. Thermoset methacrylate-based composites are used commonly as dental restorative materials, because of a relatively high cure efficiency by free-radical polymerization and excellent aesthetic qualities. However, the demands of the oral environment and the masticatory loads encountered by dental restoratives require further property improvements in these materials. Specifically, nanocomposites with improved modulus, better efficiency of the free-radical polymerization, low water sorption, improved processability, and low shrinkage are needed. Selective functionalization of the filler can lead to better interactions at the filler–matrix interphase and has been used in studies in which silica nanoparticles were silanized to varying extents using two different modifiers and then mixed with a dimethacrylate resin. A few practical advantages of the dual silanization are improved workability of the composite paste, higher filler loadings leading to better modulus values, and nanocomposites with lower polymer shrinkage.[44]

The design of cardiovascular interfaces necessitates a combination of amphiphilicity and antithrombogenicity. Amphiphilicity ensures optimal endothelial cell response at the vascular interface. Thrombogenicity refers to blood clot formation and can lead to early graft occlusion. Using reports of polyhedral oligomeric silsequioxanes (POSS) acting as an amphiphile at the water–air interface, researchers have studied the possibility of using POSS at the vascular interface. The strong intermolecular forces between constituent molecules and neighbors and the robust framework of shorter bond lengths make POSS nanocomposites more resistant to degradation. Initial work has shown that POSS nanocomposites are cytocompatible, making them potentially suitable for tissue engineering.[45] Future efforts in this field are directed at assessing the thrombogenic potential of these nanocomposites, which would be critical in their application as cardiovascular interfaces.

Concluding Remarks

We have discussed an emerging group of hybrid materials based on various polymers and nanofillers that are either used extensively or show promise in the area of biomedical materials. These novel materials vary from inorganic/ceramic-reinforced nanocomposites for mechanical enhancement to peptide-based nanomaterials in which peptides are both the filler and the matrix, with the chemistry designed to render the entire material biocompatible. Interest in these nanocomposites varies from application-oriented design to understanding a multitude of structure–property

relations. Requisite functional criteria include mechanical strength, biocompatibility, biodegradability, morphology, and a host of other parameters, depending on end use. However, at the basis of the performance of these nanocomposites are interactions between the biopolymer or synthetic polymer and the filler, which can be tuned and perfected to suit specific needs. We hope that further research into these interactions will prove valuable in contemplating the design of novel bionanocomposites for biomedical applications.

Acknowledgments

This work was partially funded by the National Science Foundation Career Award DMR-0348147 and the DuPont Young Faculty Award.

References

1. E. Ruiz-Hitzky, M. Darder, P. Aranda, *J. Mater. Chem.* **15**, 3650 (2005).
2. A.P. Alivisatos, *Science* **271**, 933 (1996).
3. A.U. Daniels, M.K.O. Chang, K.P. Andriano, *J. Appl. Biomater.* **1** (1), 57 (1990).
4. G.W. Bradley et al., *J. Bone Joint Surg.* **61** (6), 866 (1979).
5. T. Terjesen, K. Apalset, *J. Orthop. Res.* **6**, 293 (1988).
6. N. Gillett, S.A. Brown, J.H. Dumbleton, R.P. Pool, *Biomaterials* **6** (2), 113 (1985).
7. A. Uchida et al., *J. Bone Joint Surg. Br.* **72-B** (2), 298 (1990).
8. F.W. Cooke, *Clin. Orthop. Relat. Res.* **276**, 135 (1992).
9. I. Yamaguchi et al., *J. Biomed. Mater. Res.* **55** (1), 20 (2001).
10. K. Ogawa et al., *Macromolecules* **17**, 973 (1984).
11. K. Okuyama et al., *Int. J. Biol. Macromol.* **26** (4), 285 (1999).
12. H.-W. Kim, H.-E. Kim, V. Salih, *Biomaterials* **26** (25), 5221 (2005).
13. E. Cenni et al., *J. Biomater. Sci. Polym. Ed.* **11**, 685 (2000).
14. S. Mann, G.A. Ozin, *Nature* **382**, 313 (1996).
15. J.E. Zerwekh et al., *J. Orthop. Res.* **10** (4), 562 (1992).
16. F. Zhao et al., *Biomaterials* **23** (15), 3227 (2002).
17. J.L. Drury, D.J. Mooney, *Biomaterials* **24** (24), 4337 (2003).
18. H.-R. Lin, Y.-J. Yeh, *J. Biomed. Mater. Res. Part B: Appl. Biomater.* **71B** (1), 52 (2004).
19. M. Ito, Y. Hidaka, M. Nakajima, H. Yagasaki, A.H. Kafrawy, *J. Biomed. Mater. Res.* **45** (3), 204 (1999).
20. C. Du et al., *J. Biomed. Mater. Res.* **42** (4), 540 (1998).
21. C.M. Müller-Mai, S.I. Stupp, C. Voigt, U. Gross, *J. Biomed. Mater. Res.* **29** (1), 9 (1995).
22. E. Boanini et al., *Biomaterials* **27** (25), 4428 (2006).
23. U. Edlund, A.-C. Albertsson, *Adv. Polym. Sci.* **157**, 67 (2002).
24. R.L. Kronenthal, *Polymer Medicine and Surgery* (Plenum Press, New York, 1975) p. 119.
25. H. Tsuji, Y. Ikada, *Polym. Degrad. Stab.* **67**, 179 (2000).
26. N.C. Bleach et al., *Biomaterials* **23** (7), 1579 (2002).
27. H. Alexander, N. Langrana, J. Massengill, A. Weiss, *J. Biomech.* **14** (6), 377 (1981).
28. A. Majola et al., *J. Mater. Sci. Mater. Med.* **3** (1), 43 (1991).
29. V. Krikorian, D.J. Pochan, *Chem. Mater.* **15** (22), 4317 (2003).
30. V. Krikorian, D.J. Pochan, *Macromolecules* **37** (17), 6480 (2004).
31. V. Krikorian, D.J. Pochan, *Macromolecules* **38** (15), 6520 (2005).
32. J. Zhang, H. Tsuji, I. Noda, Y. Ozaki, *Macromolecules* **37** (17), 6433 (2004).
33. J. Zhang, H. Tsuji, I. Noda, Y.J. Ozaki, *Phys. Chem. B* **108** (31), 11514 (2004).
34. E. Loizou et al., *Macromolecules* **38** (6), 2047 (2005).
35. X. Zong et al., *Polymer* **43** (16), 4403 (2002).
36. M. Alexandre, P. Dubois, *Mater. Sci. Eng. R* **28**, 1 (2000).
37. Y.H. Lee et al., *Biomaterials* **26** (16), 3165 (2005).
38. R.A. Hule, D.J. Pochan, *J. Polym. Sci. Part B: Polym. Phys.* **45,** 239 (2007).
39. V. Krikorian et al., *J. Polym. Sci. Part B: Polym. Phys.* **40**, 2579 (2002).
40. B. Ozbas et al., *Macromolecules* **37** (19), 7331 (2004).
41. G.E. Lailach, G.W. Brindley, *Clays Clay Miner.* **17**, 95 (1969).
42. M. Wei et al., *J. Mater. Chem.* **15**, 1197 (2005).
43. R. Xu, E. Manias, A.J. Snyder, J. Runt, *Macromolecules* **34** (2), 337 (2001).
44. K.S. Wilson, K. Zhang, J.M. Antonucci, *Biomaterials* **26** (25), 5095 (2005).
45. R.Y. Kannan, H.J. Salacinski, P.E. Butler, A.M. Seifalian, *Acc. Chem. Res.* **38** (11), 879 (2005). □